



Eneabba Mineral Sands Phase 3

Air Quality Assessment

Final Report
Version 4

Prepared for Iluka Resources

September 2021

Project Number: 1220

Eneabba Mineral Sands Phase 3

Final Report

DOCUMENT CONTROL

Version	Description	Date	Author	Reviewer
A	Internal Review	21.07.2021	ETA (JH)	ETA (DT)
1	Final	11.08.2021	ETA (JH)	ETA (DT)
2	Final	21.08.2021	ETA (JH)	MBS
3	Final	10.09.2021	ETA (JH)	ETA (DT)
4	Final	14.09.2021	ETA (JH)	Iluka

Approval for Release

Name	Position	File Reference
Jon Harper	Director /Principal Air Quality Specialist	1220_Iluka_Phase2_AirModel_Ver4.docx

Signature



Copyright © 2021 Environmental Technologies & Analytics Pty Ltd. All rights reserved.

This document has been prepared for Iluka Resources on the basis of instructions and information provided. The report may therefore be subject to qualifications, which are not expressed. Environmental Technologies & Analytics Pty Ltd has no liability to any other person who acts or relies upon any information contained in this document without confirmation. This document is uncontrolled unless it is an original, signed copy.

Executive Summary

Iluka Resources commissioned Environmental Technologies & Analytics Pty Ltd (ETA) to undertake an air quality assessment for the Eneabba Phase 3 – Eneabba Rare Earth Refinery (ERER). The purpose of this air quality assessment is to assess the potential air quality impacts associated with the downstream processing (refining) of the rare-earth (RE) monazite.

Overview of assessment

For the purposes of the air quality assessment, the ERER consists of the following:

- Roasting and leaching – Adding acid to the heavy mineral concentrate and heating it to around 300°C thereby converting the RE minerals into a soluble form. The product from the roasting kiln is dissolved in water.
- Purification – Precipitating and removing impurities from the solution by neutralisation. The precipitate is the main waste stream, consisting of sulphates (mainly gypsum) and phosphates (mainly iron). The majority of the radioactive components of the RE are captured in this stream.
- Separation – Separating the RE elements from one another using solvent extraction technology.
- Product finishing – Precipitating the RE products from each stream. The high value products are heated and converted into oxides.
- Material transport – Transporting RE packaged products in sea containers, by road train, for export through Fremantle Port.
- Waste gas treatment - Acid recovery and off-gas cleaning from the kiln before discharging to atmosphere.

The potential impacts were determined through a dispersion modelling study, which incorporated site-specific meteorological data, emissions information, source characteristics, and the location of model receptors. Emission rates were estimated using recognised and accepted methods of emissions estimation, which included published emission factors from the NPI Emission Estimation Technique Manual for Mining (EA, 2012).

The scope of the modelling assessment is summarised below.

Modelled meteorological period	1 January to 31 December 2015
Model selection	WRF/CALMET/CALPUFF model suite
Key Pollutants	<ul style="list-style-type: none"> • particulate matter (PM) - including PM₁₀ and PM_{2.5} size fractions • nitrogen dioxide (NO₂) • sulphur dioxide (SO₂) • ammonia • acid gas as sulphur trioxide / sulphuric acid (SO₃ / H₂SO₄) <p>This assessment precludes the consideration of radiological components.</p>
Meteorological data	Three-dimensional prognostic meteorological data developed using the Weather Research and Forecasting (WRF) model.

Background Air Quality	Published air quality monitoring data for the region has been reviewed and used as a suitable proxy of existing (baseline) concentrations for particulates. There are no other significant industry sources in close proximity, therefore the assessment of the incremental cumulative contribution only accounts for background air quality where monitoring data was available.
Project Emissions	Emissions from the ERER under maximum processing and material handling assumptions formed the basis of the modelling assessment for operational configuration. Abnormal or upset operating conditions for ERER (ie. start-up and shutdown, control equipment failure) have been determined to result in emissions that are lower than normal operating conditions.
Sensitive Receptors	Discrete receptor locations were nominated to represent: <ul style="list-style-type: none"> • non-project related sensitive receptors – Township of Eneabba • closest non-project related sensitive receptors – residents outside the Township of Eneabba • other receptors – Eneabba Golf Course
Model Scenarios	The model scenarios that have been included in the assessment consider the ERER during “Normal Operations” only: <ul style="list-style-type: none"> • Scenario 1 - Normal Operations for the Project only (in isolation of other sources) • Scenario 2 - Cumulative (Project in conjunction with existing air quality (if available)) Abnormal or upset operating conditions for ERER (ie. start-up and shutdown, control equipment failure) have been determined to result in emissions that are lower than normal operating conditions.

Key findings

The model results for normal operations of the ERER at the currently advised design capacity are summarised below for the key pollutants of concern.

Nitrogen Dioxide

- There are no predicted exceedances of the assessment criteria at the sensitive receptor locations nominated.
- Modelled ground level concentrations higher than the 1-hour assessment criterion is restricted to locations within the project site.

Sulfur Dioxide

- Predicted concentrations at all sensitive receptor locations are well within the assessment criteria.
- The highest predicted 1-hour SO₂ concentrations of 20 µg/m³ occur over the project site and is well below the assessment criterion.

Sulfur Trioxide / Sulfuric acid

- Predicted concentrations at all sensitive receptor locations are well within the relevant 1-hour and 24-hour assessment criteria.
- The 1-hour assessment criterion is exceeded in the immediate vicinity of the ERER project stacks.

Particulates (as PM₁₀ and PM_{2.5})

- There are no predicted exceedances of the 24-hour PM_{2.5} assessment criterion over the model domain.
- Predicted concentrations at all sensitive receptor locations are well within the relevant annual and 24-hour PM₁₀ and PM_{2.5} criteria.
- The highest 24-hour PM₁₀ concentration exceeds the assessment criterion over a small area within the ERER project boundary.

Ammonia

- Predicted concentrations at all sensitive receptor locations are well within the relevant 1-hour assessment criteria.
- Predicted concentrations are also well below the assessment criteria in the immediate vicinity of the ERER project ammonia scrubber stack.

Generally, the predictions presented in this report incorporate a level of conservatism in the assumptions made and the dispersion modelling approach adopted. As a result, it is expected that actual ground level concentrations, attributable to the ERER project, based on its current design definition, would be lower (than modelled).

Overall, the model results show that emissions of key pollutants from the ERER project alone lead to ground level concentrations that are less than 10% of the assessment criteria, with the exception of the maximum 1-hour NO₂ concentration estimated to be approximately 30% of the assessment criteria (at Receptor 1).

These relatively low changes in predicted ground level concentrations are not expected to impact on health or amenity values of the identified area with sensitive (human) receptors.

Table of Contents

1	Introduction.....	2
	1.1 Background	2
	1.2 Scope of work.....	4
	1.3 Structure of report	4
2	Project Description	5
	2.1 Process Overview	5
	2.2 Key pollutants	6
	2.3 Air Emission Controls	7
3	Assessment methodology	8
	3.1 Overview	8
	3.2 Existing environment – meteorology, air quality and receptors.....	9
	3.2.1 Local climate and meteorology	9
	3.2.2 Existing background air quality	10
	3.2.3 Sensitive receptors and environmental values.....	13
	3.3 Emissions estimation.....	16
	3.4 Modelling	16
	3.5 Impact Assessment	16
	3.5.1 Assessment criteria.....	16
4	Modelling.....	18
	4.1 Meteorological model (WRF and CALMET).....	18
	4.1.1 WRF model	18
	4.1.2 CALMET.....	18
	4.2 CALPUFF	21
	4.3 Conversion of NO _x to NO ₂	21
5	Emissions to air estimation	23
	5.1 Emission Sources.....	23

5.2	Stack emissions	24
5.3	Upset Conditions	28
5.3.1	Roaster emission control	28
5.3.2	Calciner / dryer emission control	28
5.4	Fugitive emissions	28
5.4.1	Loading ore	28
5.4.2	Unloading ore	29
5.4.3	Bulldozing	29
5.4.4	Front end loaders	29
5.4.5	Haul Roads	29
5.4.6	Wind erosion	30
5.5	Emission summary - fugitive	30
6	Predicted air quality impact	31
6.1	Oxides of Nitrogen	31
6.2	Sulfur dioxide	34
6.3	Sulfur trioxide / Sulfuric acid	37
6.4	Particulates	40
6.5	Ammonia	47
7	Conclusions	49
7.1	Key findings	50
8	References	51
9	Acronyms and Glossary	54
10	Appendices	56
	Appendix A – Meteorology	57
	Appendix B – Emission Rates	75
	Appendix C – Emission Parameters	76

Tables

Table 2-1: Air pollutants of interest from the Project

Table 2-2: Summary of Air Emission Controls

Table 3-1: 24-hour averaged statistics of TEOM monitoring at Eneabba 2007 – 2011 ($\mu\text{g}/\text{m}^3$)

Table 3-2: Receptor coordinates (GDA20, Zone 50)

Table 3-3: Summary of adopted assessment criteria

Table 4-1: Default and revised roughness length (z_0), albedo (α) and Bowen ratio (β) used in CALMET

Table 4-2: Ratio of NO_2 to NO_x ratio with varying NO_x concentration (ppb)

Table 5-1: Characteristics of emission sources – EMSR-3

Table 5-2: Estimate of annual particulate emissions

Table 6-1: Predicted 1-hour NO_2 concentrations at receptors ($\mu\text{g}/\text{m}^3$) – Project only

Table 6-2: Predicted 1-hour SO_2 concentrations at receptors ($\mu\text{g}/\text{m}^3$) – Project only

Table 6-3: Predicted 24-hour SO_2 concentrations at receptors ($\mu\text{g}/\text{m}^3$) – Project only

Table 6-4: Predicted 1-hour $\text{SO}_3 / \text{H}_2\text{SO}_4$ concentrations at receptors ($\mu\text{g}/\text{m}^3$) – Project only

Table 6-5: Predicted 24-hour $\text{SO}_3 / \text{H}_2\text{SO}_4$ concentrations at receptors ($\mu\text{g}/\text{m}^3$) – Project only

Table 6-6: Predicted 24-hour PM_{10} concentrations at receptors ($\mu\text{g}/\text{m}^3$)

Table 6-7: Predicted 24-hour $\text{PM}_{2.5}$ concentrations at receptors ($\mu\text{g}/\text{m}^3$)

Table 6-8: Predicted 1-hour NH_3 concentrations at receptors ($\mu\text{g}/\text{m}^3$) – Project only

Figures

Figure 1-1: Project location and setting

Figure 2-1: Eneabba Stage 3 Rare Earth Refinery Process (Iluka, 2021)

Figure 3-1: Air quality assessment – study approach

Figure 3-2: Long term temperature statistics (BoM, 2021)

Figure 3-3: Long term rainfall statistics (BoM, 2021)

Figure 3-4: Location of dust deposition gauges

Figure 3-5: Monthly deposition rates ($\text{g}/\text{m}^2/\text{month}$)

Figure 3-6: Receptor locations (GDA20, Zone 50)

Figure 4-1: Image of SRTM terrain elevation used in CALMET (vertical height is exaggerated) (GDA20, Zone 50)

Figure 4-2: Scatterplot of measured NO_x and NO₂ at South Hedland within the power station plume (ETA, 2019)

Figure 5-1: Location of emission sources (Project sources are represented as stack sources while cumulative sources are represented as volume sources)

Figure 5-2: Source contributions – Phase 3

Figure 6-1: Predicted maximum 1-hour NO₂ concentrations (µg/m³)

Figure 6-2: Predicted annual NO₂ concentrations (µg/m³)

Figure 6-3: Predicted maximum 1-hour SO₂ concentrations (µg/m³)

Figure 6-4: Predicted maximum 24-hour SO₂ concentrations (µg/m³)

Figure 6-5: Predicted maximum 1-hour SO₃/H₂SO₄ concentrations (µg/m³)

Figure 6-6: Predicted maximum 24-hour SO₃/H₂SO₄ concentrations (µg/m³)

Figure 6-7: Predicted annual average PM₁₀ concentrations (µg/m³) – Project only

Figure 6-8: Predicted annual average PM₁₀ concentrations (µg/m³) – cumulative

Figure 6-9: Predicted maximum 24-hour PM₁₀ concentrations (µg/m³) – Project only

Figure 6-10: Predicted maximum 24-hour concentrations (µg/m³) – cumulative

Figure 6-11: Predicted annual average PM_{2.5} concentrations (µg/m³) – Project only

Figure 6-12: Predicted annual average PM_{2.5} concentrations (µg/m³) – cumulative

Figure 6-13: Predicted maximum 24-hour PM_{2.5} concentrations (µg/m³) – Project only

Figure 6-14: Predicted maximum 24-hour PM_{2.5} concentrations (µg/m³) – cumulative

Figure 6-15: Predicted maximum 1-hour NH₃ concentrations (µg/m³) – Project only

1 Introduction

1.1 Background

Iluka Resources (Iluka), and its predecessor companies, have undertaken mineral sands mining at Eneabba, approximately 300 km north of Perth since the 1970's. The mineral sand operations were located 6 km south west of the Eneabba townsite, 3.5 km to the west of Brand Highway (Figure 1-1). For the last 30 years Iluka has been stockpiling by-products from their Narngulu Mineral Separation Plant (MSP) within these operations. This by-product stockpile has been characterised as an ore reserve of 1.0 million tonnes grading 83.5% Heavy Mineral (HM) of which 20% is the rare-earth (RE) bearing mineral monazite.

The Eneabba Mineral Sands Recovery Phase One (EMSR-1) project was initiated to extract, wash and screen this ore to obtain a 20% monazite concentrate. The Eneabba Mineral Sands Recovery Phase Two (EMSR-2) project, nearing construction, is to upgrade the concentrate to a higher grade RE mineral product that would be a suitable for direct feed into a RE refinery, and supply downstream RE producers.

Iluka is now pursuing State and Commonwealth environmental approvals for the Phase 3 – Eneabba Rare Earth (RE) Refinery (the Project), involving the refining of the RE concentrate and other RE minerals into RE oxides. The Project will be located adjacent to the EMSR-2 plant (Figure 1-1).

Iluka and MBS Environmental Consultants commissioned Environmental Technologies & Analytics Pty Ltd (ETA) to undertake an assessment of emissions from the Project to determine the potential air quality impacts on the surrounding region.

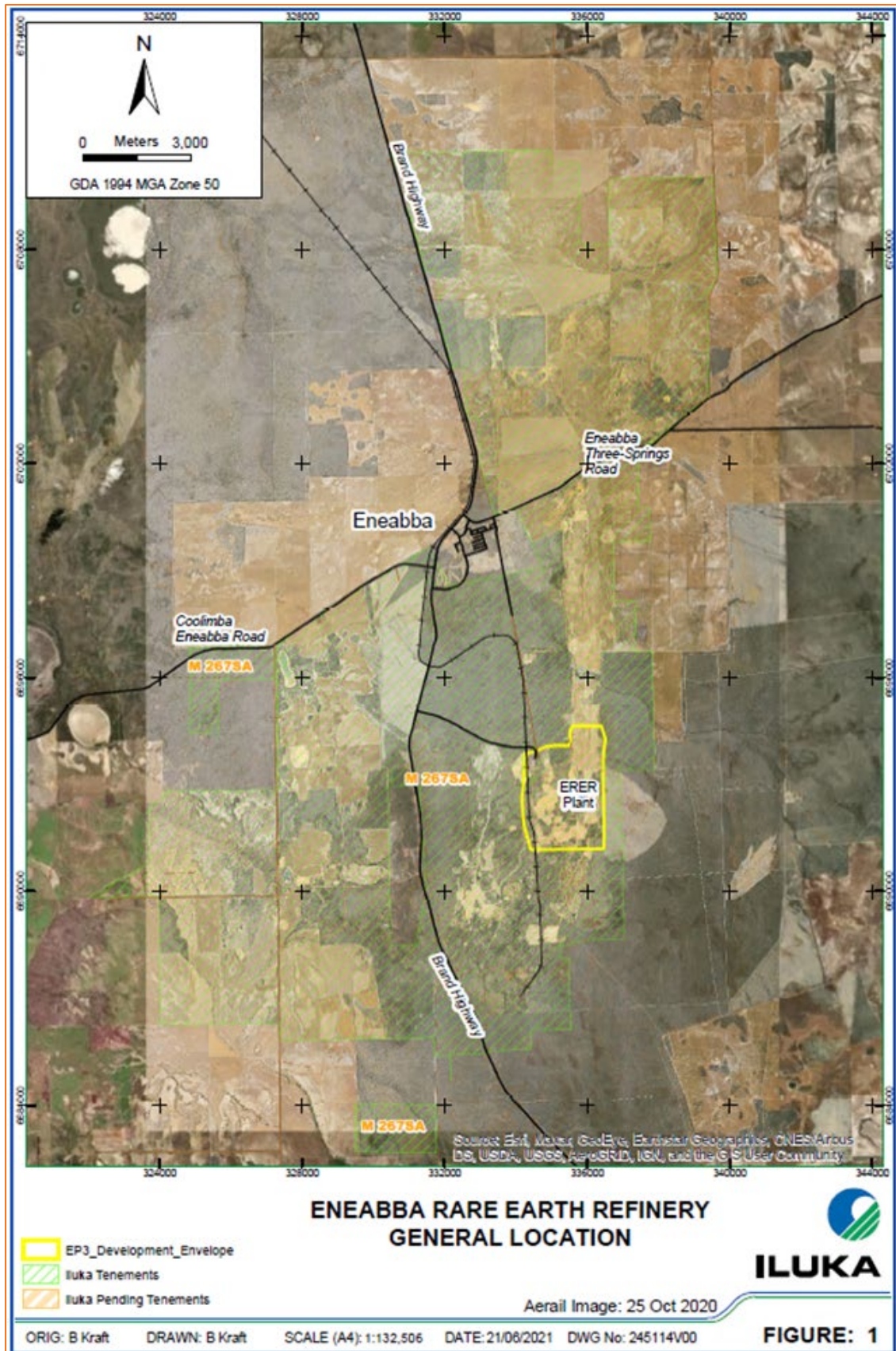


Figure 1-1: Project location and setting

1.2 Scope of work

The potential air quality impacts of the Project have been determined through a dispersion modelling study, which incorporated site-specific meteorology, and emissions information estimated for the Project for the defined nominal production capacity. The scope of the modelling has been developed, taking into account the regulatory context, available meteorological and ambient air quality monitoring data, and the nature of emissions from the process.

Reference has been made to the following key regulatory policy and guidance:

- Air Quality Modelling Guidance Notes (DoE, 2006)
- Guideline – Air Emissions, draft for external consultation (DWER, 2019)
- Environmental Factor Guideline – Air Quality (EPA, 2020)
- *Environmental Protection Act, 1986, as amended, and*
- Environmental Protection Act Regulations 1987.

1.3 Structure of report

This report describes the methods and findings of an assessment of the potential impacts to the air environment arising from the Project. The assessment includes:

- Project description in Section 2.
- Assessment methodology in Section 3.
- Details of modelling methodology and model setting in Section 4.
- Project emission estimation and operating scenarios considered in Section 5.
- Predicted concentrations and interpretation of the potential impact of the Project in Section 6.
- Conclusions of the assessment are presented in Section 7.

The appendices contain supporting information.

2 Project Description

2.1 Process Overview

A schematic process flow diagram depicting the various stages of the EMSR-3 rare earth (RE) refining process is presented in Figure 2-1.

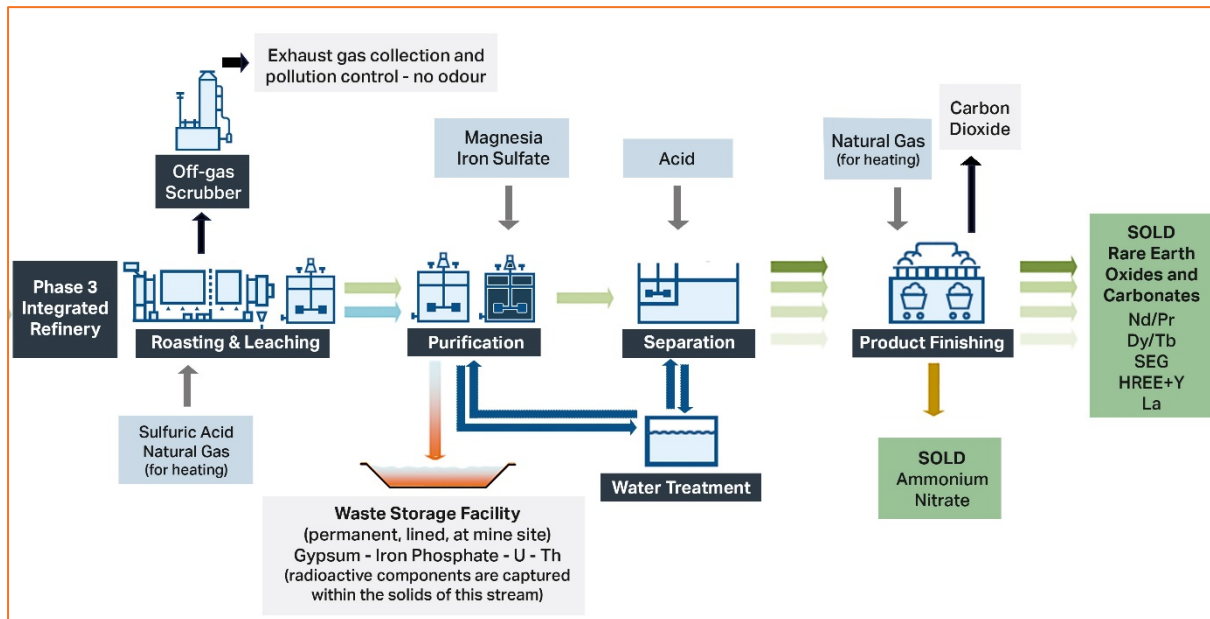


Figure 2-1: Eneabba Stage 3 Rare Earth Refinery Process (Iluka, 2021)

The main processing stages, relevant to assessment of air quality, for EMSR-3 are outlined below.

• EMSR-2:	Input of ore from EMSR-2 plant or from 3 rd party provider.
• Roasting and leaching:	Acid is added to the heavy mineral concentrate and heating it to around 300°C thereby converting the RE minerals into a soluble form. The product from the roasting kiln is dissolved in water.
• Purification:	Impurities are precipitated and removed from the solution by neutralisation, the precipitate is the main waste stream, consisting of sulphates (mainly calcium) and phosphates (mainly iron).
• Separation:	RE elements are separated from one another using solvent extraction technology.
• Product finishing:	Separated RE products are precipitated from each stream, and in the case of the high value products, are heated and converted into oxides.
• Material transport	Packaged products loaded into sea containers and transported by road train for export through Fremantle Port.

- | | |
|---|--|
| <ul style="list-style-type: none"> Waste gas treatment and Pollution Control | <p>Acid recovery and off-gas cleaning including:</p> <ul style="list-style-type: none"> Roasting Kiln Off Gas Treatment System consisting of Venturi Scrubbers, Entrainment Separator, Quench Vessel, Spray Tower Scrubber, Wet Electrostatic Precipitator, Fibre Bed Mist Eliminator and acid recovery tanks, with discharge via stack Baghouse filter systems to remove entrained particulates in calciner circuit, including – <ul style="list-style-type: none"> Dedicated system installed for each process train. Multi-compartment bag house filter to capture fine particulates |
|---|--|

Atmospheric emissions are generated during the various stages of processing the RE concentrate to recover the individual RE elements. The majority of atmospheric emissions, in relative terms, are generated from the roasting and calcination processing stage and hence will be subject to capture and treatment prior to discharge.

2.2 Key pollutants

Based on the description of the Project and processes, the key pollutants of interest to be assessed are summarised in Table 2-1. This assessment has not considered the radiological component of the RE.

Table 2-1: Air pollutants of interest from the Project

Pollutant		Description
Process Gases	NO ₂	<p>Nitrogen dioxide (NO₂) is a brownish gas with a pungent odour. It exists in the atmosphere in equilibrium with nitric oxide. The mixture of these two gases is commonly referred to as nitrogen oxides (NO_x). Nitrogen oxides are a product of combustion processes, and can arise when flame staging is non-ideal and nitrogen present in air is oxidised.</p> <p>Nitrogen dioxide can cause damage to the human respiratory tract, increasing a person's susceptibility to respiratory infections and asthma. Sensitive populations, such as the elderly, children, and people with existing health conditions are most susceptible to the adverse effects of nitrogen dioxide exposure.</p> <p>Nitrogen dioxide can also cause damage to plants, especially in the presence of other pollutants such as ozone and sulphur dioxide.</p> <p>Nitrogen oxides are also present in the reactions that lead to photochemical smog formation.</p> <p>Project sources are principally from the roasting kiln, calciners and SEGHY dryer.</p>
	SO ₂	<p>Sulphur dioxide (SO₂) is a strong-smelling, colourless gas that can irritate the lungs, and can be particularly harmful for people with asthma.</p> <p>SO₂ and other sulphur oxides can react with compounds in the atmosphere to form fine particles that reduce visibility (haze formation).</p> <p>Project sources are principally from the roasting kiln.</p>
	SO ₃	<p>When Sulfur trioxide (SO₃) is exposed to air it reacts with water vapour to form sulfuric acid (H₂SO₄). Sulfuric acid, as with other acids, is corrosive and can cause direct local effects to the skin, eyes and respiratory and gastrointestinal tracts with direct exposure to sufficient concentrations.</p> <p>Project sources are principally from the roasting kiln.</p>
	H ₂ SO ₄	

Pollutant	Description
Particulate Matter	<p>Airborne particles are a broad class of diverse substances that may be solid or liquid (liquid particles are often called aerosols) and are produced by a wide range of natural and human activities. Airborne particles are commonly classified by their size as total suspended particles (TSP), visibility reducing particles (PM₂), and inhalable particles (coarse fraction PM₁₀ and fine fraction PM_{2.5}).</p> <p>Project sources are principally from the roasting kiln, calciner dryers. Additional sources also occur from the monazite pit and transportation as part of EMSR-2.</p> <p>For the purposes of the processing described in this report, all particulate emissions are considered non-condensable.</p>
	<p>PM₁₀</p> <p>Inhalable particles are grouped into two size categories: those with a diameter of up to 10 µm (PM₁₀) and those with a diameter of up to 2.5 µm (PM_{2.5}).</p> <p>Inhalable particles are associated with increases in respiratory illnesses such as asthma, bronchitis and emphysema, with an increase in risk related to their size, chemical composition and concentration.</p> <p>Particles in the PM₁₀ size fraction have been strongly associated with increases in the daily prevalence of respiratory symptoms, hospital admissions and mortality.</p>
	<p>PM_{2.5}</p> <p>Particles in the PM_{2.5} size fraction can be inhaled more deeply into the lungs than PM₁₀, and have been associated with health effects similar to those of PM₁₀. There is some evidence to suggest that PM_{2.5} might be more deleterious to health than other size fractions. No lower limit for the onset of adverse health effects has yet been observed.</p>

2.3 Air Emission Controls

The Project has been designed to incorporate leading industry air emission control technologies to mitigate potential impacts. A summary of the key design features and control technologies to be installed for key emission sources at the Refinery is presented in Table 2-2.

Table 2-2: Summary of Air Emission Controls

Source Name	Air Emission Controls
Roasting Kiln	<ul style="list-style-type: none"> The Roasting Kiln Off Gas Treatment System will consist of Venturi Scrubbers, Entrainment Separator, Quench Vessel, Spray Tower Scrubber, Wet Electrostatic Precipitator, Fibre Bed Mist Eliminator and acid recovery tanks and a discharge stack
Calciners	<ul style="list-style-type: none"> Baghouse filter systems to remove entrained particulates. <ul style="list-style-type: none"> Dedicated system installed for each process train. Multi-compartment bag house filter to capture fine particulates.

3 Assessment methodology

This section outlines the air quality study and assessment approach. It includes the methodology applied to define the meteorological characteristics of the project area relevant to the assessment, the emission estimation, the dispersion, and the ambient assessment criteria selected for the purposes of determining the significance of the dispersion model results, and therefore the potential impact.

3.1 Overview

An overview of the air quality modelling approach is shown in Figure 1-1. Comparison of the modelled results to the assessment criteria is intended to provide an objective evaluation of the potential impact of the operations at the nearest sensitive receptors.

Further details of model settings and input parameters are provided in the subsections following.

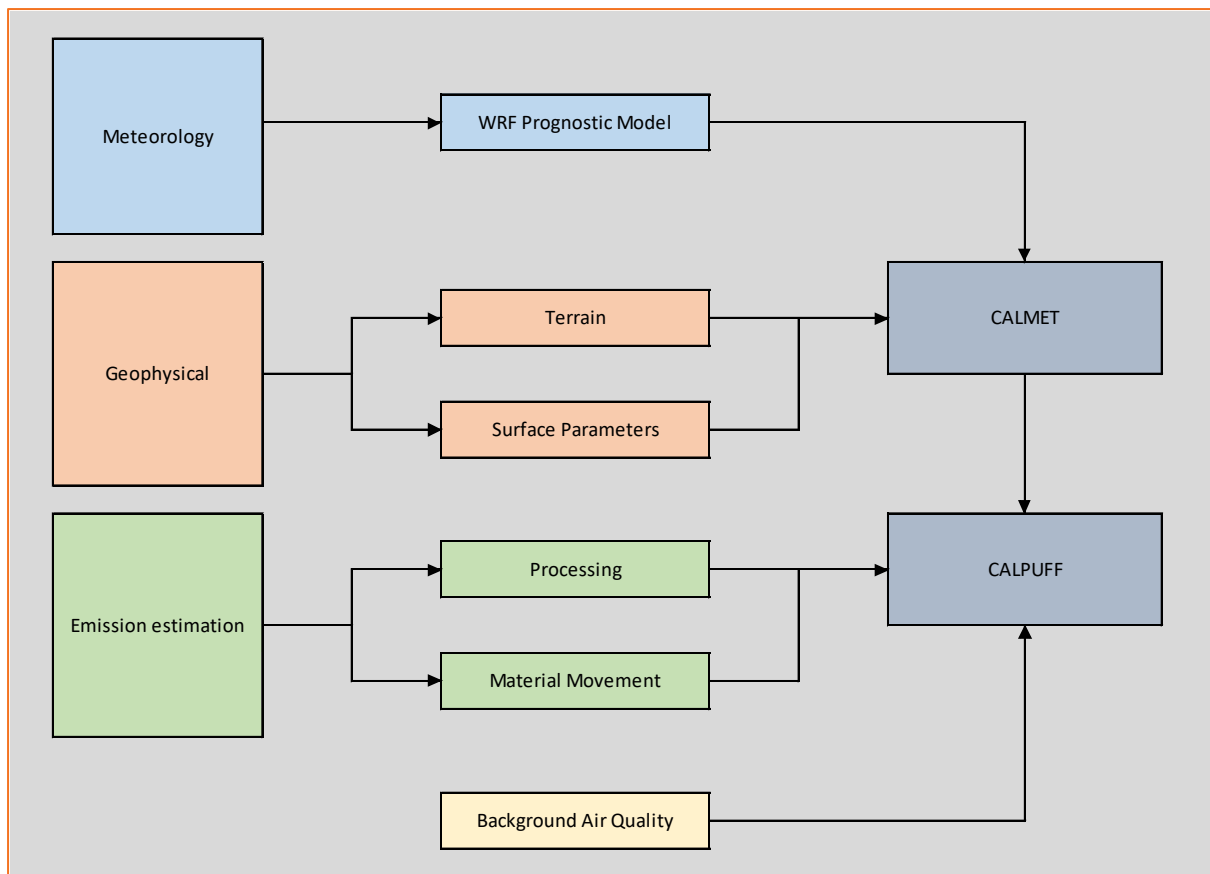


Figure 3-1: Air quality assessment – study approach

3.2 Existing environment – meteorology, air quality and receptors

The climate and meteorological characteristics of the region control the dispersion, transformation and removal (or deposition) of pollutants from the atmosphere, and therefore ambient air quality. This section outlines the key characteristics for the project location, including the receptors identified within the region.

3.2.1 Local climate and meteorology

The climate at Eneabba is characterised, according to the Koppen-Geiger classification, as “Csa” (Mediterranean climate) indicating hot, dry summers with the majority of rainfall occurring during the winter (Kottek et al (2006)). The long-term climate data for this region are sourced from the Bureau of Meteorology (BoM) meteorological station at the Badgingarra Research Station (BoM station ID: 009037), located approximately 60 km to the south of Eneabba.

The long-term temperature statistics from the BoM station at the Badgingarra Research Station are presented in Figure 3-2. From this figure it is apparent that the summer period has hot days and warm nights while the winter has cool days with cold nights, with temperatures occasionally dropping below 0°C.

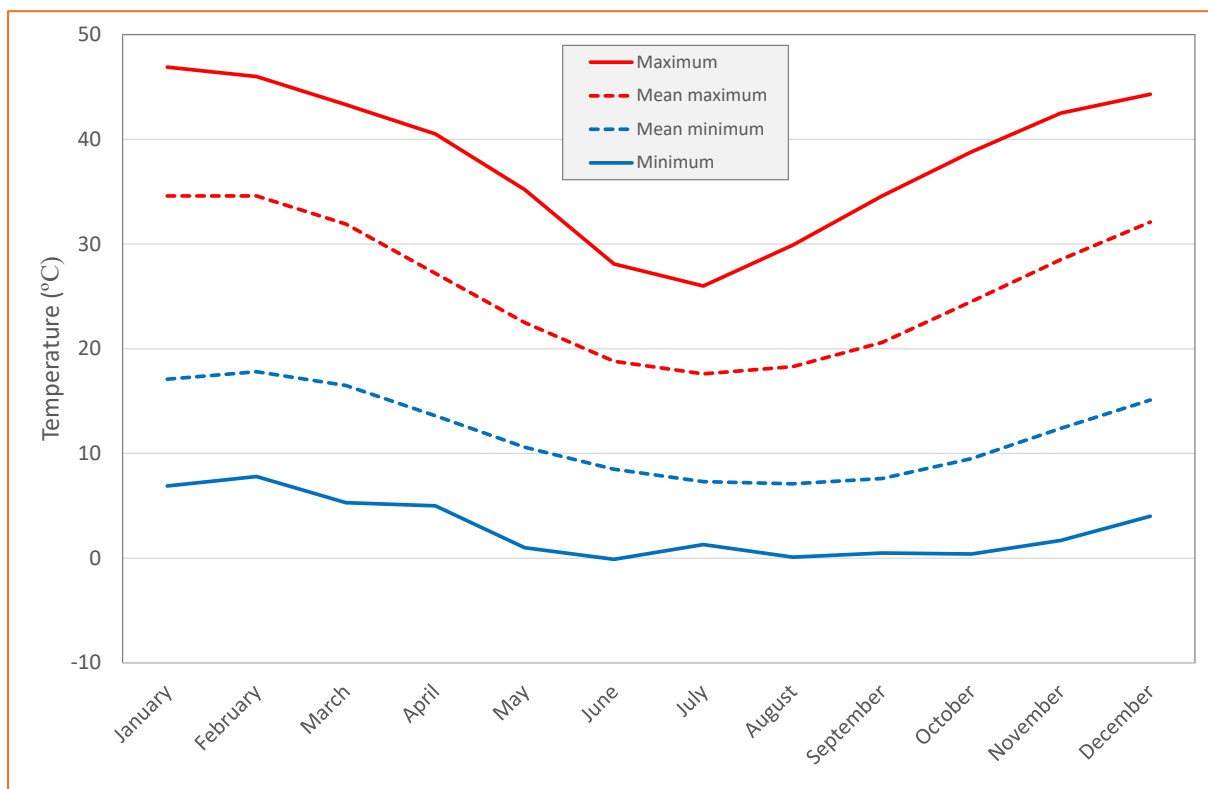


Figure 3-2: Long term temperature statistics (BoM, 2021)

The region has a mean annual rainfall of approximately 538 mm and, as presented in Figure 3-3. Rainfall varies seasonally and there is significantly more rain during the winter months.

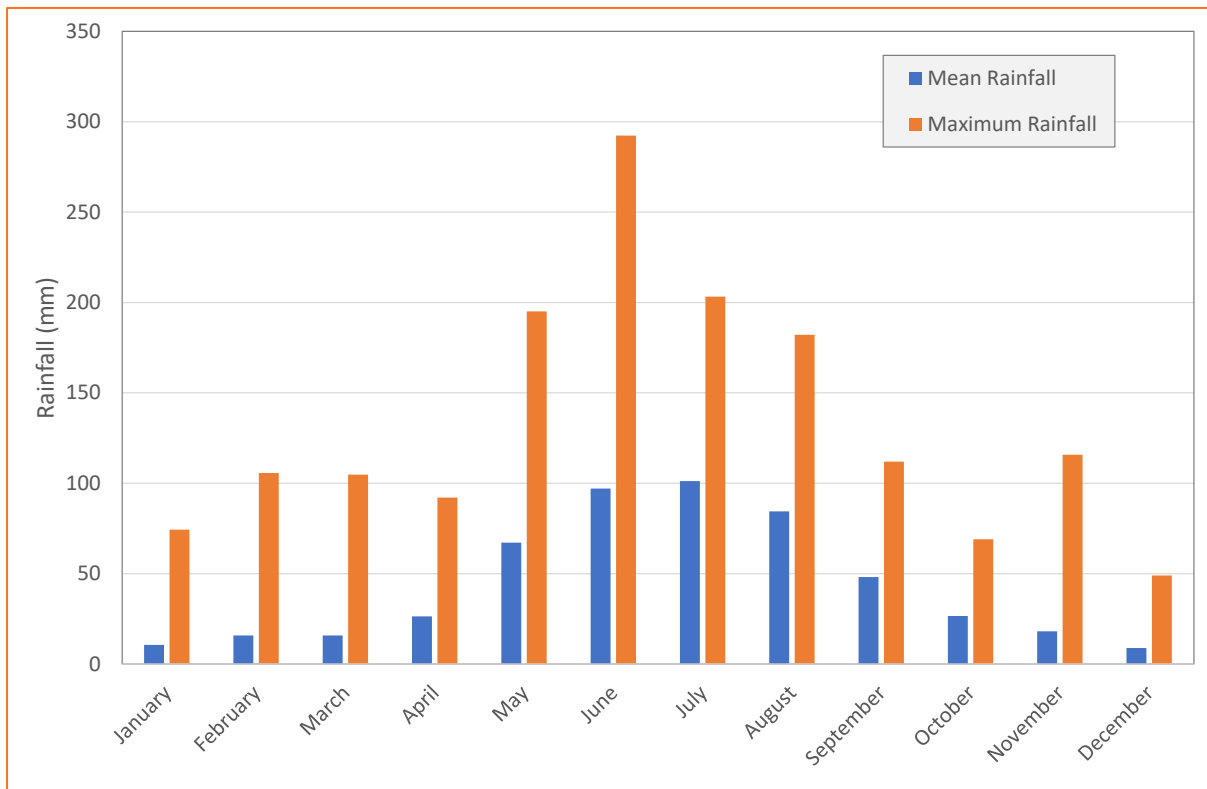


Figure 3-3: Long term rainfall statistics (BoM, 2021)

3.2.2 Existing | background air quality

There is limited ambient air quality data publicly available to describe the Project area. Ambient data is available to describe particulate matter (measured in the form of dust deposition and in the 10 micron (μm) size range).

The existing air quality in the region is expected to be influenced by natural sources such as wind erosion and bushfires. Dust may also occur due to anthropogenic activities in the study area, such as agricultural activities. When a modelling assessment is completed all of these other 'background' sources must be included as part of the representation of the air quality during the Iluka activities.

Tapered Element Oscillating Microbalance

Iluka operated a Tapered Element Microbalance (TEOM) monitor within Eneabba and the 24-hour averaged statistics from this station, for the period 2007 to 2011, are presented in Table 3-1. From these statistics the following can be surmised:

- There is a large variation in the maximum measured 24-hour averaged data from $39.6 \mu\text{g}/\text{m}^3$ in 2010 up to $165.7 \mu\text{g}/\text{m}^3$ in 2007. The annual rainfall from the BoM Badgingarra Research Station indicates that both of these years received comparable rainfall amounts (406 mm in 2007 and 374 mm in 2010) (BoM, 2021b).
- The 95th percentile concentrations are comparable across all 5 years indicating that the elevated concentrations are isolated events.
- The number of excursions of the PM_{10} NEPM criteria (Section 3.5.1) varies from zero in 2009 and 2010 up to 4 in 2008.

- As outlined in BHP (2015) the 70th percentile PM₁₀ concentration is appropriate for use as a background concentration. For this assessment the background PM₁₀ concentration of 16.8 µg/m³ will be used to simulate the 24-hour averaged concentrations as this is the maximum 70th percentile concentration over the five years of monitoring data (Table 3-1).
- For this assessment a concentration of 14.4 µg/m³ will be utilised for the annual average PM₁₀ background concentration as this represents the maximum annual average concentration over the five years of available monitoring data (Table 3-1).
- The background concentrations for PM_{2.5} will be taken as 30% of the PM₁₀ concentrations, which is the ratio of PM_{2.5} to PM₁₀ outlined in the National Pollutant Inventory (NPI) Emission Estimation Technique Manual (EETM) for Mining (EA, 2012).

Table 3-1: 24-hour averaged statistics of TEOM monitoring at Eneabba 2007 – 2011 (µg/m³)

Statistic	2007	2008	2009	2010	2011
Maximum	165.7	126.7	45.6	39.6	71.1
99 th percentile	46.8	51.6	37.4	36.0	39.3
95 th percentile	28.2	30.4	29.3	29.4	26.0
90 th percentile	22.7	24.7	24.2	23.7	20.8
70 th percentile	14.5	15.0	16.8	16.5	15.1
Annual average	13.3	13.5	14.4	13.8	13.6
Number > 50 µg/m ³	3	4	0	0	3
Valid data return (%)	97%	89%	97%	90%	73%

Dust Deposition Gauges

The primary ambient monitoring data available for the immediate region was from a series of dust deposition gauges (DDG). The DDGs provide simple non real-time measure of dust that settles out from the air, over a specified period of time, allowing a mass deposition rate of deposited matter to be calculated¹. The locations of these DDG's are presented in Figure 3-4. From this figure it is apparent that the DDGs ENE01, 02, 04, 05 and 07 are located to the south of the proposed Project, and relatively close to the historic mining areas, while DDG's ENE03, 06, 08, 09, 10 and 11 are located to the north of the Project, with DDG ENE08 being located within Eneabba.

The monthly insoluble dust deposition results from June 2012 to October 2020 from these stations is presented in Figure 3-5. The results of this monitoring indicate that each monitoring location has had elevated deposition concentrations, with the stations to the north of the operations, including ENE08 in Eneabba, tending to have a higher frequency of deposition above 4 g/m²/month. These results are not unexpected due to the agricultural operations to the north of the Project.

¹ Australian Standard AS/NZ 3580.10.1:2003 - Determination of Particulate Matter - Deposited matter - Gravimetric method.

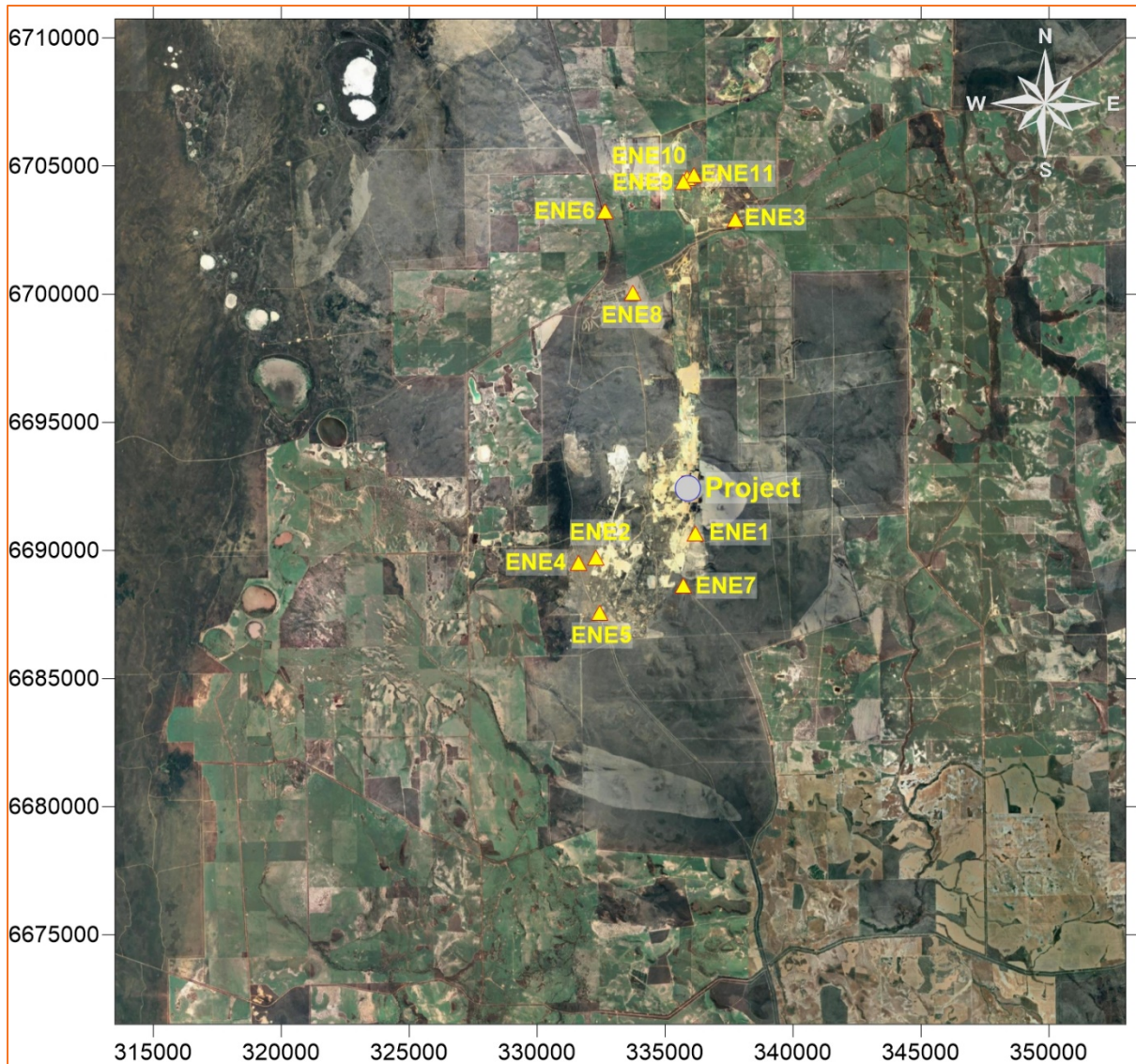


Figure 3-4: Location of dust deposition gauges

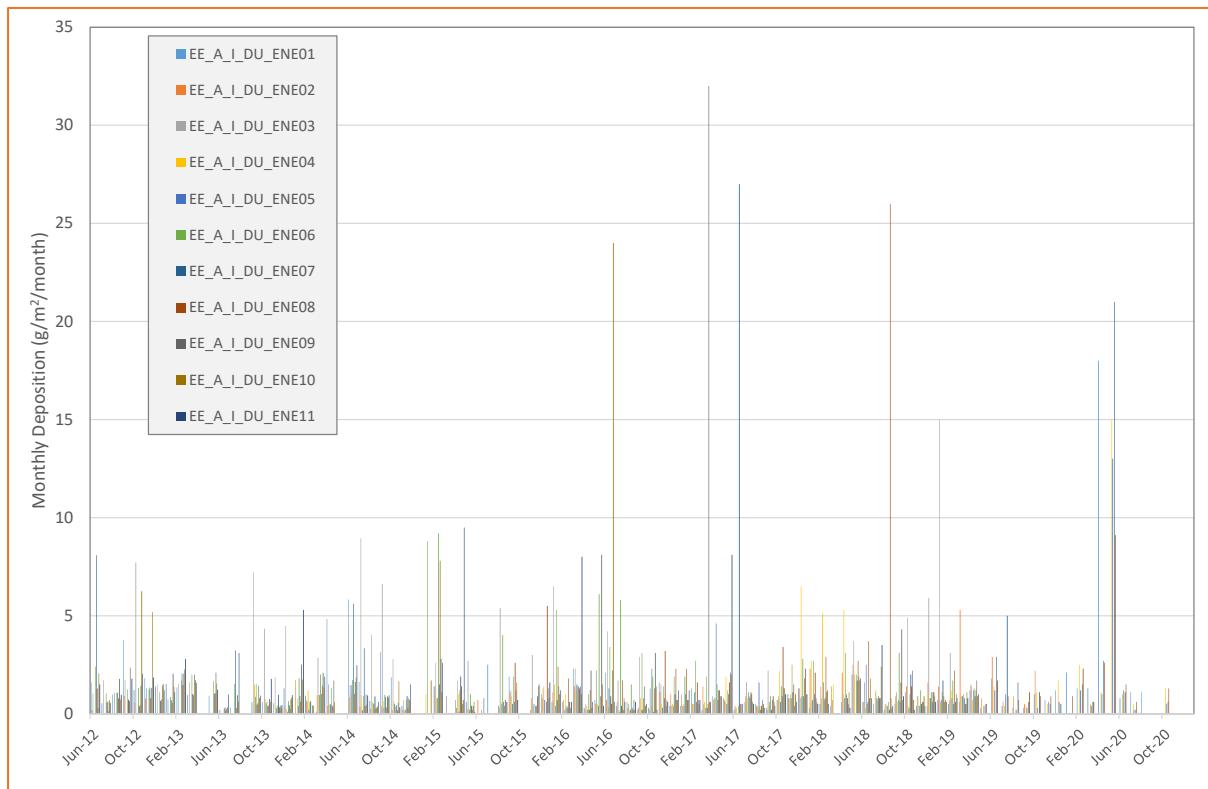


Figure 3-5: Monthly deposition rates (g/m²/month)

3.2.3 Sensitive receptors and environmental values

This modelling assessment considers the potential air quality impacts on relevant environmental values and sensitive receptors, consistent with EPA (EPA, 2020), and DWER (DWER, 2019). Consistent with the EPA's objective of air quality², relevant sensitive receptors have been identified in the vicinity of the project area. This includes sensitive (human) receptors, including locations where people are residing either on a temporary or permanent basis, noting that the current DWER guidelines excludes the consideration of on-site project related receptors as sensitive receptors. Other receptor locations have been included for information purposes to inform the assessment process. Therefore, the key receptors locations considered in the assessment are:

- The Township of Eneabba (R3 and R5)
- Residences within the region
- Eneabba Golf Course (R4)

The location of the nominated receptors in the region are presented in Figure 3-6 relative to the Project, and summarised in Table 3-2. This includes the basis for selection (ie receptor type) and the approximate distance from the Project. The relevant pollutants to be assessed at the receptors is also summarised.

² To maintain air quality and minimise emissions so that environmental values are protected (EPA, 2020).

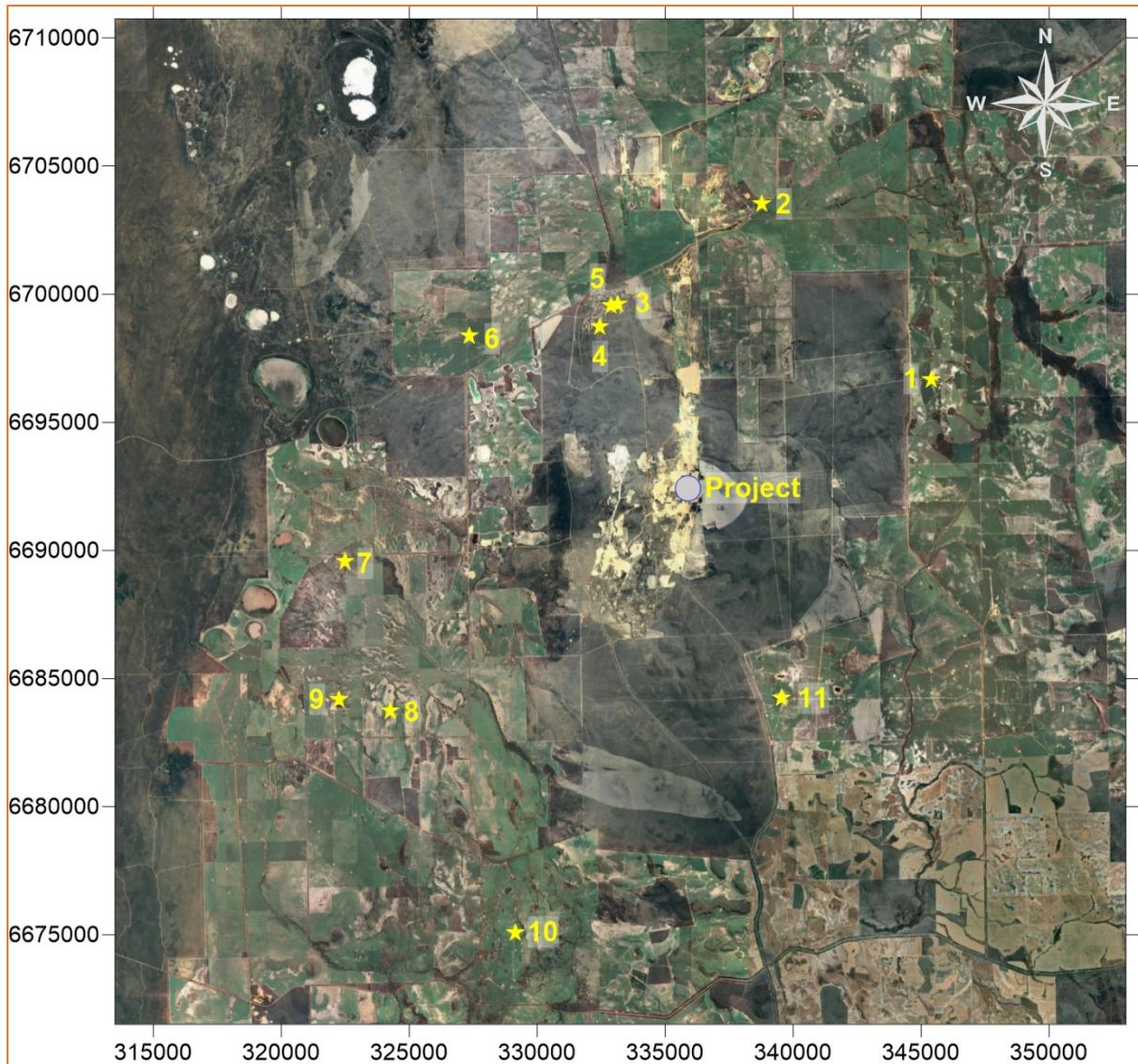


Figure 3-6: Receptor locations (GDA20, Zone 50)

Table 3-2: Receptor coordinates (GDA20, Zone 50)

Receptor	Easting	Northing	Environmental Value Receptor Type	Distance from Project (km)	Pollutant Impact Assessed				
					PM ₁₀	PM _{2.5}	NO ₂	SO ₂	H ₂ SO ₄
R1	345,397	6,696,676	Residence	10.4	✓	✓	✓	✓	✓
R2	338,774	6,703,524	Residence	11.6	✓	✓	✓	✓	✓
R3	333,149	6,699,618	Residence (Eneabba)	7.9	✓	✓	✓	✓	✓
R4	332,443	6,698,724	Golf Course (Eneabba)	7.3	✓	✓	✓	✓	✓
R5	332,892	6,699,549	Residence (Eneabba)	7.9	✓	✓	✓	✓	✓
R6	327,337	6,698,381	Residence	10.5	✓	✓	✓	✓	✓
R7	322,486	6,689,562	Residence	13.7	✓	✓	✓	✓	✓
R8	324,248	6,683,733	Residence	14.4	✓	✓	✓	✓	✓
R9	322,264	6,684,184	Residence	15.9	✓	✓	✓	✓	✓
R10	329,153	6,675,075	Residence	18.6	✓	✓	✓	✓	✓
R11	339,541	6,684,232	Residence	8.9	✓	✓	✓	✓	✓

3.3 Emissions estimation

The principal emission sources associated with the operation of the EMSR-3 project have been identified by Iluka and comprise various refinery point sources (process stacks).

The emissions related to material handling from mining of the monazite ore, transport of ore, and products, to and between EMSR-1, EMSR-2 and the Project has been considered. The emission rates were estimated using recognised and accepted methods of emissions estimation, which included published emission factors from the NPI EETM for Mining (EA, 2012). Further detail is contained in Section 5.

3.4 Modelling

The modelling has been conducted using the Weather Research and Forecasting (WRF) model, a mesoscale numerical weather prediction model coupled with the CALMET/CALPUFF model suite.

The WRF model was used to develop a three-dimensional wind field across the model area, which in turn was used as input to CALMET to form the final meteorological dataset used for modelling. Air dispersion modelling was conducted using CALPUFF. The model has been used to predict ground level concentrations across the model domain and at identified receptor locations of relevance to the assessment. Modelling setup is further detailed in Section 4.

The potential air quality impacts associated with the Project have been considered in isolation.

Air dispersion modelling was conducted using CALPUFF – the dispersion module of the CALMET/CALPUFF suite of models.

3.5 Impact Assessment

Ground-level concentrations of pollutants predicted at nominated receptors and the surrounding environment were compared with the relevant air quality assessment criteria. This assessment has considered the potential impact attributable to the Project, as well as the cumulative (background or existing air quality in conjunction with the Project) impact. The basis for this is summarised in Table 3-1.

Modelling results, at nominated receptors, are compared to the numerical value of the criteria, and assessed as being either above or below the numerical value. It is important to note that, as a risk-based assessment approach is normally applied to the assessment of air quality, a modelled result above the numerical value is not an indicator of unacceptable impact, but is an indication that the potential risk for impact requires further consideration.

3.5.1 Assessment criteria

Modelled ground level concentrations for particles (as PM₁₀ and PM_{2.5}), and process gases (NO_x, SO₂ and H₂SO₄) have been compared to ambient air quality assessment criteria to determine the potential risk of impact on nearest sensitive receptors.

The assessment criteria adopted for this study are primarily based on the DWER (2019) guidelines, which also reference the numerical values from the ambient air quality standards specified in the Ambient Air Quality NEPM (NEPC, 2021). The most recent amendment to the Ambient Air Quality NEPM standards for NO₂ and SO₂ (as varied 15 April 2021) are not reflected in the DWER (2019) guidelines. As the numerical values of the amended NEPM (2021), for NO₂ and SO₂ are more stringent, these have been adopted here to inform the assessment in regard to future regulatory requirements.

For the process gas, H₂SO₄, the DWER (2019) guidelines specify a 1-hour average assessment criteria. As DWER (2019) does not include a 24-hour average value for H₂SO₄, assessment criteria from the Ontario Ministry of the Environment Ambient Air Quality Criteria (AAQC) has also been referenced. These AAQCs are not a regulatory value, and are defined as a concentration of a contaminant in air that is protective against adverse effects on health and/or the environment. The AAQCs are used in Ontario (Canada) to assess general (ambient) air quality resulting from all sources of a contaminant to air. They are derived by a process that reviews scientific information about the effects of contaminants on health and the environment, and are generally based on the most sensitive effect identified. On this basis, the referencing of the AAQC for 24-hour average for H₂SO₄ is used as suitable proxy in the absence of a Western Australian or Australian derived criteria (MECP, 2020).

The ambient air quality assessment criteria adopted in this study are shown in Table 3-3.

Table 3-3: Summary of adopted assessment criteria

Pollutant	Air quality assessment criteria applicable at sensitive receptor locations				Reference	
	Concentration ¹ (µg/m ³)		Averaging Period	Allowable Exceedances		Environmental value protected
	referenced to 0°C	referenced to 25°C				
PM ₁₀	50	46	24-hour	exception event	Human health	
	25	23	annual	none		
PM _{2.5}	25	23	24-hour	exception event		
	8	7	annual	none		
NO ₂	164	150	1-hour	none		
	31	28	annual	none		
SO ₂	286	262	1-hour	none		
	57	52	24-hour	none		
SO ₃ / H ₂ SO ₄	20	18	1-hour	none		
	5	5	24-hour	none		
NH ₃	-	330	1-hour	none		

4 Modelling

For this assessment, air dispersion modelling has been conducted using CALPUFF (Version 6.42, Level: 110325). Although simplistic steady state models, such as AERMOD, would be suitable to model particulate emissions from the Project, the CALMET/CALPUFF suite was chosen to ensure that the model is suitable for more complex assessments such as power station and additional processing.

The model has been used to predict ground level concentrations across the model domain. The potential air quality impacts associated with the Project have been considered in isolation of other emission sources. The model was configured to predict the ground-level concentrations on a rectangular grid. The model domain was defined with the Southwest corner of the grid cell at 313.500 km Easting and 6671.750 km Northing (GDA94, Zone 50). The 2015 calendar year was selected based on the results of the statistical study presented in Appendix A.

Specifics for the modelling configuration are described further in this section.

4.1 Meteorological model (WRF and CALMET)

The meteorology component of a dispersion model is a key element for the effectiveness or representativeness of the dispersion model outputs. Both upper air and surface information are needed for modelling (or assumptions).

4.1.1 WRF model

In the absence of adequate onsite meteorological data, the Weather Research and Forecast (WRF V3.7) model (<http://wrf-model.org/index.php>) was used to generate hourly 3-dimensional data for the region. WRF is the next-generation mesoscale numerical weather prediction system. The model was primarily designed to serve both operational forecasting and atmospheric research. WRF features multiple dynamical cores, a 3-dimensional variational data assimilation system and a software architecture allowing for computational parallelism and system extensibility. Further details on WRF are provided in Appendix A.

4.1.2 CALMET

The 3-Dimensional meteorological data generated by WRF was input to CALMET for further processing to the finer resolution used in the dispersion modelling. This procedure will be referred to as the 'WRF-CALMET methodology'. The output from the CALMET meteorological model is then used to drive the pollution dispersion in the CALPUFF model.

CALMET is a three-dimensional meteorological pre-processor that includes a wind field generator containing objective analysis and parameterised treatments of slope flows, terrain effects and terrain blocking effects. The pre-processor produces fields of wind components, air temperature, relative humidity, mixing height and other micro-meteorological variables to produce the three-dimensional, spatially, and temporally varying meteorological fields that are utilised in the CALPUFF dispersion model.

CALMET requires several datasets to resolve the surface and upper air meteorology occurring for each hour of the year:

- land use and topographical data,
- surface and upper air observations or gridded prognostic meteorological model data.

Shuttle Radar Topography Mission (SRTM) data with 30 m resolution was input into the CALMET model to indicate terrain heights within the model domain (Figure 4-1). CALMET also requires geophysical data including gridded fields of land use categories. The newly released European Space Agency Climate Change Initiative Land Cover (ESACCI-LC) dataset was used for this study. This unique dataset providing land cover for each 300x300 meters pixel of the terrestrial surface of the Earth, was produced from the reprocessing and the interpretation of 5 different satellite missions, including NOAA-AVHRR HRPT, SPOT-Vegetation, ENVISAT-MERIS FR and RR, ENVISAT-ASAR, and PROBA-V. The ESACCI-LC categories were then converted into USGS land-use categories for assimilation by CALMET.

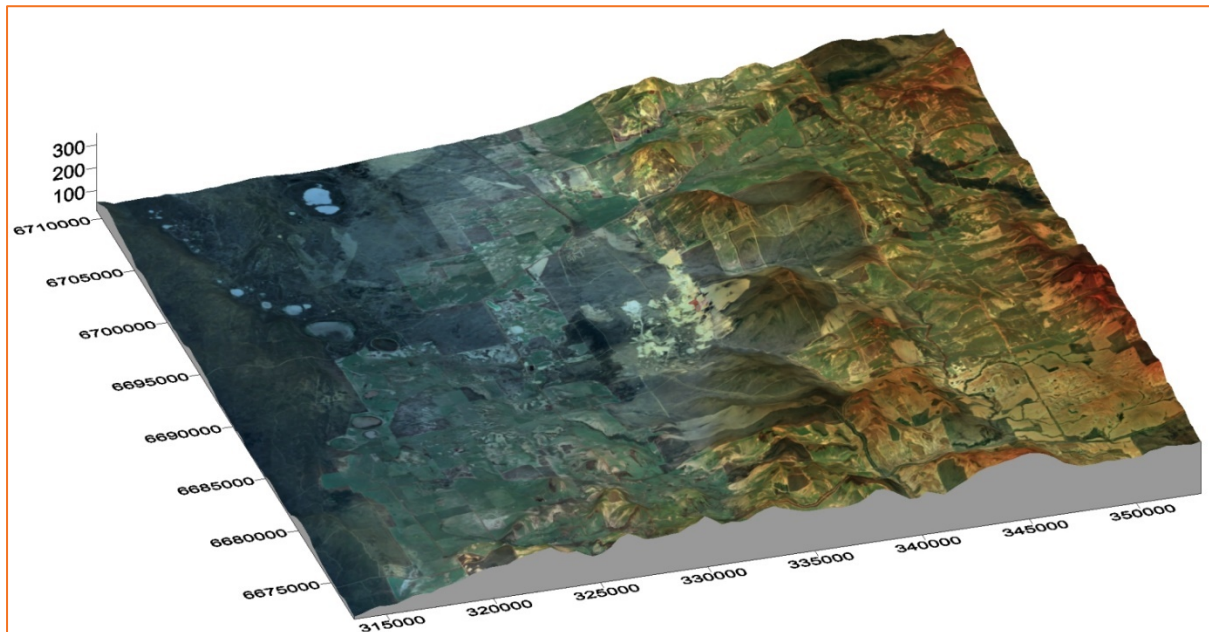


Figure 4-1: Image of SRTM terrain elevation used in CALMET (vertical height is exaggerated) (GDA20, Zone 50)

The default USGS³ biophysical parameters (i.e., roughness length, albedo, Bowen ratio) used in CALMET are based on North American vegetation types and are sometime unrepresentative of Australia. Consequently, parameters were revised based on local measurements (where available) and the literature. Roughness length was determined from Ozflux measurement data at Gingin for banksia shrubland (designated shrubland in CALMET) and wandoo woodland at Collie (designated forest in CALMET) respectively (Siberstein, 2015; Beringer, 2018). The roughness lengths (z_0) were calculated from the measured standard deviation of wind speed (σ_u), wind speed (u) and anemometer height (z) at Gingin and Collie (Beljaars, 1987):

$$\frac{\sigma_u}{u} = \frac{1}{\ln\left(\frac{z}{z_0}\right)}$$

An average roughness length of 0.23 m was thus determined for shrubland and 0.29 m for forest. The former calculated value falls between the roughness lengths given for Mediterranean shrubland in Hagemann (2002) and Peel et al., (2005), while the later calculated value is confirmed by Peel et al. (2005) for southwestern

³ United States Geological Service

Western Australian forests. Other roughness length values were sourced from Hagemann (2002) and Peel et al. (2005).

Average Bowen ratios were obtained from 30-minute average latent and sensible heat flux measurements for local shrub and forest land cover types (Siberstein, 2015; Beringer, 2018), and were calculated as follows:

$$\beta = \frac{Q_h}{Q_e}$$

Where Q_h and Q_e are sensible and latent heat fluxes, respectively.

Other biophysical parameters such as albedo and leaf area indices were also assigned to the various land-use types to reflect the specific nature of Australian vegetation. These values were sourced from Hagemann (2002) and Peel *et al* (2004).

The default CALMET geophysical parameters and the revised values based on local measurements and the literature, is summarised in Table 4-1.

Table 4-1: Default and revised roughness length (z_o), albedo (α) and Bowen ratio (β) used in CALMET

Land-use	Default USGS			Revised		
	Z_o	α	β	Z_o	α	β
Urban	1.0	0.18	1.5	0.23 ^d	0.18	1.5
Cropland	0.25	0.15	1.0	0.06 ^b	0.2 ^b	1.0
Grassland	0.05	0.25	1.0	0.04 ^c	0.2 ^{b, c}	1.0
Shrubland	0.05	0.25	1.0	0.23 ^a	0.15 ^c	1.3a
Forest	1.0	0.10	1.0	0.29 ^a	0.14 ^b	1.2a
Water	0.001	0.10	0.0	0.001	0.10	0.0
Barren	0.05	0.3	1.0	0.005 ^c	0.28 ^c	4.0

- a. Calculated
- b. From Peel et. Al., (2005)
- c. From Hagemann (2002)
- d. Yang et al. (2014)

CALMET was run in “no-obs” mode. This means that the meteorology was entirely driven by the gridded prognostic meteorological model (i.e. WRF) output. This approach allows a more spatially varying 3-dimensional meteorological field to be developed in CALMET than from a few isolated weather stations.

The model was run for a 159 x 158 grid domain at a spatial resolution of 250 m. Vertically, the model consists of 12 levels extending to 3,000 m, with seven levels below 300 m for better resolution of the atmosphere in the layers where pollution dispersion is most likely to occur. The southwest corner coordinates of the domain were 313.500 km Easting and 6671.750 km Northing (UTM Zone 50 S).

A discussion of selected CALMET results is provided in the Appendices.

4.2 CALPUFF

CALPUFF is the dispersion module of the CALMET/CALPUFF suite of models. It is a multi-layer, multi species, non-steady-state puff dispersion model that can simulate the effects of time-varying and space-varying meteorological conditions on pollutant transport, transformation and removal. The model contains algorithms for near-source effects such as building downwash, partial plume penetration, sub-grid scale interactions as well as longer range effects such as pollutant removal, chemical transformation, vertical wind shear and coastal interaction effects. The model employs dispersion equations based on a Gaussian distribution of pollutants across released puffs and considers the complex arrangement of emissions from point, area, volume and line sources (Scire et al., 2000). It is listed by the USEPA as an alternative regulatory dispersion model for assessing certain near-field applications involving complex meteorological conditions (US Federal Register, 2017), and is used extensively throughout Australia for regulatory assessments of industrial facilities.

The CALPUFF model was set to calculate concentrations on a set grid (gridded receptors). The model domain was defined as 39.75 km in the east-west and 39.5 km in the north-south direction at a spacing of 250 m x 250 m. Given the terrain of the region (Figure 4-1) this grid spacing is deemed appropriate to capture potential topographical impacts and dispersion characteristics. Emissions from the processing plant were modelled as point sources. Emissions resulting from mining and hauling The emission estimation process is outlined in Section 5.

4.3 Conversion of NO_x to NO₂

The atmospheric transformation of nitric oxide (NO) must be accounted for in the modelling, and in particular the estimation of NO₂ from modelled NO_x concentrations. The amount of NO₂ in the exhaust stream as it is released from combustion sources is typically in the order of 5-10% of total NO_x (expressed as NO₂ equivalents). However, following release, the NO₂ proportion of the emitted NO_x changes through complex photochemical reactions of atmospheric ozone (O₃) and NO_x.

There are several alternative approaches to account for the transformation of NO to NO₂ that occurs after the exhaust gases are discharged. For this assessment, the ambient ratio method (ARM) was used to calculate the concentration of NO₂. In this method an empirical NO_x /NO₂ relationship can be derived from monitoring data and used as an alternative to the ozone limiting method (OLM), which is not feasible for this location owing to a lack of ozone measurement data.

For this assessment the conversion determined in the assessment of the BHP Yarnima Power Station in Newman (ETA, 2019) was utilised, and is considered suitably representative. Hourly NO₂ and NO_x measurement data at the South Hedland monitoring station was filtered for wind directions blowing directly from the Port Hedland power station to the monitor. This served to exclude any other sources and allows a degree of confidence in NO_x to NO₂ conversion rates within a gas-fired power station plume. Figure 4-2 shows the NO_x to NO₂ ratio for the Port Hedland power station plume used in this study. As the relationship between NO_x to NO₂ is non-linear, especially for higher NO_x concentrations, a table of NO₂/NO_x ratios varying with NO_x concentration is formulated from the values in Figure 4-2 (Table 4-2). The tabulated ratios are then applied within the CALPOST postprocessor to determine NO₂ values from the range of modelled NO_x concentrations.

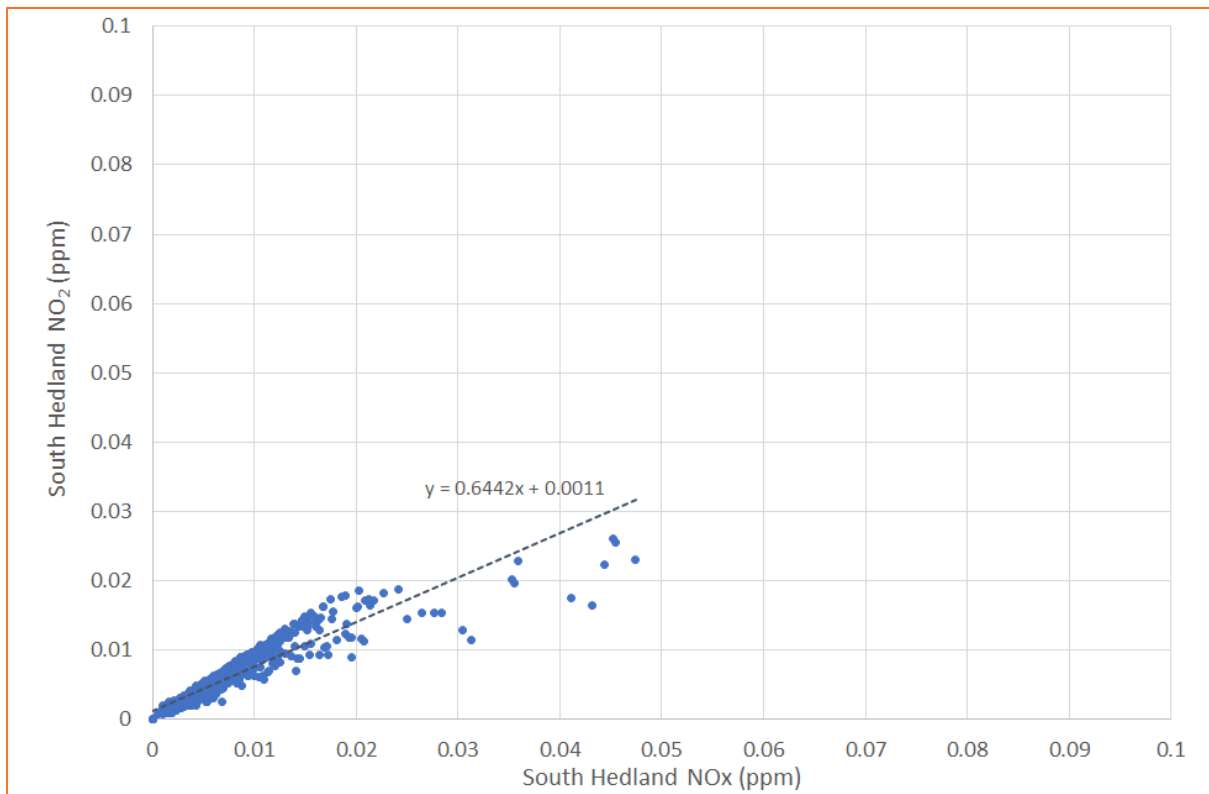


Figure 4-2: Scatterplot of measured NO_x and NO₂ at South Hedland within the power station plume (ETA, 2019)

Table 4-2: Ratio of NO₂ to NO_x ratio with varying NO_x concentration (ppb)

NO _x	0.73	1	1.2	1.9	3.9	7.3	12.3	16.8	22.1	27.7	32.5	35.9	44	50
NO ₂ :NO _x	1	1	0.93	0.93	0.91	0.89	0.86	0.82	0.74	0.71	0.61	0.51	0.5	0.44

5 Emissions to air estimation

This section outlines the emission estimation process for the Project. Emission estimates are sourced from this inventory for inclusion in the dispersion model. It includes the emissions from mine operations, facilities and associated infrastructure including the road network. Emissions from all key sources associated with the Project have been identified according to accepted methods. The emphasis of the emission estimation and modelling is on the potential impact from the operating phase of the Project. Emission estimation of construction activities is excluded from the assessment due to their intermittent nature over the life of the Project.

5.1 Emission Sources

The key emission sources for the operating phase of the Project are generally associated with:

- The Project:
 - Stack emissions from the roaster, calciners, boiler and ammonia scrubber.
- Cumulative (EMSR-2)
 - material handling from loading and unloading activities involving
 - loading trucks
 - unloading trucks
 - bulldozing
 - wheel-generated dust from haulage
 - wind erosion from stockpiles and open areas (inclusive of pits and waste rock landforms)

The locations of the identified emission sources are presented in Figure 5-1. Note that the project, at the time of this assessment, is within the initial design stage and the actual location of the stack sources may vary by up to 500m from what has been used in this assessment.

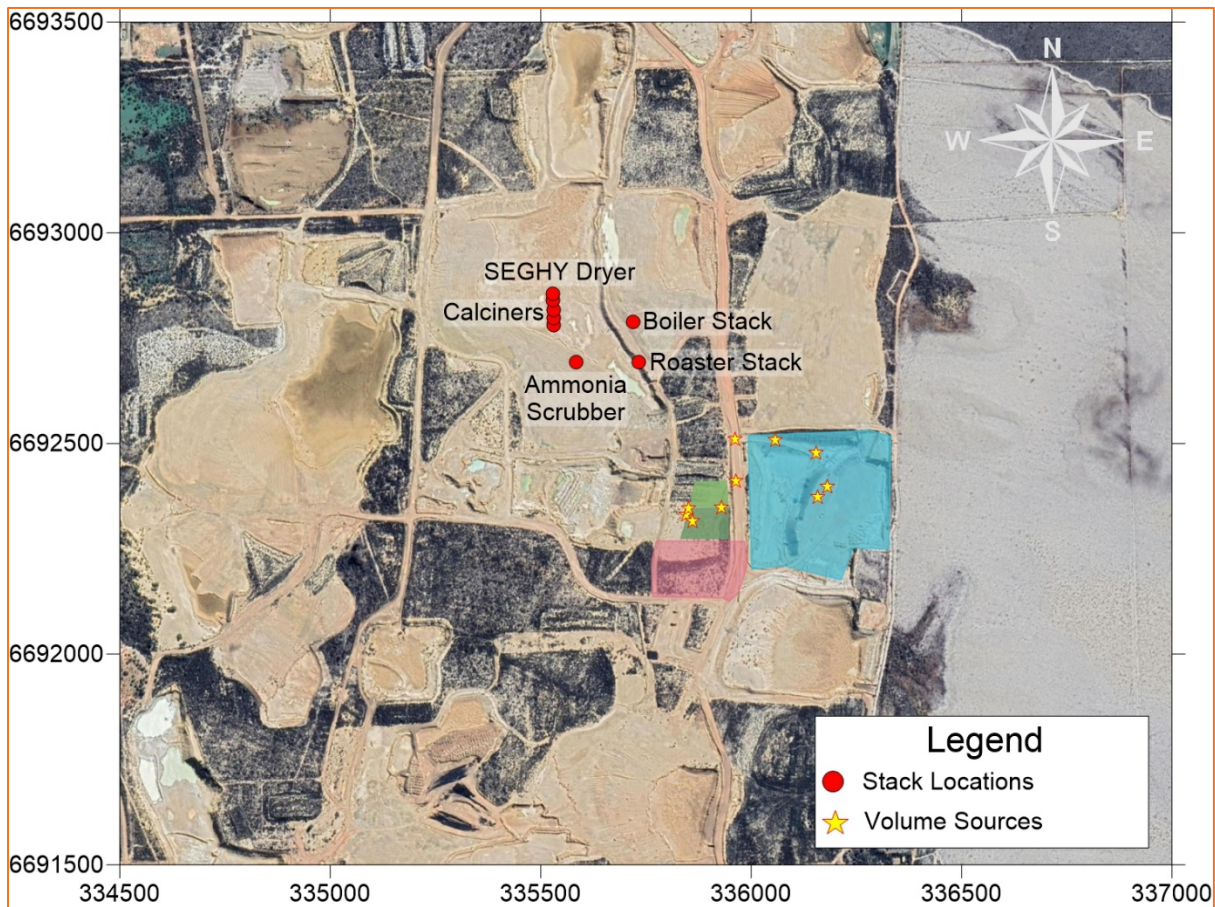


Figure 5-1: Location of emission sources (Project sources are represented as stack sources while cumulative sources are represented as volume sources)

5.2 Stack emissions

The principal emission sources associated with the operation of the Refinery have been identified by Iluka and comprise of various point sources (process stacks).

A summary of the characteristics of the Refinery emission sources used as input to the model is presented in Table 5-1. Each point source is defined in terms of physical characteristics (stack location, height above ground, and diameter), exhaust characteristics (exit velocity and temperature), and pollutant emission rate. The emission estimates were derived from information provided by Iluka, based upon the performance specifications for emission control equipment and other process design information including information verified by Vendors. These emission estimates are based on what can be described as a reliable conservative representation of emissions (i.e. a reasonable limit of expected emissions but not a gross over-estimate).

The relative contribution of the various sources to the total Refinery emissions under normal operations is shown in Figure 5-2.

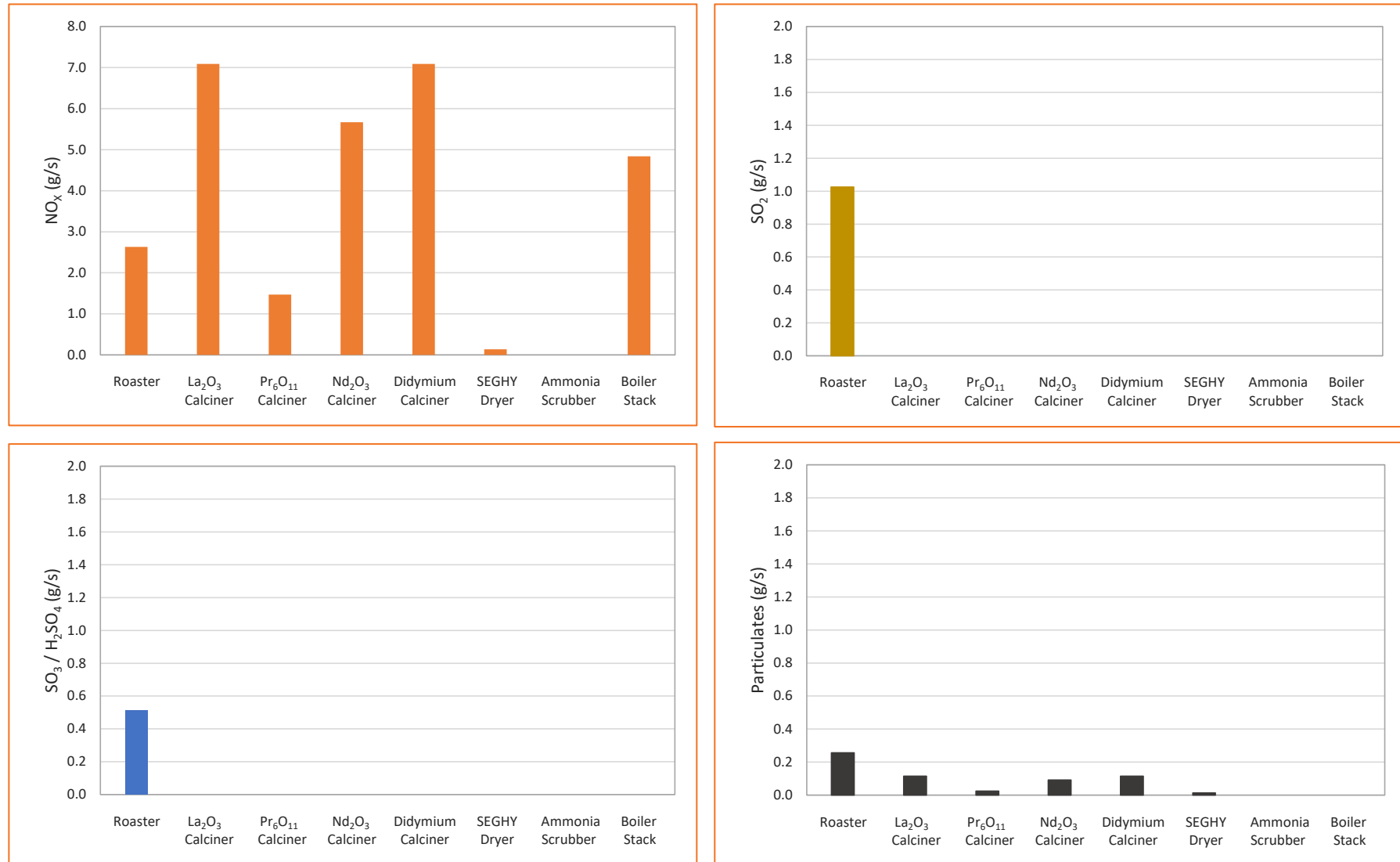


Figure 5-2: Source contributions – Phase 3

Table 5-1: Characteristics of emission sources – EMSR-3

Source Reference No.		1	2	3	4	5	6	7	8
Source Name		Roaster	La ₂ O ₃ Calciner	Pr ₆ O ₁₁ Calciner	Nd ₂ O ₃ Calciner	Didymium (NdPrOxide) Calciner	SEGHY Dryer	Ammonia Scrubber	Boiler Stack
Parameter	Units								
Location ⁴	mE	335,931	335,931	335,931	335,930	335,930	335,930	335,584	335,719
	mN	6,692,335	6,692,322	6,692,314	6,692,307	6,692,300	6,692,292	6,692,693	6,692,788
Stack Release Height	m (agl)	50	12	12	12	12	12	5	15
Stack Diameter	mm	750	1250	700	1250	1250	250	500	800
Temperature	°C	80	400	400	400	400	120	40	394
Volumetric Flow	Nm ³ /h	18,450	8,287	1,719	6,630	8,287	957	5,865	35,652
Exit Velocity	m/s	15	6.5	4.3	5.2	6.5	7.8	8.3	12
Emission Concentration									
NO _x (NO ₂ equivalent)	mg/Nm ³ (dry)	513	3078	3078	3078	3078	513	-	-
SO ₂		200	-	-	-	-	-	-	-
SO ₃		100	-	-	-	-	-	-	-
H ₂ SO ₄		100	-	-	-	-	-	-	-
Particulates		50	50	50	50	50	50	50	-
Emission Rate									
NO _x (NO ₂ equivalent)	g/s	2.63	7.09	1.47	5.67	7.09	0.14	-	4.84
SO ₂		1.02	-	-	-	-	-	-	-
SO ₃		0.51	-	-	-	-	-	-	-
H ₂ SO ₄		0.51	-	-	-	-	-	-	-

⁴ As outlined in Section 5.1 the actual locations of stacks may vary by up to 500m.

Source Reference No.		1	2	3	4	5	6	7	8
Particulates		0.26	0.12	0.02	0.09	0.12	0.01	-	-
Ammonia		-	-	-	-	-	-	0.08	-

5.3 Upset Conditions

5.3.1 Roaster emission control

There are two potential upset conditions that may impact the emissions from the roaster: cold start ups and shutdowns (planned or emergency). An outline of each of these conditions, and the planned engineering solutions are as follows:

- Cold start-ups will be undertaken initially without feed to the roaster. Once the system is stable and the offgas cleaning systems are fully operational, feeds will be brought online ensuring all systems remain in control during that process. As a result of this procedure the initial emissions will be lower than the normal operational state.
- During planned shutdowns the feed will be taken off the kiln and the system will be allowed to cool the until roaster emissions are low enough to guarantee no extraneous emissions through the stack without the offgas cleaning system. Once the roaster offgas has reduced to where there will be no risk of emission without gas cleaning will the offgas system be shut down. During planned shutdowns this process is expected to take several hours.
- Emergency shutdowns of all but equipment that feeds the offgas cleaning system will be the same as a normal shut down since no additional damage or emissions can occur by a crash shut down.

In the event of grid power failure emergency power will be supplied via an auxiliary generator. This auxiliary generator will only be used to allow controlled shutdown of the critical systems after which the generator will also be shut down.

5.3.2 Calciner / dryer emission control

For the calciners and dryers the primary emission control consists of ducting for particulate removal into baghouses. In the case failure of the calciner or dryer particulate removal system then the feed for that calciner or dryer will be shut down to reduce the potential of emission excursion. Within the baghouses there will be an online monitoring system, and in the event that leakages occur those baghouses will be shut down until the issue is rectified.

As for the roasters (Section 5.3.1), the extraction system will start ahead of feed introduction and will be the last to stop to ensure emissions are within the approved limits.

Given the planned cold start up and shutdown, including emergency, procedures outlined in this section there is no requirement to model upset conditions as part of this assessment.

5.4 Fugitive emissions

The fugitive emissions for this assessment are derived from the recovery of material from the monazite storage area and transportation to the facility. As outlined in Section 1.1 this process is a component of EMSR1 but has been included in the emission estimation / modelling process for a cumulative assessment.

5.4.1 Loading ore

Emissions for loading material at the monazite storage facility in the adjacent EMSR-2 plant have been calculated using the default value from Section 1.1.2 of Appendix A in the EETM for Mining (EA, 2012) for excavators and front end loaders on overburden of:

- PM₁₀: 0.012 kg/t.

These values were utilised as the alternative, which is the USEPA equation for batch loading, results in emission factors that are unrealistically low (EA, 2012). The emissions were determined by the total forecast annual tonnage of 113,000 tonnes and the assumption that loading operations occur for 12 hours each day.

The emission factor for PM_{2.5} emissions is taken as 28% of the PM₁₀ emissions. The statistics of the annual emissions for loading for PM₁₀ are contained in Appendix B.

5.4.2 Unloading ore

Emissions for unloading the monazite ore have been calculated using the default values from Section 1.1.6 of Appendix A in the EETM for Mining (EA, 2012) of:

- PM₁₀: 0.0043 kg/t.

The emissions were determined by the total tonnage of ore and the assumption that unloading operations occur for 12 hours each day.

The emission factor for PM_{2.5} emissions is taken as 30% of the PM₁₀ emissions as per the fraction of PM_{2.5} in PM₁₀ from the particle sizes in Table 5-1. The statistics of the annual emissions for loading for PM₁₀ are contained in Appendix B.

5.4.3 Bulldozing

Emissions for the operation of bulldozers within the monazite storage area have been determined using the equation outlined in Section 1.1.5 as outlined in Appendix A of the EET for Mining (EA, 2012). The silt and moisture contents used were the defaults listed in the manual (10% moisture, 2% silt).

The emission factor for PM_{2.5} emissions is taken as 30% of the PM₁₀ emissions as per the fraction of PM_{2.5} in PM₁₀ from the particle sizes in Table 5-1. The statistics of the annual PM₁₀ emissions for bulldozing are contained in Appendix B.

5.4.4 Front end loaders

Emissions for the operation of front end loaders (FEL), within the EMSR-1 and EMSR-2 facilities, used the default emission factor listed in Appendix A of the EET for Mining (EA, 2012) for overburden. These factors are:

- PM₁₀: 0.012 kg/tonne

The operation of FELs is assumed to be for 12 hours per day.

The emission factor for PM_{2.5} emissions is taken as 30% of the PM₁₀ emissions as per the fraction of PM_{2.5} in PM₁₀ from the particle sizes in Table 5-1. The statistics of the annual emissions for loading for PM₁₀ are contained in Appendix B.

5.4.5 Haul Roads

To determine emissions from wheel-generated dust along the haul roads the default equation for 'unpaved roads' from wheels from the EETM for Mining (EA, 2012) was utilised (Equation 2). For this assessment the following average weights were utilised:

- The weight of the haul trucks was taken as 56.3 tonnes – being the average of an empty and fully laden CAT772G haul truck and the default silt content of 10% was utilised.

Equation 1: $EF_{(kg/VKT)} = \frac{0.4536}{1.6093} \times k \times \left(\frac{s(\%)}{12}\right)^a \times \left(\frac{W(t)}{3}\right)^b$

Where: k = constant (TSP = 4.9, PM₁₀ = 1.5)
 $s(\%)$ = silt content (%)
 $W(t)$ = vehicle mass (t)
 a = constant (TSP = 0.7, PM₁₀ = 0.9)
 b = constant (0.45)

5.4.6 Wind erosion

The default emission factor for wind erosion in the EET for Mining (EA, 2012) is a constant emission of 0.2 kg/ha/hr which, while potentially suitable for the calculation of annual emissions, is not suitable for inclusion in atmospheric modelling. The primary reason for this is that it assumes a constant emission rate, regardless of the wind speed.

This assessment used the modified Shao equation outlined in SKM (2005) which allows for both a wind speed threshold (wind speed at which wind erosion commences) and an increase in emissions with increasing wind speed. The modified Shao equation is represented as Equation 3:

Equation 2: $PM_{10(g/m^2/s)} = k \times \left\{ WS^3 \times \left(1 - (WS_0^2/WS^2) \right) \right\}$ $WS > WS_0$
 $PM_{10(g/m^2/s)} = 0$ $WS < WS_0$

Where: WS = wind speed (m/s)
 WS_0 = threshold for particulate matter lift off (m/s)
 k is a constant

For this assessment the wind speed threshold (WS_0) was set at 5.5 m/s and the k constant was set at 2.45×10^{-7} . This results in an overall emission rate of 0.4 kg/ha/hr for PM₁₀ from open areas, which is higher than the emission rate of 0.2 kg/ha/hr specified in the EETM for Mining (EA, 2012), and ensures that the modelling is conservative. The emission factor for TSP is taken as twice that of the PM₁₀ emissions while PM_{2.5} emissions are taken as 30% of the PM₁₀ emissions (Table 5.1).

5.5 Emission summary - fugitive

A summary of the estimated annual emissions from the Project is shown in Table 5-2. As outlined in Section 5.3.1 the emission estimation was based on the forecast tonnage of 113,000 tonnes and the assumption that loading operations occur for 12 hours each day.

Table 5-2: Estimate of annual particulate emissions

Project Activity	PM ₁₀	PM _{2.5}
Loading	2,938	881
Unloading	1,053	316
Bulldozers	10,409	3,123
FEL	1,469	441
Haul Roads	3,822	1,147
Wind Erosion	7,894	2,368
TOTAL (kg/yr)	27,585	8,275

6 Predicted air quality impact

Comparison of the modelled results to the assessment criteria is intended to provide an objective evaluation of the potential impact of the operations at the nearest sensitive receptors. Modelled ground-level concentrations for key air pollutants have been compared to ambient air quality assessment criteria to determine the potential impacts.

As outlined in the description of the project, atmospheric emissions are generated during the various stages of processing the RE concentrate to recover the individual RE elements. The majority of atmospheric emissions, in relative terms, will be generated from the roasting and calcination processing stage, and hence will be subject to capture and treatment prior to discharge. The model scenarios consider the EMRS-3 during “Normal Operations” only⁵:

- Scenario 1 – Normal Operations for the Project only (in isolation of other sources).
- Scenario 2 – Cumulative (Project in conjunction with existing PM₁₀ and PM_{2.5} air quality).

6.1 Oxides of Nitrogen

The modelled results for NO₂, at the sensitive receptors discussed in Section 3.2.3 are presented statistically in Table 6-1.

- Receptor 1 has the highest predicted 1-hour average concentration of 43 µg/m³. This value is 29% of the criterion (referenced to ambient conditions (25 °C, 101.3 kPa).
- The predicted annual average and maximum 1-hour ground level concentrations at the remaining receptors are also well within the relevant assessment criteria for the EMSR-3 project in isolation of other emissions.

Table 6-1: Predicted 1-hour NO₂ concentrations at receptors (µg/m³) – Project only

Receptor	Maximum	2 nd Highest	99 th Percentile	90 th Percentile	70 th Percentile	Average
R1	43.4	37.2	12.8	0.1	0.0	0.4
R2	37.1	37.0	12.6	0.3	0.0	0.4
R3	36.8	35.1	19.0	1.1	0.0	0.7
R4	37.4	37.4	21.4	1.2	0.0	0.8
R5	37.3	36.0	18.6	1.1	0.0	0.7
R6	25.6	25.3	11.3	0.6	0.0	0.5
R7	19.0	17.6	8.2	0.5	0.0	0.3
R8	18.3	16.2	5.4	0.2	0.0	0.2
R9	17.5	15.1	5.4	0.2	0.0	0.2

⁵ Abnormal or upset operating conditions for EMRS-3 (ie. start-up and shutdown, control equipment failure) have not been modelled to date. These upset operating conditions have been determined to result in emissions that are lower than normal operating conditions (Section 5.3).

Receptor	Maximum	2 nd Highest	99 th Percentile	90 th Percentile	70 th Percentile	Average
R10	14.1	13.8	1.8	0.0	0.0	0.1
R11	37.4	37.4	6.3	0.0	0.0	0.2

Assessment criteria: 164 $\mu\text{g}/\text{m}^3$ referenced to STP (0 °C, 101.3 kPa), and 150 $\mu\text{g}/\text{m}^3$ referenced to ambient conditions (25 °C, 101.3 kPa).

The predicted isopleths (contours) for ground level concentrations of NO₂ indicate that:

- Maximum predicted 1-hour concentrations indicates an area of exceedance of the assessment criterion (150 $\mu\text{g}/\text{m}^3$) over the facility (Figure 6-1), noting that there are no sensitive receptors in this area.
- Annual average concentrations across the modelled domain are predicted to be lower than the assessment criteria for the EMSR-3 project in isolation of other emissions (Figure 6-2).

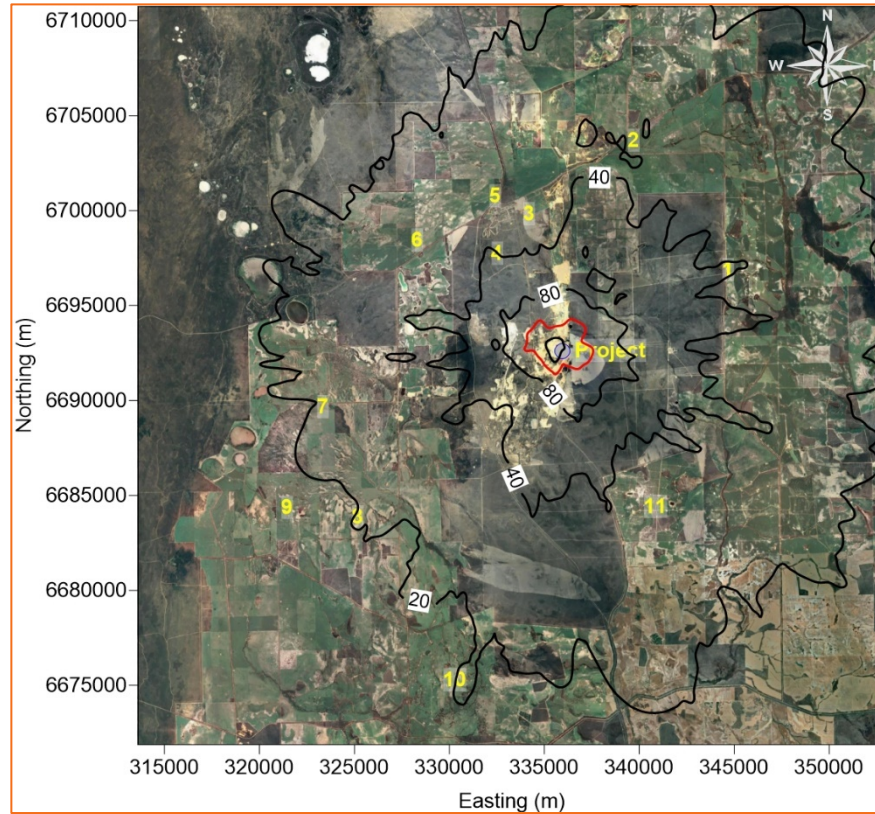


Figure 6-1: Predicted maximum 1-hour NO₂ concentrations (µg/m³)

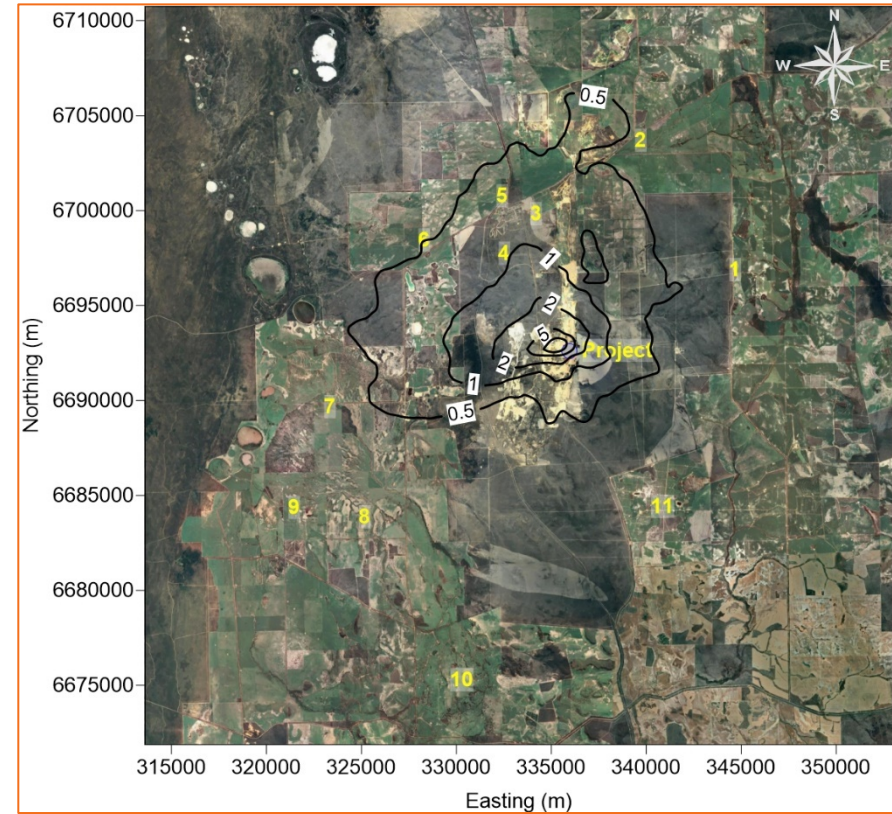


Figure 6-2: Predicted annual NO₂ concentrations (µg/m³)

6.2 Sulfur dioxide

The modelled results for SO₂ at the sensitive receptors are presented statistically in Table 6-2 and Table 6-3. The tables show that:

- The highest predicted 1-hour ground level concentration of 3 µg/m³ occurs at Receptor 1.
- The highest predicted 24-hour ground level concentration of 0.4 µg/m³ occurs at Receptors 2 and 4.
- Predicted concentrations at all receptors are well within the assessment criteria.

Table 6-2: Predicted 1-hour SO₂ concentrations at receptors (µg/m³) – Project only

Receptor	Maximum	2 nd Highest	99 th Percentile	90 th Percentile	70 th Percentile	Average
R1	3.0	2.0	0.3	0.0	0.0	0.01
R2	2.2	2.0	0.5	0.0	0.0	0.02
R3	1.5	1.4	0.7	0.0	0.0	0.02
R4	1.6	1.6	0.8	0.0	0.0	0.03
R5	1.5	1.4	0.7	0.0	0.0	0.02
R6	1.0	0.9	0.4	0.0	0.0	0.01
R7	0.7	0.6	0.3	0.0	0.0	0.01
R8	0.7	0.6	0.2	0.0	0.0	0.01
R9	0.7	0.6	0.2	0.0	0.0	0.01
R10	0.7	0.5	0.0	0.0	0.0	0.00
R11	1.9	1.6	0.2	0.0	0.0	0.01

Assessment criteria: 286 µg/m³ referenced to STP (0 °C, 101.3 kPa), and 262 µg/m³ referenced to ambient conditions (25 °C, 101.3 kPa).

Table 6-3: Predicted 24-hour SO₂ concentrations at receptors (µg/m³) – Project only

Receptor	Maximum	2 nd Highest	99 th Percentile	90 th Percentile	70 th Percentile	Average
R1	0.2	0.2	0.1	0.0	0.0	0.01
R2	0.4	0.2	0.2	0.1	0.0	0.02
R3	0.2	0.2	0.2	0.1	0.0	0.02
R4	0.4	0.2	0.2	0.1	0.0	0.03
R5	0.2	0.2	0.2	0.1	0.0	0.02
R6	0.2	0.1	0.1	0.0	0.0	0.01
R7	0.1	0.1	0.1	0.0	0.0	0.01
R8	0.1	0.1	0.1	0.0	0.0	0.01
R9	0.1	0.1	0.1	0.0	0.0	0.01
R10	0.1	0.1	0.0	0.0	0.0	0.00
R11	0.2	0.2	0.1	0.0	0.0	0.01

Assessment criteria: 57 µg/m³ referenced to STP (0 °C, 101.3 kPa), and 52 µg/m³ referenced to ambient conditions (25 °C, 101.3 kPa).

The predicted isopleths (contours) for ground level concentrations of SO₂ indicate that:

- Highest predicted 1-hour SO₂ concentrations of 20 µg/m³ occur over the Iluka project site and is well below the relevant assessment criterion of 262 µg/m³ (Figure 6-3).
- Maximum predicted 24-hour concentration of 2 µg/m³, occurring within the boundary of the EMSR-3 project is approximately 4% of the assessment criterion of 52 µg/m³ (Figure 6-4).

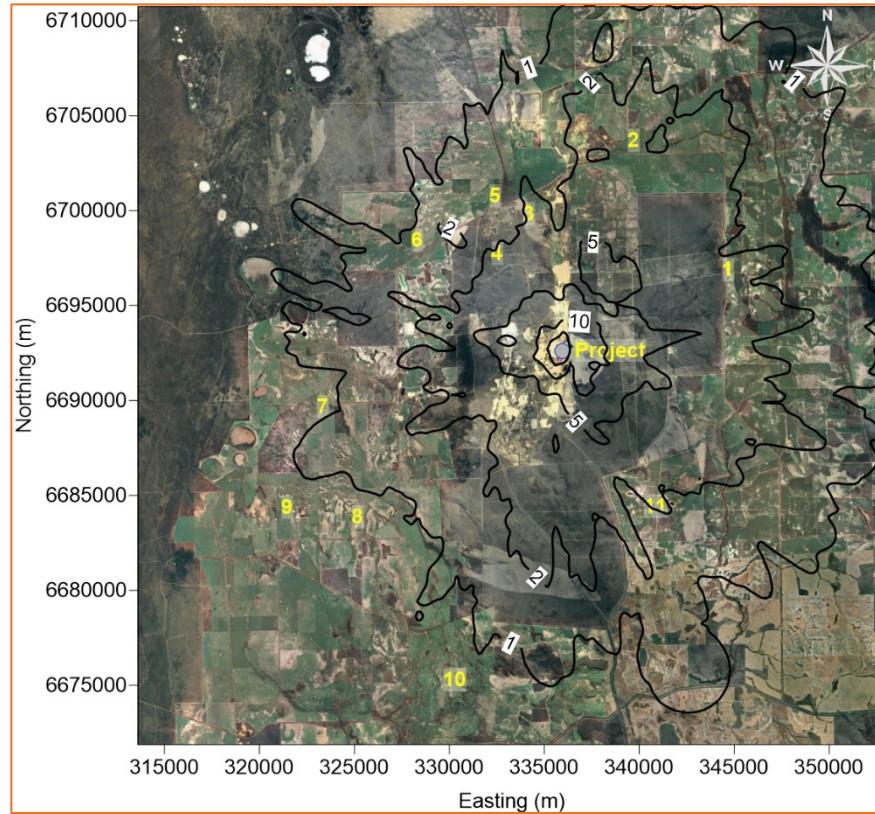


Figure 6-3: Predicted maximum 1-hour SO₂ concentrations (µg/m³)

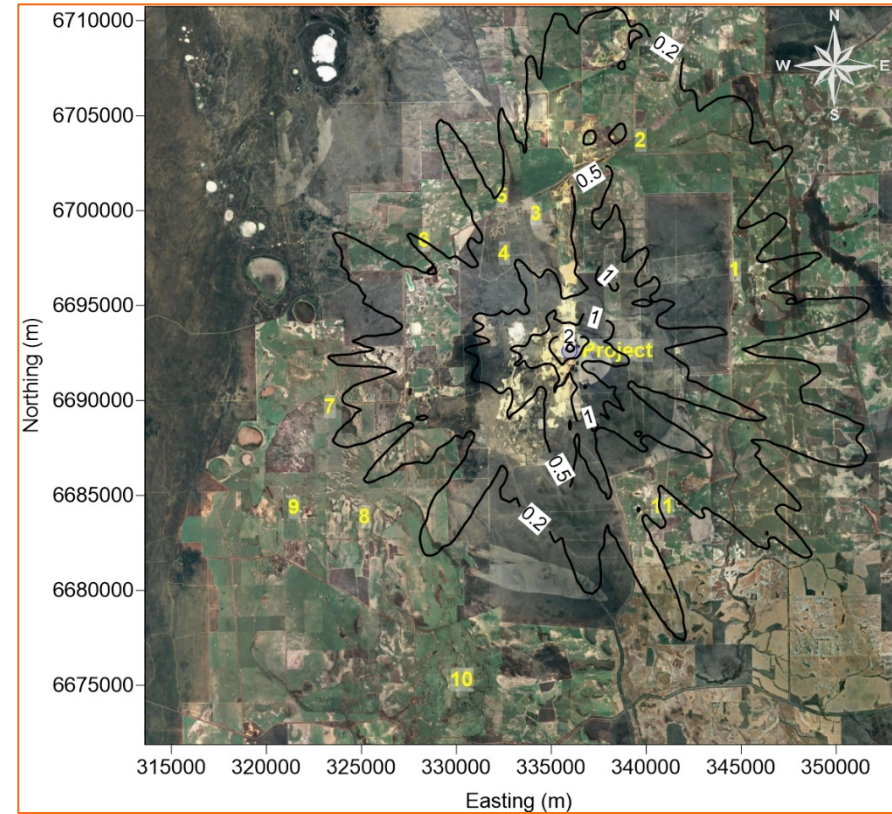


Figure 6-4: Predicted maximum 24-hour SO₂ concentrations (µg/m³)

6.3 Sulfur trioxide / Sulfuric acid

The modelled results for SO₃/H₂SO₄ at the sensitive receptors are presented statistically in Table 6-4 and Table 6-5. The results at the selected receptors indicate that:

- The highest predicted 1-hour concentration of 1.2 µg/m³ occurring at Receptor 1 is approximately 7% of the assessment criterion of 18 µg/m³.
- The highest predicted 24-hour concentration of 0.19 µg/m³ (at Receptor 4) is approximately 4% of the assessment criteria of 5 µg/m³.
- All other predicted sensitive receptor concentrations are well below the relevant criteria.

Table 6-4: Predicted 1-hour SO₃ / H₂SO₄ concentrations at receptors (µg/m³) – Project only

Receptor	Maximum	2 nd Highest	99 th Percentile	90 th Percentile	70 th Percentile	Average
R1	1.2	1.2	0.1	0.0	0.0	0.01
R2	1.3	1.3	0.3	0.0	0.0	0.01
R3	0.9	0.8	0.4	0.0	0.0	0.01
R4	0.9	0.9	0.5	0.0	0.0	0.01
R5	1.0	0.9	0.4	0.0	0.0	0.01
R6	0.5	0.5	0.2	0.0	0.0	0.01
R7	0.4	0.4	0.2	0.0	0.0	0.01
R8	0.4	0.3	0.1	0.0	0.0	0.00
R9	0.4	0.3	0.1	0.0	0.0	0.00
R10	0.3	0.3	0.0	0.0	0.0	0.00
R11	0.9	0.7	0.1	0.0	0.0	0.00

Assessment criteria: 20 µg/m³ referenced to STP (0 °C, 101.3 kPa), and 18 µg/m³ referenced to ambient conditions (25 °C, 101.3 kPa).

Table 6-5: Predicted 24-hour SO₃ / H₂SO₄ concentrations at receptors (µg/m³) – Project only

Receptor	Maximum	2 nd Highest	99 th Percentile	90 th Percentile	70 th Percentile	Average
R1	0.12	0.11	0.08	0.02	0.00	0.01
R2	0.21	0.14	0.11	0.03	0.00	0.01
R3	0.13	0.12	0.11	0.05	0.01	0.01
R4	0.19	0.11	0.09	0.05	0.01	0.01
R5	0.13	0.11	0.10	0.04	0.01	0.01
R6	0.09	0.07	0.07	0.02	0.01	0.01
R7	0.08	0.07	0.05	0.02	0.00	0.01

Receptor	Maximum	2 nd Highest	99th Percentile	90th Percentile	70th Percentile	Average
R8	0.06	0.06	0.04	0.01	0.00	0.00
R9	0.06	0.04	0.03	0.01	0.00	0.00
R10	0.04	0.03	0.02	0.00	0.00	0.00
R11	0.09	0.09	0.07	0.01	0.00	0.00

Assessment criteria: 7 $\mu\text{g}/\text{m}^3$ referenced to STP (0 °C, 101.3 kPa), and 5 $\mu\text{g}/\text{m}^3$ referenced to ambient conditions (25 °C, 101.3 kPa).

The predicted isopleths (contours) for ground level concentrations of $\text{SO}_3/\text{H}_2\text{SO}_4$ across the modelled domain indicate that:

- The assessment (1-hour) criterion is not achieved in the vicinity of the Project stacks (Figure 6-5), noting that this is not considered a sensitive receptor location.
- The highest predicted 24-hour concentrations of 1 $\mu\text{g}/\text{m}^3$, are found immediately over the operations, and is 20% of the assessment criteria relevant (7 $\mu\text{g}/\text{m}^3$) to off-site sensitive receptors (Figure 6-6).

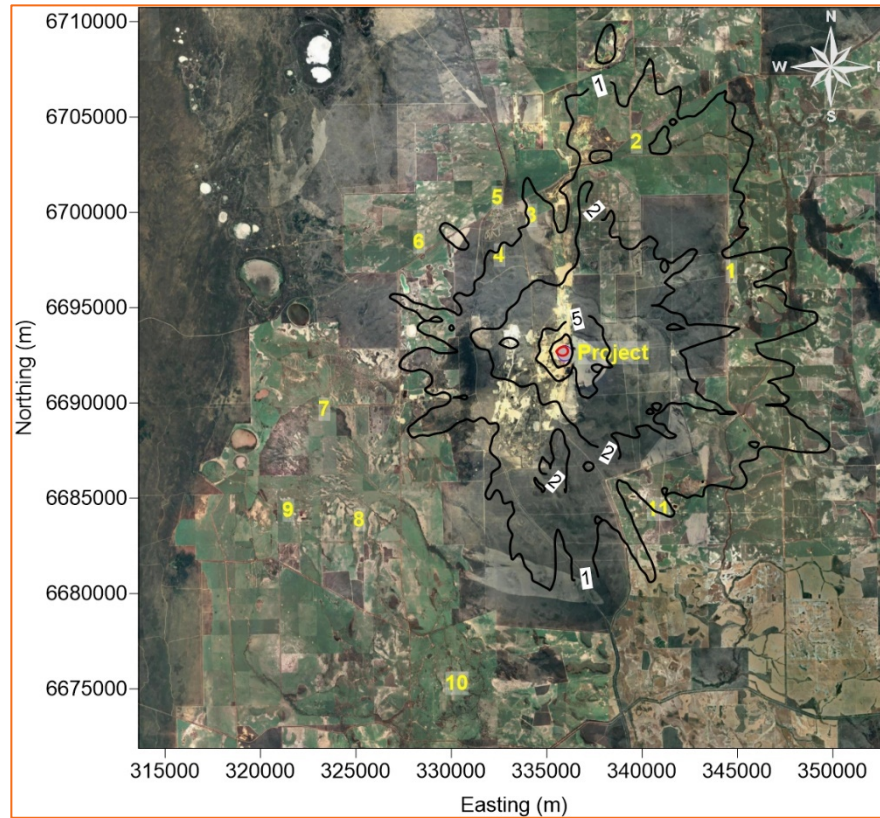


Figure 6-5: Predicted maximum 1-hour SO₃/H₂SO₄ concentrations (µg/m³)

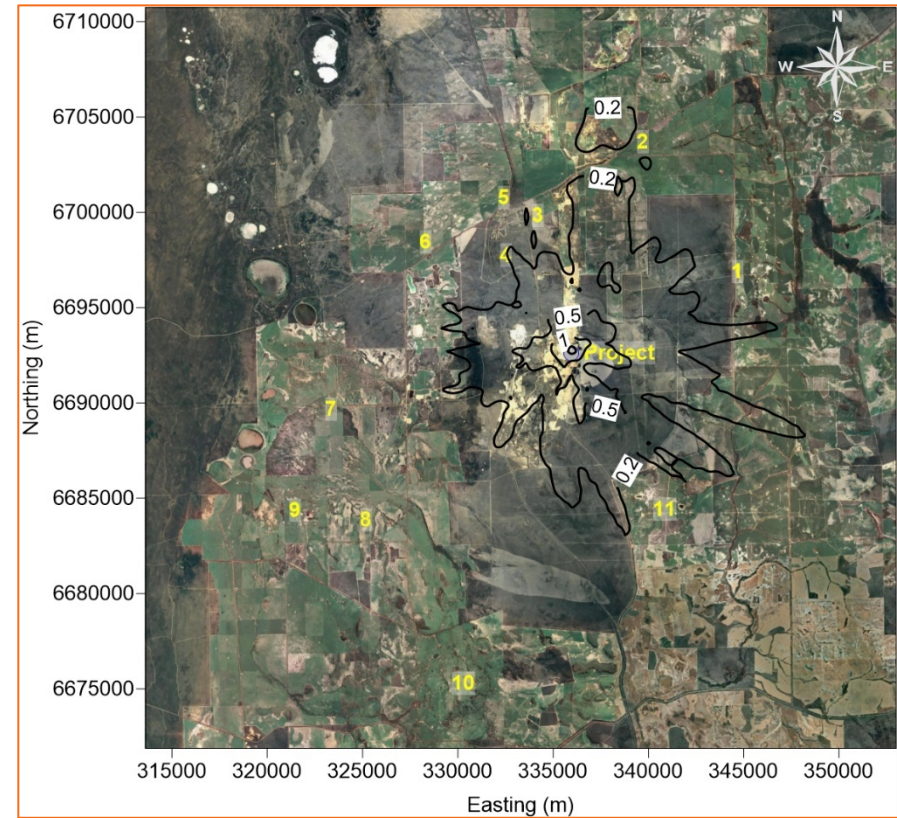


Figure 6-6: Predicted maximum 24-hour SO₃/H₂SO₄ concentrations (µg/m³)

6.4 Particulates

The modelled results for PM_{10} are presented at the sensitive receptors, for the Project in isolation and cumulatively, in Table 6-6 while the predicted concentrations, at the sensitive receptors, for $PM_{2.5}$ are presented in Table 6-7. The background concentrations are outlined in Section 3.2.2.

The results at the selected receptors indicate that:

- The predicted 24-hour concentration of both PM_{10} and $PM_{2.5}$ are within the relevant assessment criteria at all receptors with the Project in isolation and cumulatively.
- Predicted annual average concentrations are also within the relevant assessment criteria.

The predicted isopleths (contours) for ground level concentrations of particulates are presented as follows:

- The predicted annual average PM_{10} concentrations are presented in Figure 6-7 for the Project in isolation and in Figure 6-8 for the cumulative prediction.
- The predicted maximum 24-hour PM_{10} concentrations are presented in Figure 6-9 for the Project in isolation and in Figure 6-10 for the cumulative prediction.
- The predicted annual average $PM_{2.5}$ concentrations are presented in Figure 6-11 for the Project in isolation and in Figure 6-12 for the cumulative prediction.
- The predicted maximum 24-hour $PM_{2.5}$ concentrations are presented in Figure 6-13 for the Project in isolation and in Figure 6-14 for the cumulative prediction.

The figures show that:

- The highest 24-hour PM_{10} concentration across the modelled domain occurs in a small area within the Project boundary. While this result is higher than the assessment criteria, this location is not considered a sensitive receptor location.
- The modelled 24-hour $PM_{2.5}$ concentration is lower than the assessment criteria across the model domain.
- Annual average PM_{10} and $PM_{2.5}$ concentrations are well within the relevant criteria outside of the Project area.

Table 6-6: Predicted 24-hour PM₁₀ concentrations at receptors (µg/m³)

Receptor	Project only						Cumulative					
	Maximum	6 th Highest	99 th Percentile	90 th Percentile	70 th Percentile	Average	Maximum	6 th Highest	99 th Percentile	90 th Percentile	70 th Percentile	Average
R1	0.2	0.1	0.1	0.0	0.0	0.01	17.0	17.0	16.9	16.9	16.9	14.4
R2	0.2	0.1	0.1	0.0	0.0	0.01	17.0	17.0	16.9	16.9	16.9	14.4
R3	0.3	0.2	0.2	0.1	0.0	0.03	17.1	17.1	17.0	17.0	16.9	14.5
R4	0.4	0.3	0.3	0.1	0.0	0.04	17.2	17.1	17.1	17.1	17.0	14.5
R5	0.3	0.2	0.2	0.1	0.0	0.03	17.1	17.1	17.0	17.0	16.9	14.5
R6	0.2	0.1	0.1	0.1	0.0	0.02	17.0	17.0	16.9	16.9	16.9	14.5
R7	0.2	0.1	0.1	0.1	0.0	0.02	17.0	17.0	16.9	16.9	16.9	14.5
R8	0.1	0.1	0.1	0.0	0.0	0.01	16.9	16.9	16.9	16.9	16.9	14.4
R9	0.1	0.1	0.1	0.0	0.0	0.01	16.9	16.9	16.9	16.9	16.9	14.4
R10	0.1	0.0	0.0	0.0	0.0	0.00	16.9	16.9	16.8	16.8	16.8	14.4
R11	0.2	0.1	0.1	0.0	0.0	0.01	17.0	17.0	16.9	16.9	16.8	14.4

Assessment criteria: 24-hour average of 50 µg/m³ referenced to STP (0 °C, 101.3 kPa), and 46 µg/m³ referenced to ambient conditions (25 °C, 101.3 kPa); annual average of 25 µg/m³ referenced to STP (0 °C, 101.3 kPa), and 23 µg/m³ referenced to ambient conditions (25 °C, 101.3 kPa);

Table 6-7: Predicted 24-hour PM_{2.5} concentrations at receptors (µg/m³)

Receptor	Project only						Cumulative					
	Maximum	6 th Highest	99 th Percentile	90 th Percentile	70 th Percentile	Average	Maximum	6 th Highest	99 th Percentile	90 th Percentile	70 th Percentile	Average
R1	0.05	0.03	0.04	0.01	0.00	0.00	5.1	5.0	5.0	5.0	5.0	4.3
R2	0.07	0.04	0.04	0.01	0.00	0.00	5.1	5.1	5.0	5.0	5.0	4.3
R3	0.09	0.06	0.07	0.03	0.01	0.01	5.1	5.1	5.1	5.1	5.0	4.3
R4	0.11	0.08	0.08	0.03	0.01	0.01	5.1	5.1	5.1	5.1	5.1	4.3
R5	0.09	0.07	0.07	0.03	0.01	0.01	5.1	5.1	5.1	5.1	5.0	4.3
R6	0.06	0.04	0.04	0.02	0.01	0.01	5.1	5.1	5.0	5.0	5.0	4.3
R7	0.05	0.04	0.04	0.02	0.00	0.01	5.1	5.1	5.0	5.0	5.0	4.3
R8	0.04	0.02	0.03	0.01	0.00	0.00	5.0	5.0	5.0	5.0	5.0	4.3
R9	0.03	0.03	0.03	0.01	0.00	0.00	5.0	5.0	5.0	5.0	5.0	4.3
R10	0.02	0.01	0.01	0.00	0.00	0.00	5.0	5.0	5.0	5.0	5.0	4.3
R11	0.05	0.03	0.03	0.01	0.00	0.00	5.0	5.0	5.0	5.0	5.0	4.3

Assessment criteria: 24-hour average of 50 µg/m³ referenced to STP (0 °C, 101.3 kPa), and 46 µg/m³ referenced to ambient conditions (25 °C, 101.3 kPa); annual average of 25 µg/m³ referenced to STP (0 °C, 101.3 kPa), and 23 µg/m³ referenced to ambient conditions (25 °C, 101.3 kPa);

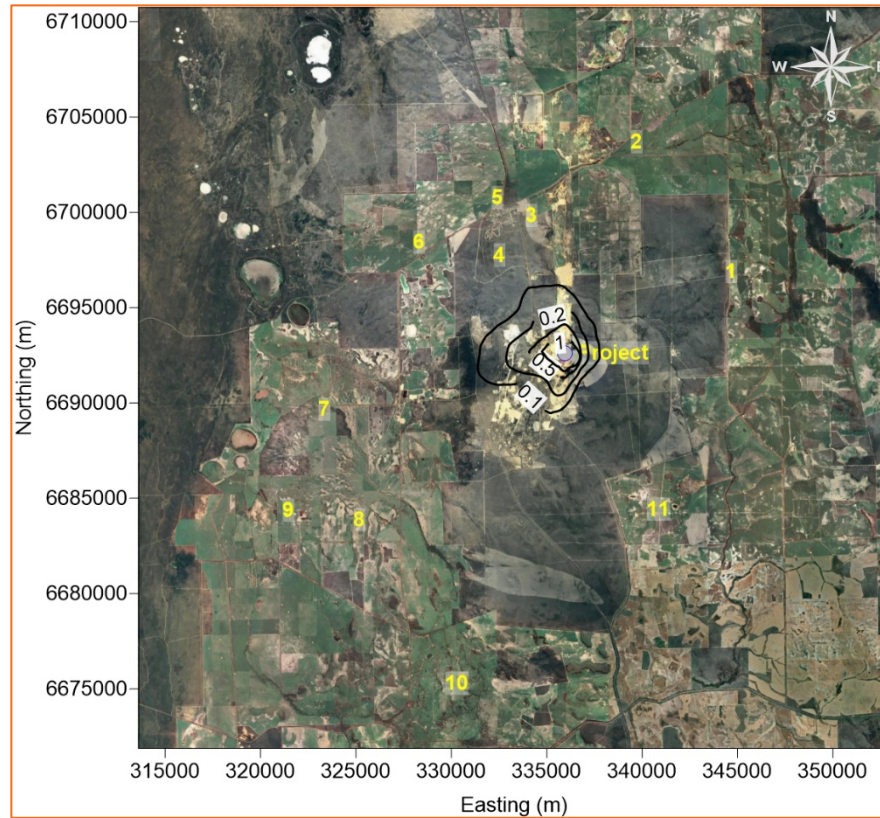


Figure 6-7: Predicted annual average PM₁₀ concentrations (µg/m³) – Project only

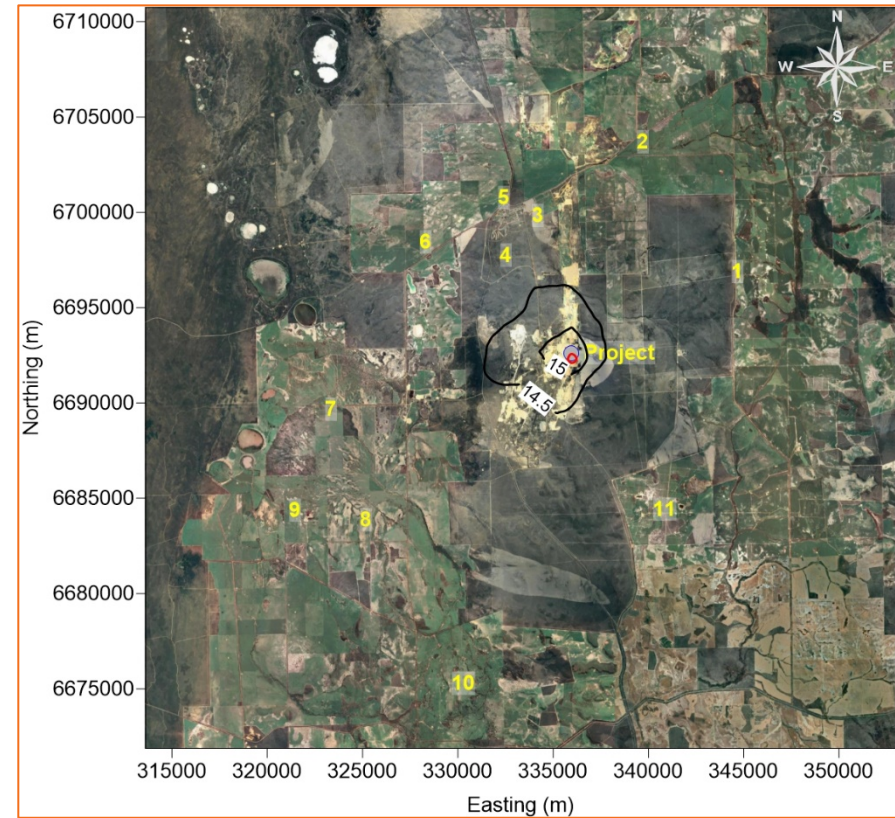


Figure 6-8: Predicted annual average PM₁₀ concentrations (µg/m³) – cumulative

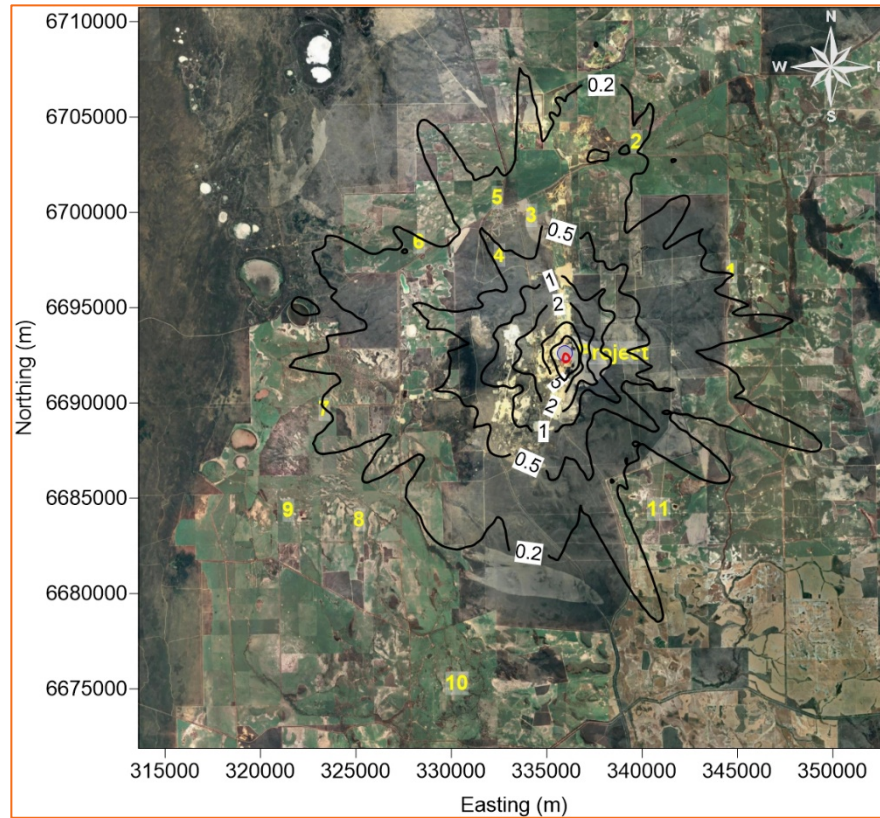


Figure 6-9: Predicted maximum 24-hour PM₁₀ concentrations (µg/m³) – Project only

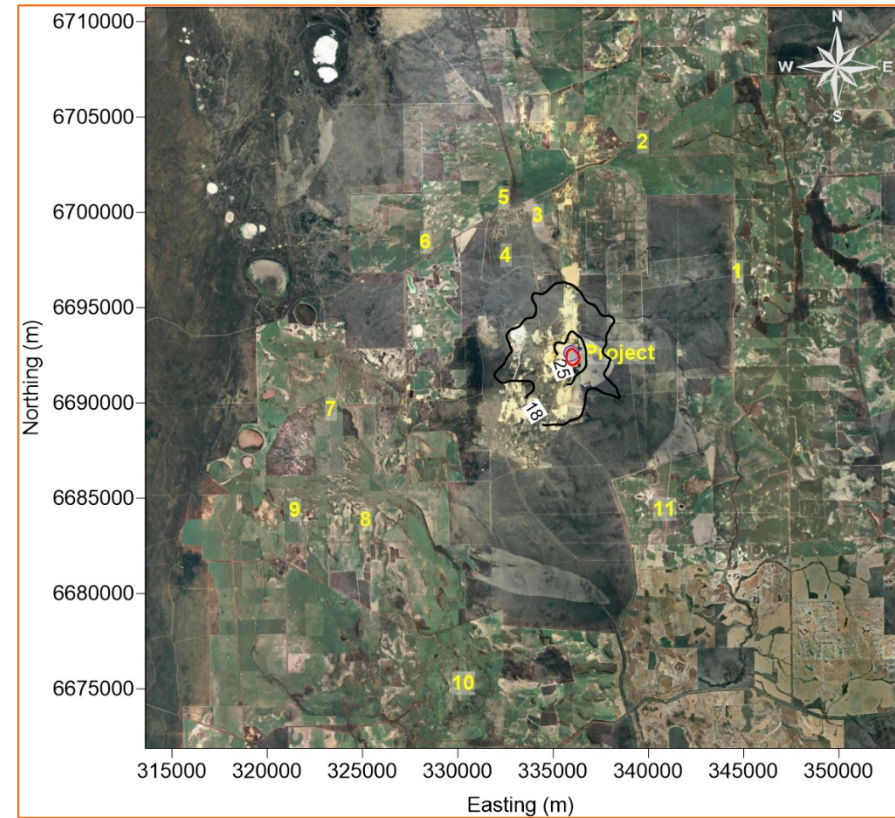


Figure 6-10: Predicted maximum 24-hour concentrations (µg/m³) – cumulative

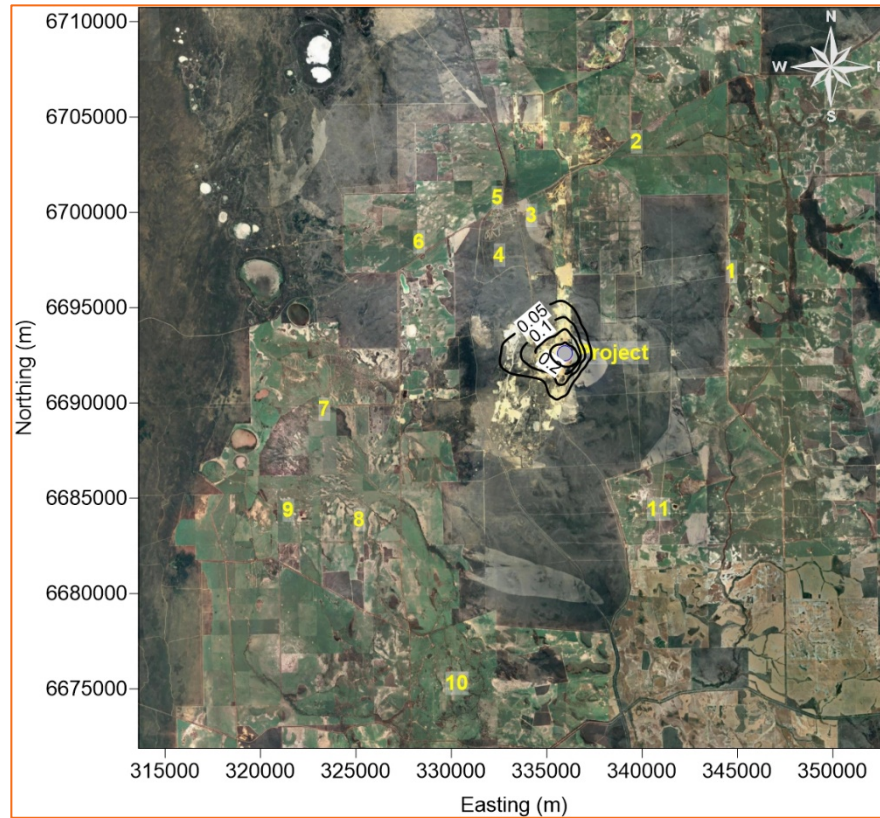


Figure 6-11: Predicted annual average PM_{2.5} concentrations (µg/m³) – Project only

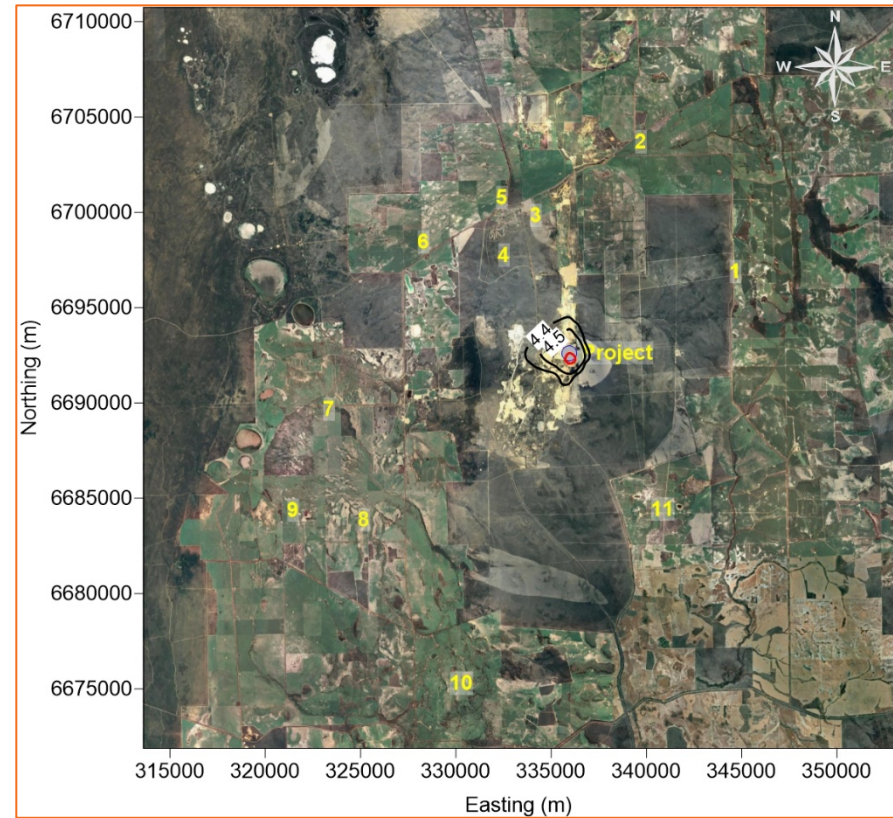


Figure 6-12: Predicted annual average PM_{2.5} concentrations (µg/m³) – cumulative

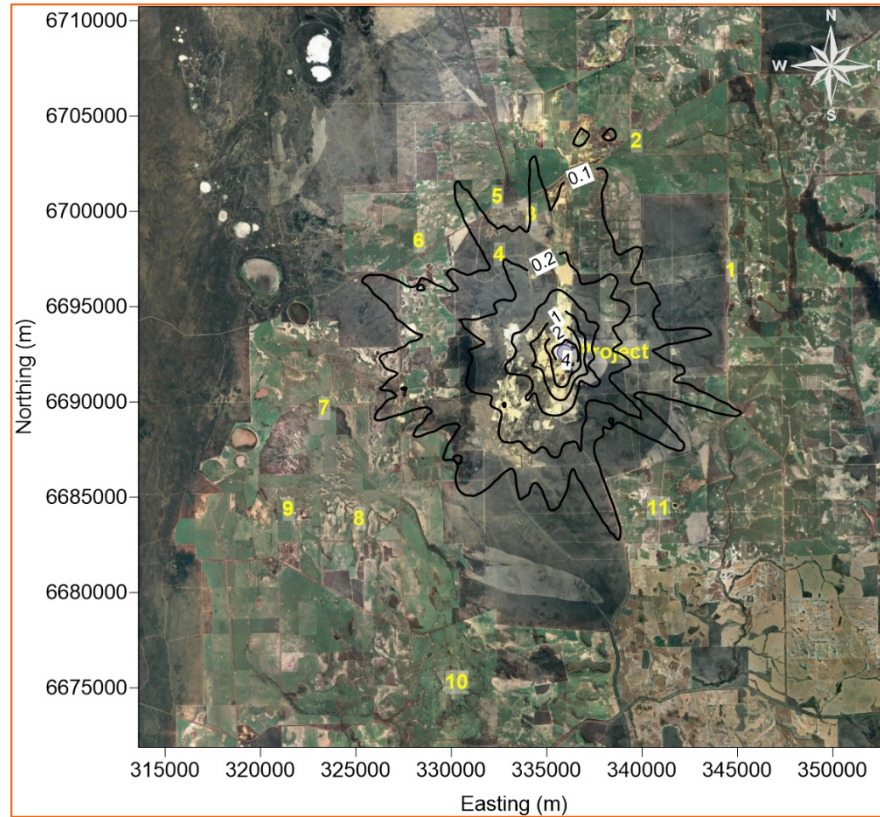


Figure 6-13: Predicted maximum 24-hour PM_{2.5} concentrations ($\mu\text{g}/\text{m}^3$) – Project only

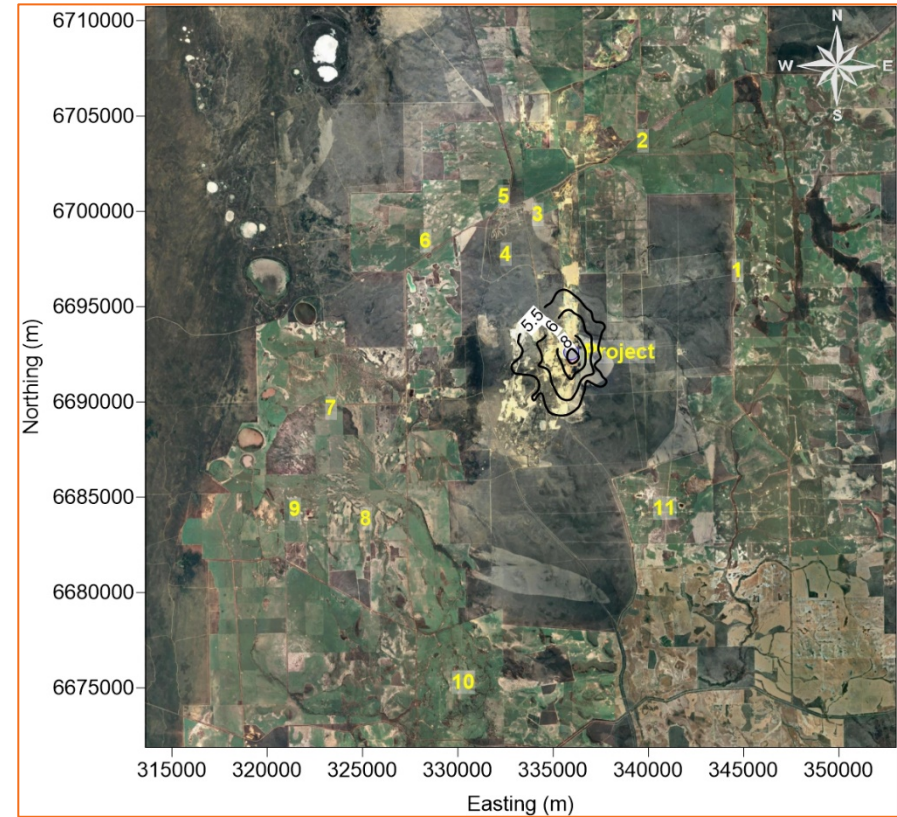


Figure 6-14: Predicted maximum 24-hour PM_{2.5} concentrations ($\mu\text{g}/\text{m}^3$) – cumulative

6.5 Ammonia

The modelled results for NH₃ at the sensitive receptors are presented statistically in Table 6-8. The results at the selected receptors indicate that:

- The highest predicted 1-hour concentration of 0.3 µg/m³ occurring at Receptor 1 is less than 0.1% of the assessment criterion of 330 µg/m³.

Table 6-8: Predicted 1-hour NH₃ concentrations at receptors (µg/m³) – Project only

Receptor	Maximum	2 nd Highest	99 th Percentile	90 th Percentile	70 th Percentile	Average
R1	0.2	0.1	0.0	0.0	0.0	0.0
R2	0.1	0.1	0.0	0.0	0.0	0.0
R3	0.2	0.2	0.1	0.0	0.0	0.0
R4	0.3	0.3	0.1	0.0	0.0	0.0
R5	0.3	0.2	0.1	0.0	0.0	0.0
R6	0.1	0.1	0.0	0.0	0.0	0.0
R7	0.1	0.1	0.0	0.0	0.0	0.0
R8	0.1	0.1	0.0	0.0	0.0	0.0
R9	0.1	0.1	0.0	0.0	0.0	0.0
R10	0.1	0.0	0.0	0.0	0.0	0.0
R11	0.1	0.1	0.0	0.0	0.0	0.0

Assessment criterion: 330 µg/m³ referenced to ambient conditions (25 °C, 101.3 kPa).

The predicted isopleths (contours) for ground level concentrations of NH₃ across the modelled domain indicate that:

- The impacts are well within the assessment (1-hour) criterion even in the immediate vicinity of the ammonia scrubber stack (Figure 6-15).

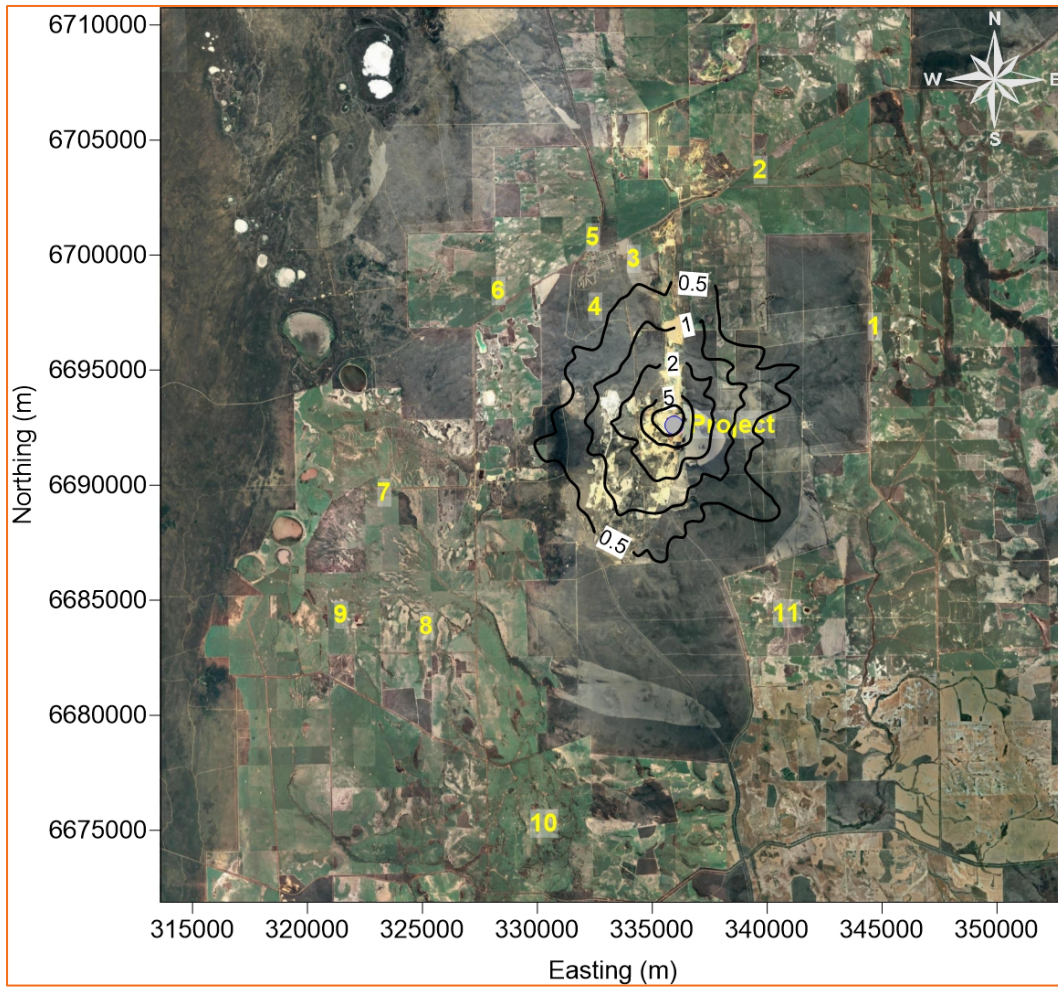


Figure 6-15: Predicted maximum 1-hour NH₃ concentrations (µg/m³) – Project only

7 Conclusions

An air quality assessment has been conducted to determine potential impacts associated with the operation of the Project, in support of the environmental approval.

The scope of the modelling assessment is summarised below.

Modelled meteorological period	1 January to 31 December 2015
Model selection	WRF/CALMET/CALPUFF model suite
Key Pollutants	<ul style="list-style-type: none"> particulate matter (PM) – including PM₁₀ and PM_{2.5} size fractions, and dust deposition nitrogen dioxide (NO₂) sulphur dioxide (SO₂) acid gas as sulphur trioxide / sulphuric acid (SO₃ / H₂SO₄) ammonia (NH₃) <p>This assessment precludes the consideration of radiological components.</p>
Meteorological data	Three-dimensional prognostic meteorological data developed using the Weather Research and Forecasting (WRF) model.
Background Air Quality	<p>Published air quality monitoring data for the region has been reviewed and used as a suitable proxy of existing (baseline) concentrations for key pollutants.</p> <p>There are no other significant industry sources in the in close proximity, therefore the assessment of the incremental cumulative contribution only accounts for background air quality where monitoring data was available.</p>
Project Emissions	<p>Emissions from the EMRS-3 under maximum processing and material handling assumptions formed the basis of the modelling assessment for operational configuration.</p> <p>Abnormal or upset operating conditions for EMRS-3 (ie. start-up and shutdown, control equipment failure) have not been modelled to date, as project designs are preliminary. These will need to be defined and modelled in future.</p>
Sensitive Receptors	<p>Discrete receptor locations were nominated to represent:</p> <ul style="list-style-type: none"> non-project related sensitive receptors – Township of Eneabba closest non-project related sensitive receptors – residents outside the Township of Eneabba other receptors – Eneabba Golf Course
Model Scenarios	<p>The model scenarios that have been included in the assessment consider the Project:</p> <ul style="list-style-type: none"> Scenario 1 – Normal Operations for the Project only (in isolation of other sources) Scenario 2 – Cumulative (Project in conjunction with existing air quality (if available))

7.1 Key findings

The model results for normal operations of the Project at the currently advised design capacity are summarised below for the key pollutants of concern.

Nitrogen Dioxide

- There are no predicted exceedances of the assessment criteria at the sensitive receptors.
- An exceedance of the 1-hour assessment criterion is restricted to occurring immediately over the project site.

Sulphur Dioxide

- Predicted concentrations at all sensitive receptor locations are well within the assessment criteria.
- Highest predicted 1-hour SO₂ concentrations of 20 µg/m³ occur over the project site and is well below the assessment criterion.

Sulphur Trioxide / Sulphuric acid

- Predicted concentrations at all sensitive receptor locations are well within the relevant 1-hour and 24-hour assessment criteria.
- The 1-hour assessment criterion is exceeded in the immediate vicinity of the Project stacks.

Particulates (as PM₁₀ and PM_{2.5})

- Predicted concentrations at all sensitive receptor locations are well within the relevant annual and 24-hour PM₁₀ and PM_{2.5} criteria.
- There are no predicted exceedances of the 24-hour PM_{2.5} assessment criterion over the model domain.
- The highest 24-hour PM₁₀ concentration exceeds the assessment criterion over a small area within the project boundary.

Ammonia

- Predicted concentrations at all sensitive receptor locations are well within the assessment criteria.
- Highest predicted 1-hour NH₃ concentrations of 10 µg/m³ occur over the project site and is well below the assessment criterion.

Generally, the predictions presented in this report incorporate a level of conservatism in the assumptions made and the dispersion modelling approach adopted. As a result, it is expected that actual ground level concentrations, attributable to the Project, based on its current design definition, would be lower (than modelled).

Overall, the model results show that emissions of key pollutants from the Project alone lead to ground level concentrations that are less than 10% of the assessment criteria, with the exception of the maximum 1-hour NO₂ concentration estimated to be approximately 30% of the assessment criteria (at Receptor 1).

These relatively low changes in predicted ground level concentrations are not expected to impact on health or amenity values of the identified area with sensitive (human) receptors.

The modelled cumulative impact (with background concentrations included) has not been undertaken to date due to an absence of representative local data, and no other operating sources in the immediate vicinity.

8 References

Beljaars, A. (1987). On the memory of wind standard deviation for upstream roughness. *Boundary-Layer Meteorology*. **38**, 95–101.

Beringer, J. (2018). Collie OzFlux: Australian and New Zealand Flux Research and Monitoring hdl: 102.100.100/70007

BHP (2015). Pilbara Strategic Environmental Assessment – Cumulative Air Quality Assessment. https://www.bhp.com/-/media/bhp/regulatory-information-media/iron-ore/western-australia-iron-ore/0000/report-appendices/160316_ironore_waio_pilbarastrategicassessment_state_appendix9.pdf

BoM (2021). http://www.bom.gov.au/climate/averages/tables/cw_009037.shtml

BoM (2021b).

http://www.bom.gov.au/jsp/ncc/cdio/weatherData/av?p_nccObsCode=139&p_display_type=dataFile&p_start Year=&p_c=&p_stn_num=009037

DoE (2006). Air Quality Modelling Guidance Notes. Department of Environment, Western Australia.

Department of Water and Environment Regulation (DWER) (2019). Guideline Air Emissions. Activities regulated under the: Environmental Protection Act 1986 Environmental Protection Regulations 1987. Draft for external consultation, October 2019. Government of Western Australia.

Environment Australia (EA) 2012. National Pollutant Inventory Emission Estimation Technique Manual for Mining Version 3.1, Environment Australia, Canberra, Australia.

http://www.npi.gov.au/handbooks/approved_handbooks/mining.html

Environmental Protection Authority (EPA) (2020). Environmental Factor Guideline – Air Quality. Environmental Protection Authority, Western Australia. April 2020. Available at:

https://www.epa.wa.gov.au/sites/default/files/Policies_and_Guidance/EFG%20-%20Air%20Quality%20-%2003.04.2020.pdf

Environment Australia (2012a) National Pollutant Inventory Emission Estimation Technique Manual for Mining Version 3.1, Environment Australia, Canberra, Australia. Online at: http://www.npi.gov.au/handbooks/approved_handbooks/mining.html

Golder, D., (1972). Relations among Stability Parameters in the Surface Layer, *Boundary-Layer Meteorology*, **3**: 47-58

Hagermann S. (2002) An Improved Land Surface Parameter Dataset for Global and Regional Climate Models, Max Planck Institute for Meteorology, MPI Report 336.

Kottek, M., J. Grieser, C. Beck, B. Rudolf, and F. Rubel (2006). World Map of the Köppen-Geiger climate classification updated. *Meteorol. Z.*, **15**, 259-263. DOI: 10.1127/0941-2948/2006/0130. Available at: [http://koeppen-geiger.vu-wien.ac.at/Lettau, H. \(1969\). Note on Aerodynamic Roughness-Parameter Estimation on the Basis of Roughness-Element Description, *Journal of Applied Meteorology*, **8**, 828-832.](http://koeppen-geiger.vu-wien.ac.at/Lettau, H. (1969). Note on Aerodynamic Roughness-Parameter Estimation on the Basis of Roughness-Element Description, <i>Journal of Applied Meteorology</i>, 8, 828-832.)

Ministry of the Environment, Conservation and Parks, Human Toxicology and Air Standards Section, Technical Assessment and Standards Development Branch, Ontario Ministry of the Environment, Conservation and Parks

(MECP). 2020. Ambient Air Quality Criteria. MECP, Toronto, ON, Canada. Available at: <https://files.ontario.ca/mecp-ambient-air-quality-criteria-list-en-2020-05-01.pdf>.

NEPC. (2015). National Environment Protection (Ambient Air Quality) Measure. National Environment Protection Council, Australia.

NEPC (2021). National Environment Protection (Ambient Air Quality) Measure. Available at: <https://www.legislation.gov.au/Details/C2004H03935>.

NERDDC (1988). Air Pollution from Surface Coal Mining: Measurement, Modelling and Community Perception, Project No. 921, National Energy Research Development and Demonstration Council, Canberra.

NSW EPA (2017). Approved Methods for the Modelling and Assessment of Air Pollutants in New South Wales. New South Wales Environment Protection Authority. Online at: <https://www.epa.nsw.gov.au/-/media/epa/corporate-site/resources/air/approved-methods-for-modelling-and-assessment-of-air-pollutants-in-nsw-160666.pdf?la=en&hash=D4131297808565F94E13B186D8C70E7BD02B4C3D>

Peel, D.R., Pitman, A.J., Hughes, L.A., Narisma, G.T. and, R.A. Pielke Sr (2004) The impact of realistic biophysical parameters for eucalypts on the simulation of the January climate of Australia, *Environmental Modelling & Software*, **20**, 595-612

Perry, S.G., A.J. Cimorelli, et al. (2005). AERMOD: A Dispersion Model for Industrial Source Applications. Part II: Model 52 performance against 17 Field Study Databases. *Journal of Applied Meteorology* 44(5):694-708.

Scire, J. S., Robe, F. R., Fernau, M. E., Yamartino, R. J., (2000). A User's Guide for the CALPUFF Dispersion Model (Version 5). Earth Tech Inc., Concord, Massachusetts.

Scire, J. S., Robe, F. R., Fernau, M. E., Yamartino, R. J., (2011). CALPUFF Modeling System Version 6 User Instructions. Earth Tech Inc., Concord, Massachusetts

Seinfeld, J. and S. Pandis (2006). *Atmospheric Chemistry and Physics: From Air Pollution to Climate Change*. Hoboken, New Jersey, John Wiley & Sons, Inc.

Silberstein, R. (2015) Gingin OzFlux: Australian and New Zealand Flux Research and Monitoring hdl: 102.100.100/22677

USEPA (1998). Western surface coal mining, AP-42 Chapter 11.9, United States Environment Protection Agency Office of Air Quality Planning and Standards.

USEPA (2006). Unpaved Roads, AP-42 Chapter 13.2.2, United States Environment Protection Agency Office of Air Quality Planning and Standards.

USEPA (2006b). Aggregate handling and storage piles, AP-42 Chapter 13.2.4, United States Environment Protection Agency Office of Air Quality Planning and Standards.

USEPA (2006c). Industrial wind erosion, AP-42 Chapter 13.2.5, United States Environment Protection Agency Office of Air Quality Planning and Standards.

USEPA (2015). Technical Support Document (TSD) for NO₂-related AERMOD Modifications. United States Environment Protection Agency, July 2015.

USEPA (2016). Guideline on Air Quality Models (Appendix W to 40 CFR Part 51). United States Environment Protection Agency, December 2016.

Yang, T., Nadimpalli, K. and Cechet, B. (2014). Local Wind Assessment in Australia: Computation Methodology for Wind Multipliers. Record 2014/33. Geoscience Australia, Canberra.

<http://dx.doi.org/10.11636/Record.2014.033>

9 Acronyms and Glossary

Acronym	Description
AGV	Ambient guideline value, as defined by DWER
AQQC	Ambient Air Quality Criteria, as defined by the MECP
BoM	Bureau of Meteorology
BWS	Belt wash station
C	Degrees Celsius (temperature)
CLP	Leaching and Purification plant
DDG	Dust Deposition Gauge
DoE	Department of Environment (now DWER)
DWER	Department of Water and Environmental Regulation
EE	Emissions estimation
EET	Emissions Estimation Technique
EETM	Emissions Estimation Technique Manual
EF	Emission factor
EMRS-1	Eneabba Mineral Sands Recovery Phase One Project
EMRS-2	Eneabba Mineral Sands Recovery Phase Two Project
EMRS-3	Eneabba Mineral Sands Recovery Phase Three Project
EPA	Environmental Protection Authority Western Australia, Australia
EPAV	Environmental Protection Authority Victoria, Australia
ETA	Environmental Technologies & Analytics Pty Ltd
FEL	Front end loader
GLC	Ground Level Concentration
g/m ² /month	Grams per square metre per month
g/s	grams per second
h/yr	Hours per year

Acronym	Description
H ₂ SO ₄	Sulphuric acid (gas)
HM	Heavy minerals
kg	kilogram
kg/t	kilogram per tonne
kg/yr	kilograms per year
kPa	kiloPascals
km	kilometre
m	metre
m/s	metres per second
MECP	Ministry of the Environment, Ontario, Canada
mm	millimetre
MSP	Narngulu Mineral Separation Plant
.Mt	Million tonnes
Mtpa	Million tonnes per annum
NEPC	National Environment Protection Council
NEPM	National Environmental Protection Measure
NH ₃	Ammonia
NO	Nitrogen oxide
NO ₂	Nitrogen dioxide
NO _x	Oxides of nitrogen
NPI	National Pollutant Inventory
NSW	New South Wales
O ₃	Ozone
PM	Particulate matter, small particles and liquid droplets that can remain suspended in air.
PM _{2.5}	Particulate matter with an aerodynamic diameter of 2.5 µm or less.

Acronym	Description
PM ₁₀	Particulate matter with an aerodynamic diameter of 10 µm or less.
RE	Rare earth
SO ₂	Sulphur dioxide
SO ₃	Sulphur trioxide
STP	Standard temperature and pressure
t	Tonnes
t/h	Tonnes per hour
tpa	tonnes per annum

Acronym	Description
tph	tonnes per hour
TS	Transfer station
TSP	Total suspended particulates
µg/m ³	micro grams (one millionth of a gram) per cubic metre
µm	micrometre
USEPA	United States Environment Protection Agency
WRF	Weather Research and Forecasting Model

10 Appendices

Appendix A – Meteorology	57
Appendix B – Emission Rates	75
Appendix C – Emission Parameters	76

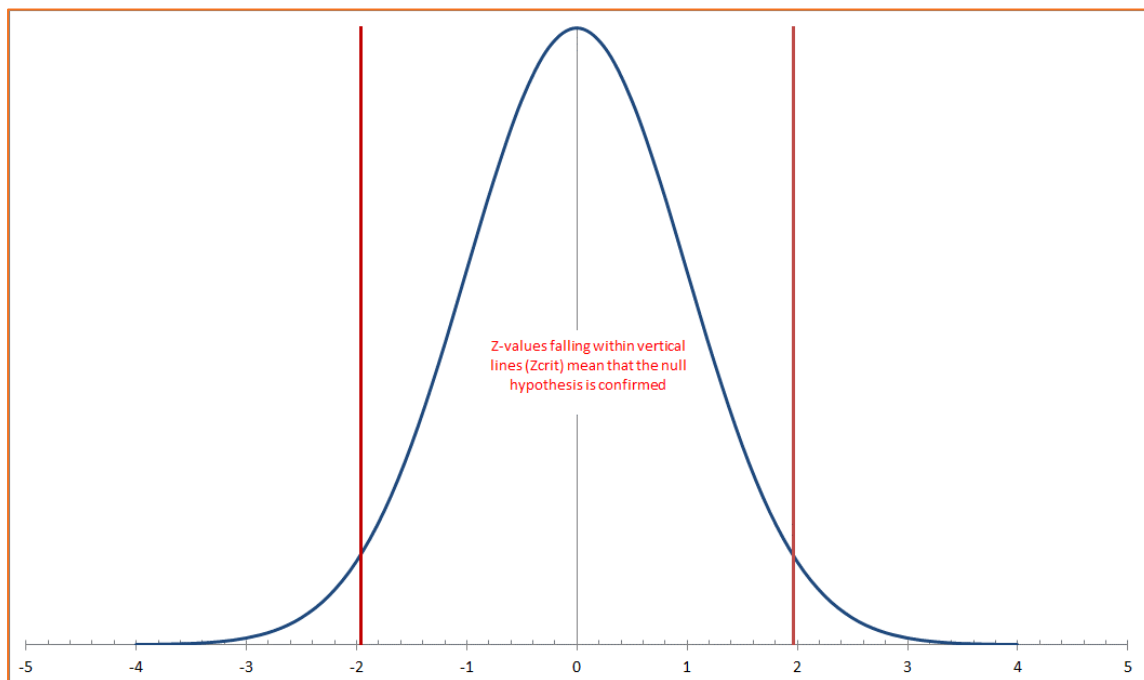
Appendix A – Meteorology

A.1: Selection of Representative Year

Generally, a minimum of one year of meteorological data is acceptable for dispersion modelling in Australia and New Zealand. The data must, however, adequately represent worst-case meteorological conditions and the data should be assessed in terms of representativeness against climatic averages. In other words, the meteorology for selected years must be deemed representative of the “normal” range of conditions in the area.

To determine the year of meteorological data to use for the dispersion modelling, 10-years of historical surface observations from the BoM station at Badgingarra⁶ (2011 to 2020 inclusive) were reviewed. The Mann-Whitney U test was used to statistically identify the representative modelling year based on recorded scalar meteorological parameters including wind speed and temperature.

The null hypothesis is that there is no significant difference between hourly values in an individual year and the hourly averages for long term average values. If values fall within the vertical lines (at 5% confidence interval, two tailed), then accept the null hypothesis (Appendix Figure 1). The null hypothesis is that there is no significant difference between hourly values in an individual year and the hourly averages for long term average values. The graph below shows that if values fall within the vertical lines (at 5% confidence interval, two tailed), then accept the null hypothesis. Note that only scalars were assessed (i.e., temperature and wind speed). Wind direction was assessed through radar plots.

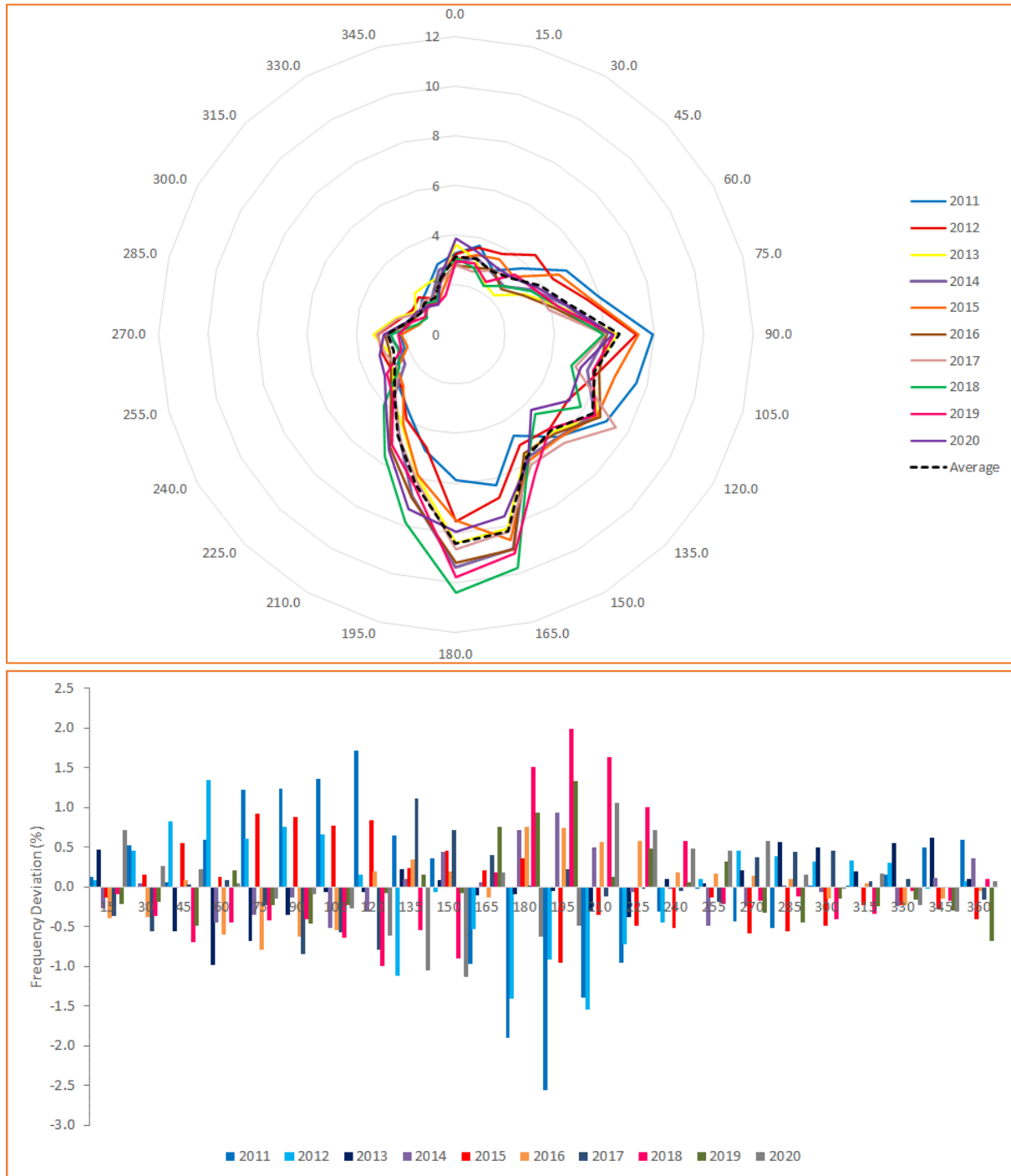


Appendix Figure 1: Null Hypothesis for Mann-Whitney U test

⁶ Badgingarra is located approximately 55 km to the south-southeast of Iluka operations.

Wind direction and speed

The average wind direction radar plots for 2011 to 2020 at Badgingarra are compared in Appendix Figure 2 (upper). Except for 2011, the wind direction pattern is generally consistent across all years. There are only minor inter-annual differences in wind direction for years 2012 to 2020, with deviations from the 10-year mean of <1.5% and less for any direction for all years except 2011, 2012 and 2018 (Appendix Figure 2, lower).

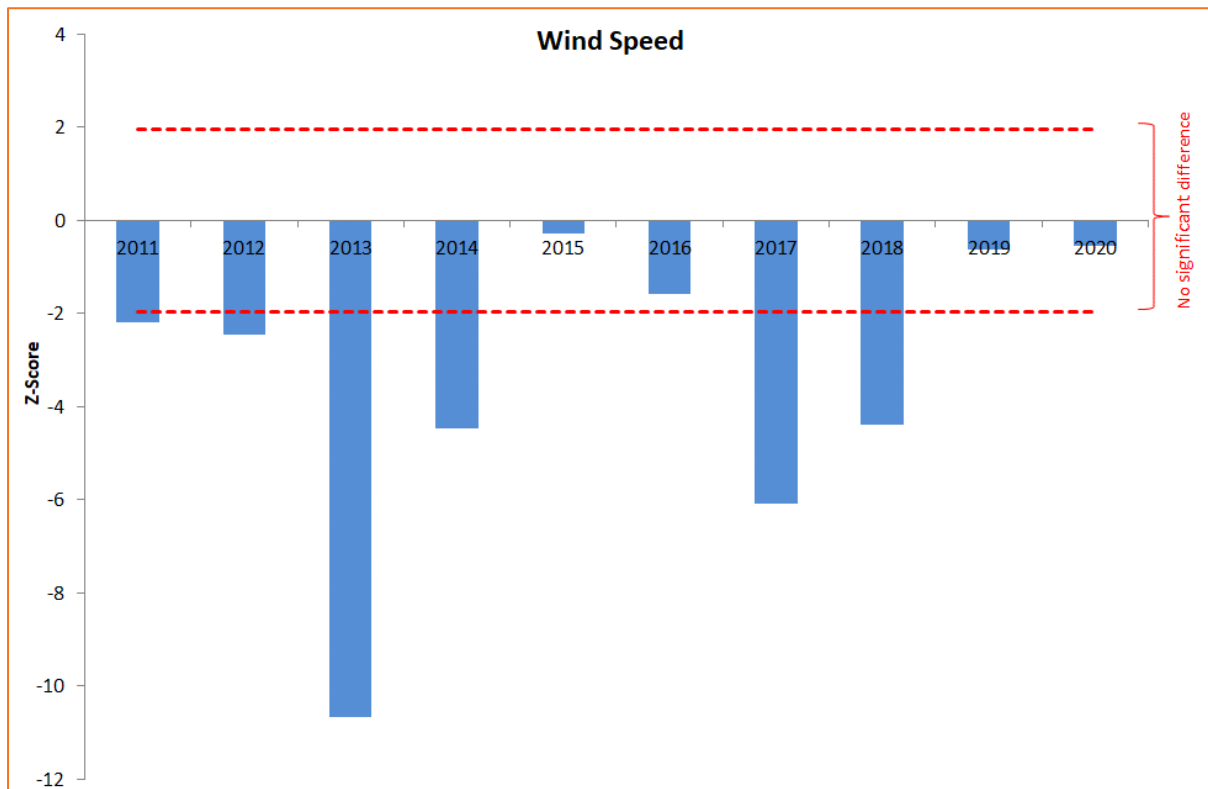


Appendix Figure 2: Wind direction radar plot (upper) and frequency deviation from the 10-year mean (lower) for Badgingarra (2011-2020)

The wind speed statistics for the 10 years is shown in Appendix Table 1. Some outlier wind speeds are apparent in the table. The more objective Mann-Whitney U test results for wind speed indicate that 2015, 2016, 2019 and 2020 were representative of 10 year mean conditions at the 5% confidence interval (Appendix Figure 3).

Appendix Table 1: Statistics of wind speed in m/s for the period 2011-2020.

Year	Min	10% ^{ile}	50% ^{ile}	90% ^{ile}	Max
2011	0	2.1	5.1	8.3	16.1
2012	0	2.1	5.0	8.0	15.4
2013	0	1.8	4.8	8.1	13.0
2014	0	2.0	5.0	8.3	14.4
2015	0	2.1	5.1	8.2	14.1
2016	0	2.1	5.0	8.3	13.4
2017	0	2.0	4.9	8.1	15.0
2018	0	1.9	5.0	8.4	15.0
2019	0	2.1	5.1	8.4	16.4
2020	0	2.0	5.1	8.5	15.8



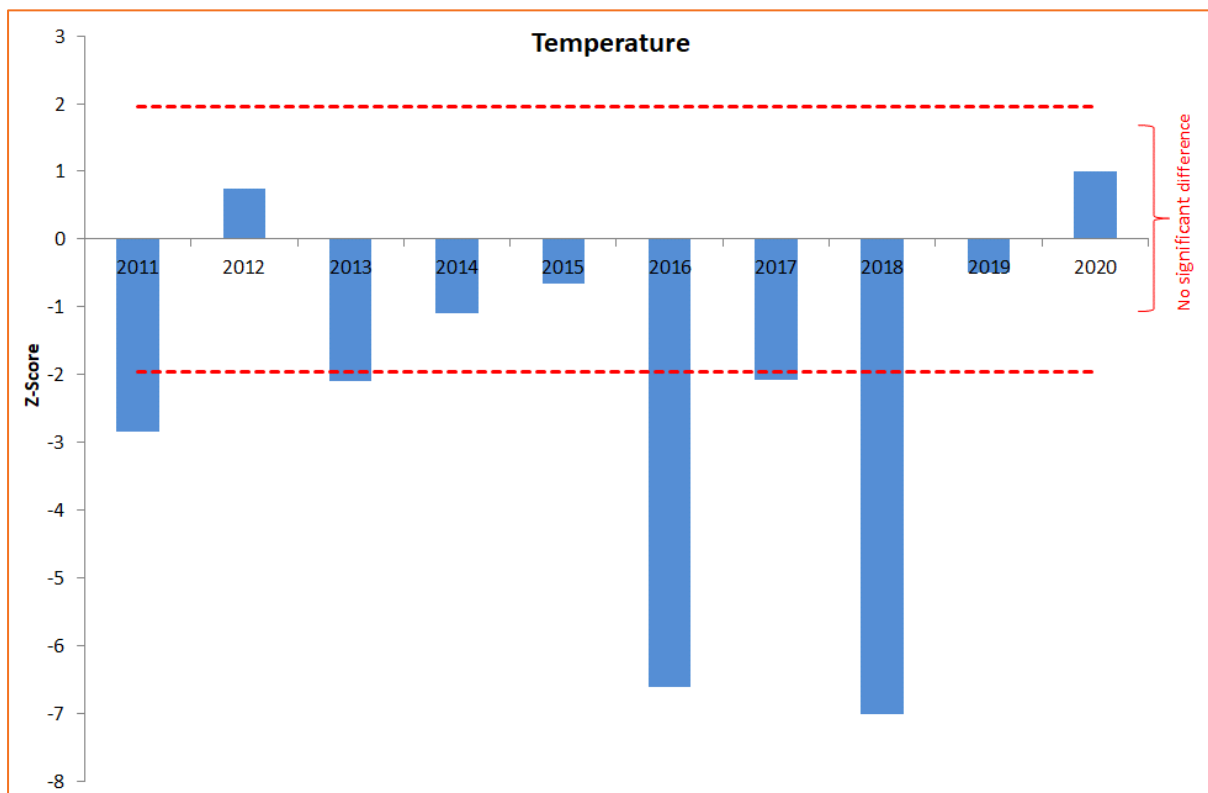
Appendix Figure 3: Mann-Whitney U test result for wind speed for Badgingarra.

Temperature

The temperature statistics for the 10 years is shown in Appendix Table 2. The Mann-Whitney U test results for temperature indicate that hourly temperature values during 2012, 2014, 2015, 2019 and 2020 were not significantly different to the hourly averages for long term average values (Appendix Figure 4).

Appendix Table 2: Statistics of Temperature in °C for the period 2011-2020.

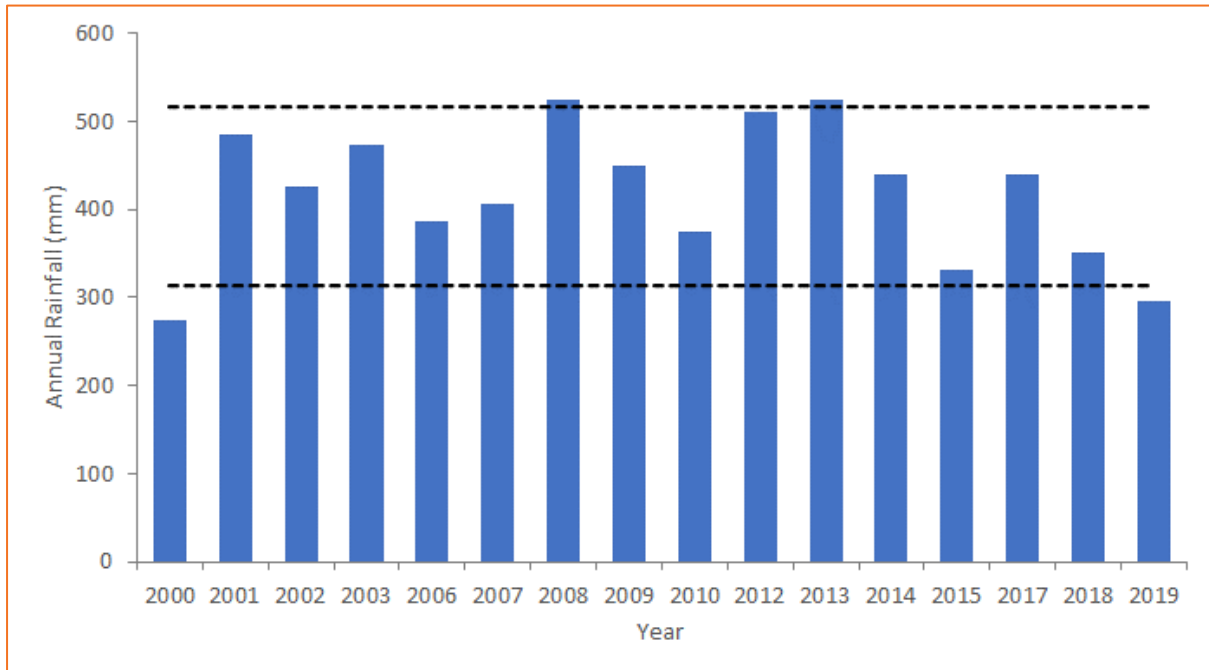
Year	Min	10% ^{ile}	50% ^{ile}	90% ^{ile}	Max
2011	3.7	10.2	18.8	29.4	40.7
2012	2.3	10.0	18.4	28.5	40.3
2013	4.1	9.5	18.3	28.9	41.3
2014	4.6	10.0	18.4	28.8	44.2
2015	3.0	10.2	18.5	28.8	42.3
2016	2.4	8.2	17.6	28.8	42.7
2017	2.6	9.9	18.2	28.5	42.4
2018	3.4	9.6	17.7	27.7	40.6
2019	4.0	9.9	18.5	29.2	42.6
2020	0.0	10.3	18.5	28.5	42.8



Appendix Figure 4: Mann-Whitney U test result for temperature for Badgingarra.

Rainfall

The annual rainfall at Badgingarra for the 16-year period (2000-2019)⁷ is displayed in Appendix Figure 5. There is a significant variation of rainfall between each year. During the 2000 to 2019 period, only 2000, 2008, 2013 and 2019 all fall outside the 10th and 90th percentile long-term rainfall totals. This indicates that these years had no major “outlier” annual rainfall totals.



Appendix Figure 5: Median annual rainfall at Jandakot between 1994 and 2020. Dotted lines indicate 27-year 10th and 90th percentile rainfall values.

Selected representative year

In summary:

- For wind speeds 2012, 2014, **2015**, 2019 and 2020 were not statistically different to longer term conditions.
- For temperature 2012, 2014, **2015**, 2019 and 2020 were not significantly different to longer term average values.
- Wind direction displayed little significant interannual variability (except for 2012 and 2018).
- Rainfall, although highly variable, showed that 2001, 2002, 2003, 2006, 2007, 2009, 2010, 2014, **2015**, 2017 and 2018 all fell within the 10th and 90th percentile 30-year rainfall totals.

This section therefore shows that **2015** can be considered largely representative of longer-term average conditions. The meteorological variables affecting dispersion, namely wind speed, temperature and direction compare favourably to the long-term average conditions.

⁷ Several years were excluded due to incomplete data.

A.2: Weather Research and Forecast Model

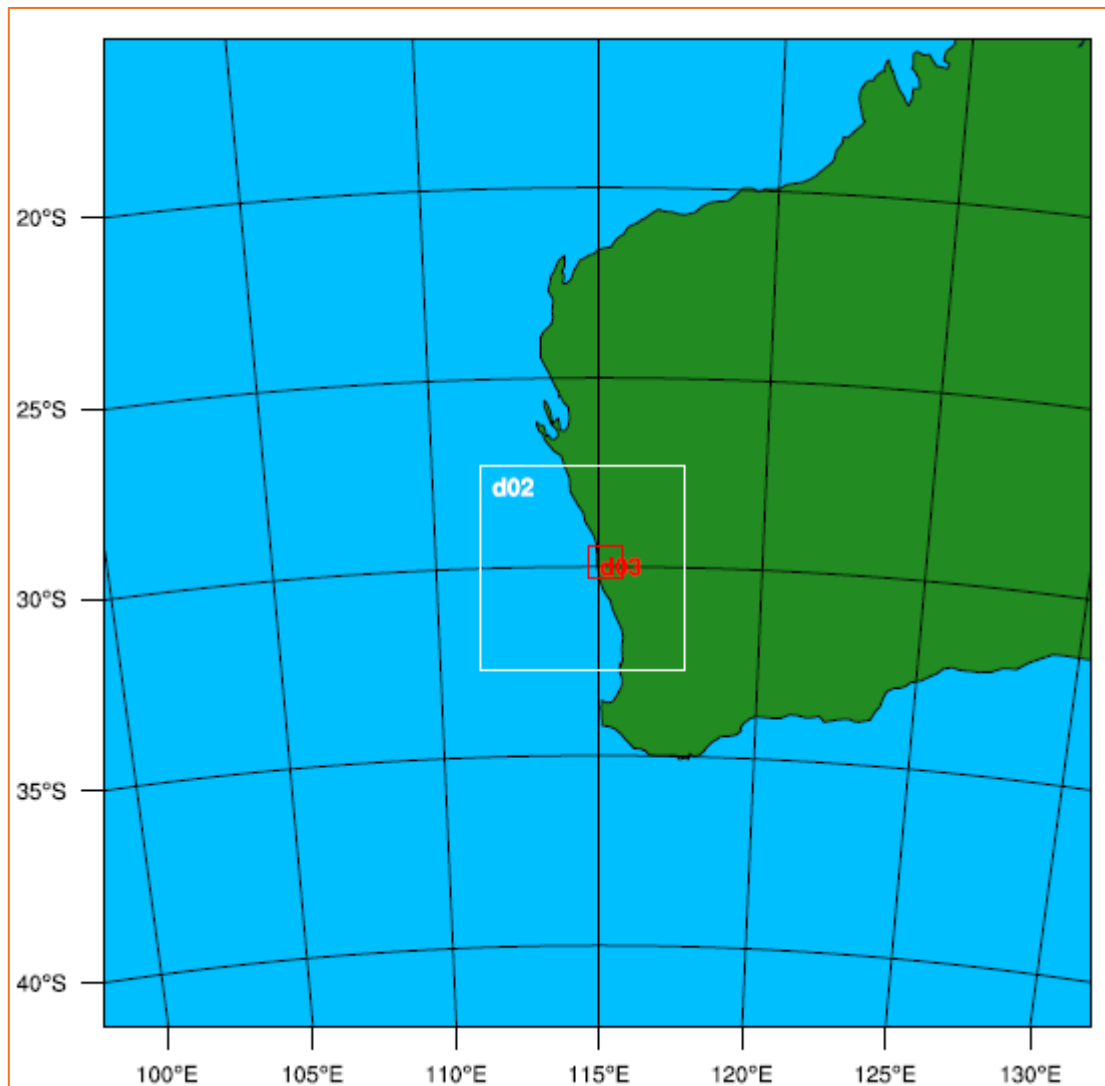
WRF was developed (and continues to be developed) in the United States by a collaborative partnership including the National Center for Atmospheric Research (NCAR), the National Oceanic and Atmospheric Administration (the National Center for Environmental Prediction (NCEP), the Forecast Systems Laboratory (FSL), the Air Force Weather Agency (AFWA), the Naval Research Laboratory, the University of Oklahoma, the Federal Aviation Administration (FAA) and others. (WRF, 2012).

WRF is a fully compressible, Eulerian, non-hydrostatic meso-scale numerical model developed by the National Center for Atmospheric Research (NCAR) and the National Oceanic and Atmospheric Administration (NOAA) in the United States. WRF is suitable for a broad spectrum of applications across scales ranging from metres to thousands of kilometres. The model utilises global reanalysis⁸ data to produce fine-scale 3-dimensional meteorological fields that considers local terrain and land-use effects.

WRF was run with a three-nest structure (30 km, 6 km, and 1.2 km horizontal grid space resolution) centred on 29.0°S and 115.276°E. This is shown in Appendix Figure 6. The model vertical resolution consists of 38 eta levels⁹.

⁸ Global modelling using observed climate data for temperature, wind speed, and pressure. The observations are analysed; interpolated onto a system of grids and the model initialised with this data.

⁹ Eta levels are terrain-following vertical coordinates near the ground, and purely isobaric above a prescribed level of approximately 400 hPa (~ 7,000m)



Appendix Figure 6: WRF model domains.

Physics options in WRF are to represent atmospheric radiation, surface, and boundary layer as well as cloud and precipitation processes. The physics options selected for the modelling are based on the results of a sensitivity study undertaken over southwestern Western Australia, where simulations of 14 combinations of land surface model, longwave radiation scheme, shortwave radiation scheme, cumulus scheme, planetary boundary layer scheme, surface layer scheme and microphysics schemes were compared to observations (Kala et. al., 2015). The combination of physics options found to produce the most accurate results, were used in this study, and are summarised in Appendix Table 3.

Appendix Table 3: WRF Physics Options Selected for Model

	Domain 1	Domain 2	Domain 3	Explanatory Notes
mp_physics	4	4	4	WRF Single-moment 5-class Scheme
ra_lw_physics	1	1	1	Rapid radiative transfer model scheme
ra_sw_physics	1	1	1	Dudhia scheme for cloud and clear sky absorption and scattering
Radt	10	10	10	Time step for radiation schemes
sf_sfclay_physics	1	1	1	MM5 based on MOST
sf_surface_physics	2	2	2	Noah land surface model with 6 soil layers
bl_pbl_physics	1	1	1	Non-local K-scheme with entrainment layer
bltdt	0	0	0	Boundary layer time step (0=every time step)
cu_physics	1	1	0	Kain-Fritsch scheme using mass flux approach for domain 1 only.
cutd	5	5	5	Cumulus physics time step (minutes)

Six-hourly global final analysis synoptic data (from <http://nomads.ncdc.noaa.gov/data/gfsan/>) was used to initialise the model and provide boundary conditions.

Land-use and terrain data was sourced from the United State Geological Services (USGS) database. Inspection of the land-use indicates an acceptable resolution and category for the model area with shrub land being the dominant vegetation type. A review of the Vegparm.tbl¹⁰ reveals that these are based on North American parameterisations, with marked seasonal differences to allow for winter snow cover. These are clearly inappropriate for Australia, and specifically Western Australia. A non-seasonally varying roughness length value of 0.29 m and 0.4 m was therefore assigned to the eucalyptus forest and shrub land category based on a study by Peel *et al.* (2004). Albedo was also set to 0.2 based on values cited in Peel *et al.* (2004).

The selection of an appropriate Land Surface Model (LSM) is critically important to provide the boundary conditions at the land-atmosphere interface because:

- The Planetary Boundary Layer (PBL) schemes are sensitive to surface fluxes.
- The cloud/cumulus schemes are sensitive to the PBL structures.
- There is a need to capture mesoscale circulations forced by surface variability in albedo, soil moisture/temperature and land use.

The Noah Land-Surface Model was selected in this case to account for the sub-grid-scale fluxes. This sophisticated scheme provides 4 quantities to the parent atmospheric model (WRF), namely:

- surface sensible heat flux
- surface latent heat flux
- upward longwave radiation
- upward (reflected) shortwave radiation.

¹⁰ A table consisting of land-use specific surface roughness, albedo, and Bowen ratio.

A.3: CALMET Results

Wind speed and direction

Selected meteorological variables were extracted from the gridded CALMET output for a point corresponding to the Iluka operations. The general features of the 10 m winds illustrated in the annual and seasonal wind rose diagrams for the period from January – December 2015 are shown in Appendix Figure 7.

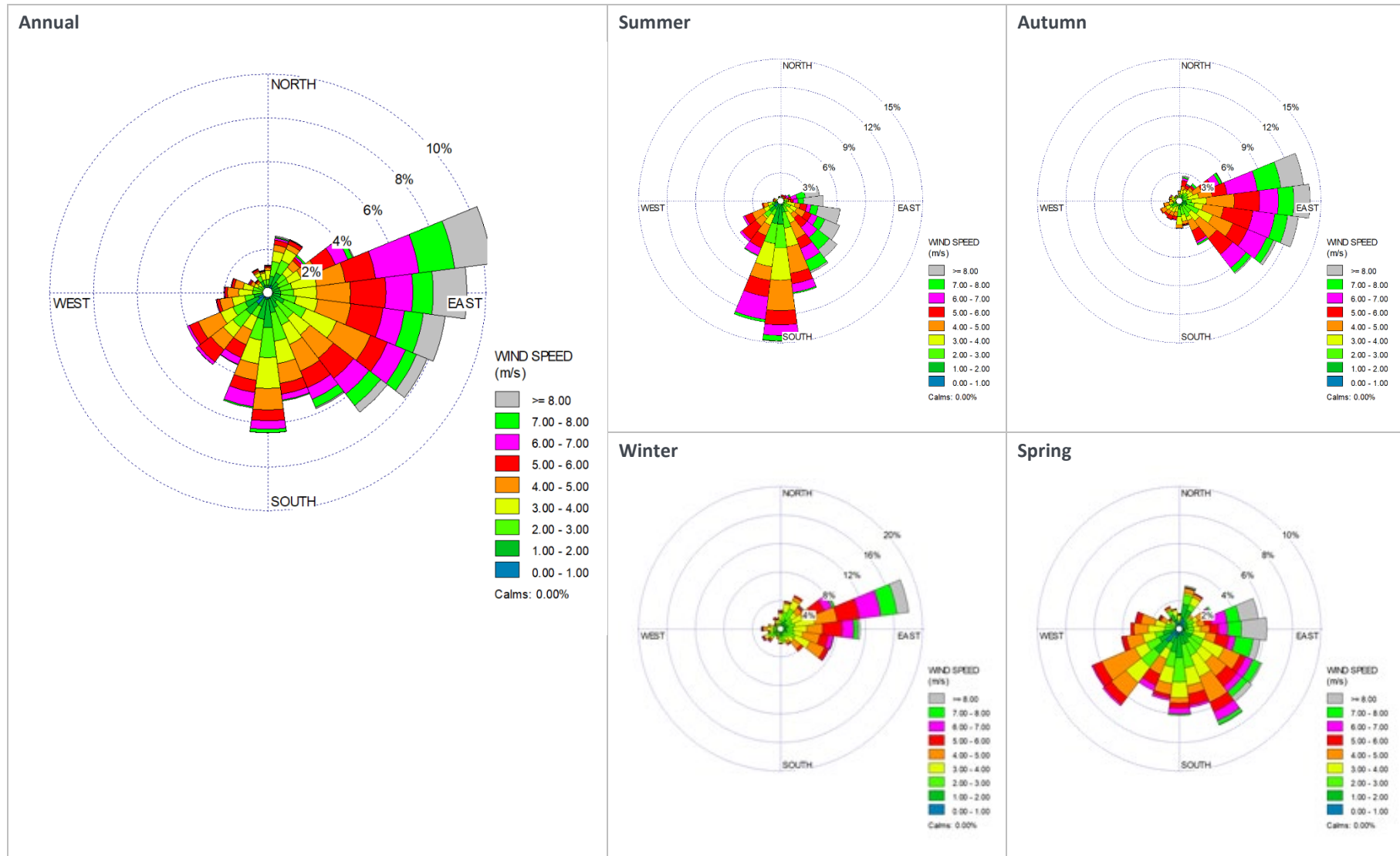
The wind rose summarises the model wind statistics of the frequency of occurrence of winds by direction and strength. The bars correspond to the 16 compass points – N, NNE, NE, etc. The bar at the top of each wind rose diagram represents winds blowing from the north (i.e., northerly winds), and so on. The length of the bar represents the frequency of occurrence of winds from that direction for the corresponding wind speed categories.

The major features of the wind rose for the site are as follows:

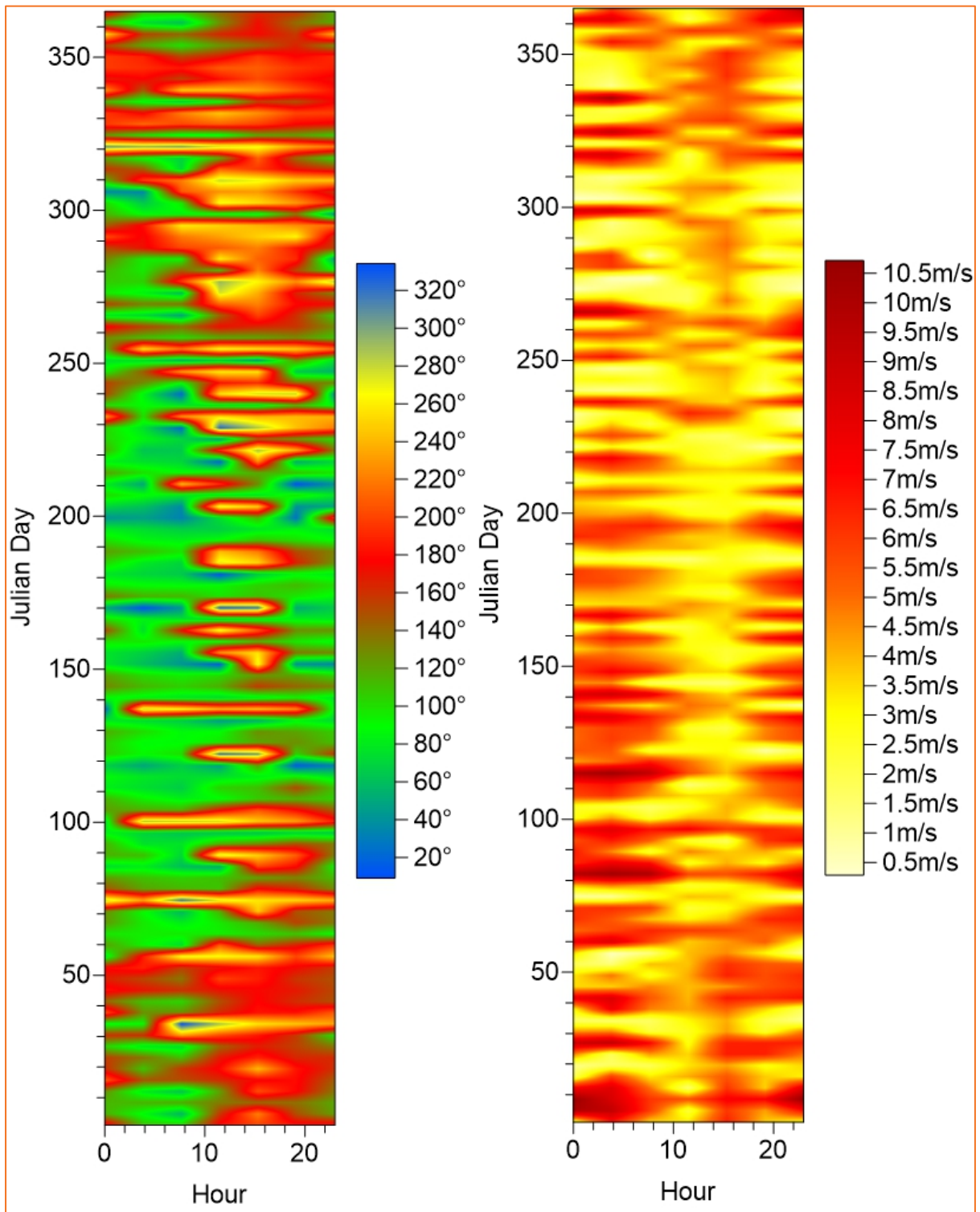
- Annual wind rose:
 - wind direction is predominantly from the east-northeast to southeast, with a secondary peak from the south.
 - Highest frequency of average speeds (> 8 m/s) occur with winds from the east-northeast.
 - Winds from the northwest are relatively uncommon.
 - Highest frequency of light winds occurs from the south.
- Summer wind rose:
 - Winds are predominantly from the south.
 - Strongest winds are from the east-northeast to southeast.
 - Highest frequency of light winds occurs from the south.
- Autumn wind rose:
 - Winds are predominantly from the east-northeast to southeast.
 - Strongest winds are from these directions.
 - Winds from the northwest are rare.
- Winter wind rose:
 - Winds are predominantly from the east-northeast.
- Spring wind rose:
 - Winds during this season do not display a predominant direction, with easterly, southeasterly and southwesterly winds most common.

The diurnal and annual cycle of modelled wind speed and direction during 2015 at a point corresponding to the Iluka operations is presented as a day/time (Hovmöller) plot (Appendix Figure 8). This plot allows the visualisation of the variation of wind by time of day as well as day of year. The figure on the left shows that wind direction is predominantly from the east during the night and mornings, especially during winter, with westerly flow on occasions. Southerly wind is evident after 10 am on most days during summer, with easterly flow on occasions. The figure on the right shows that wind speeds are generally stronger at night, particularly during summer/autumn.

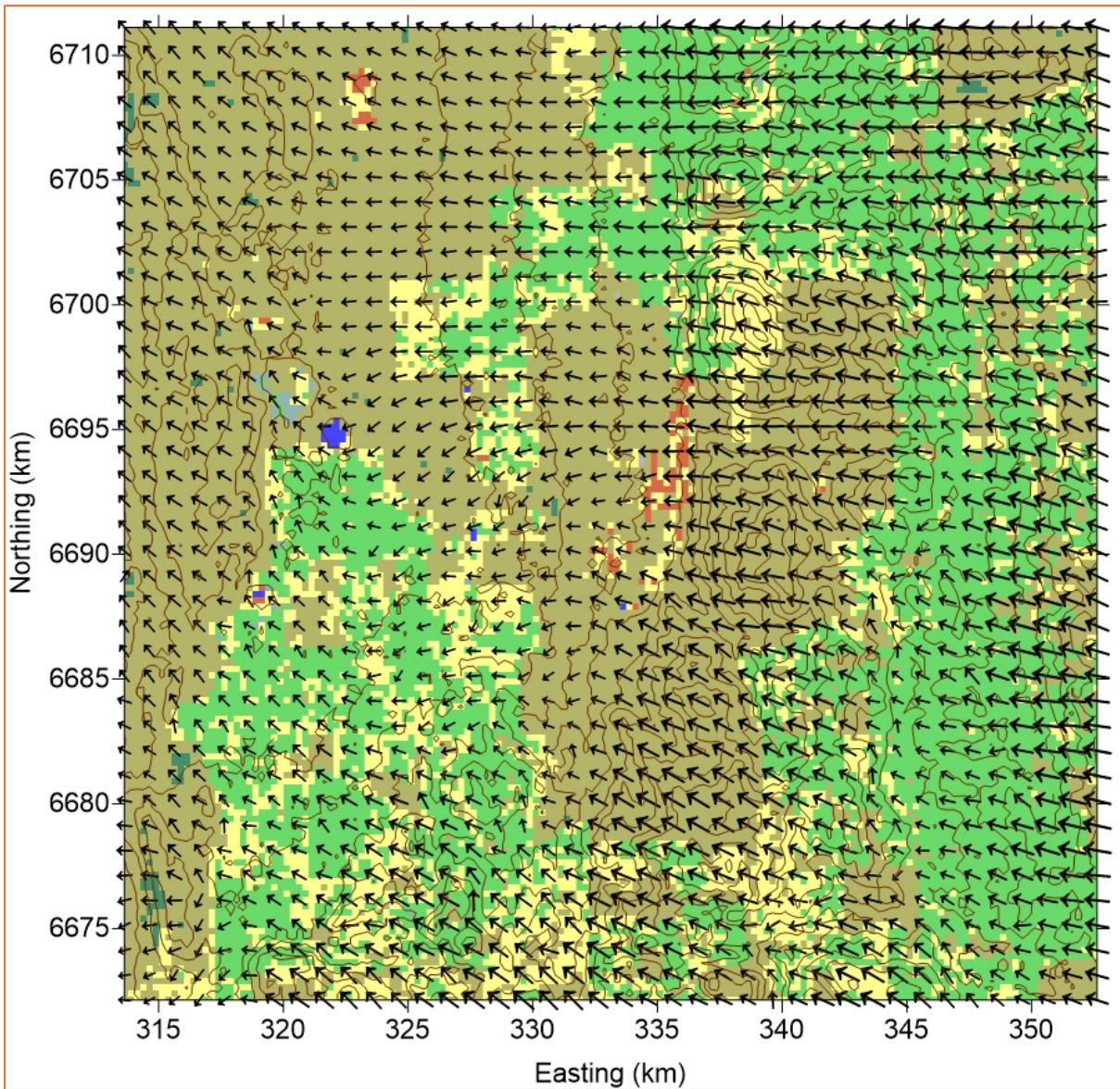
An example of CALMET-generated surface wind vectors for 4 am on 20 January is shown in Appendix Figure 9. Terrain influence on the wind, with terrain blocking effects as well as higher speeds over elevated areas to the east, is evident.



Appendix Figure 7: Annual and seasonal wind roses for Iluka site - January to December 2015 (extracted from CALMET).



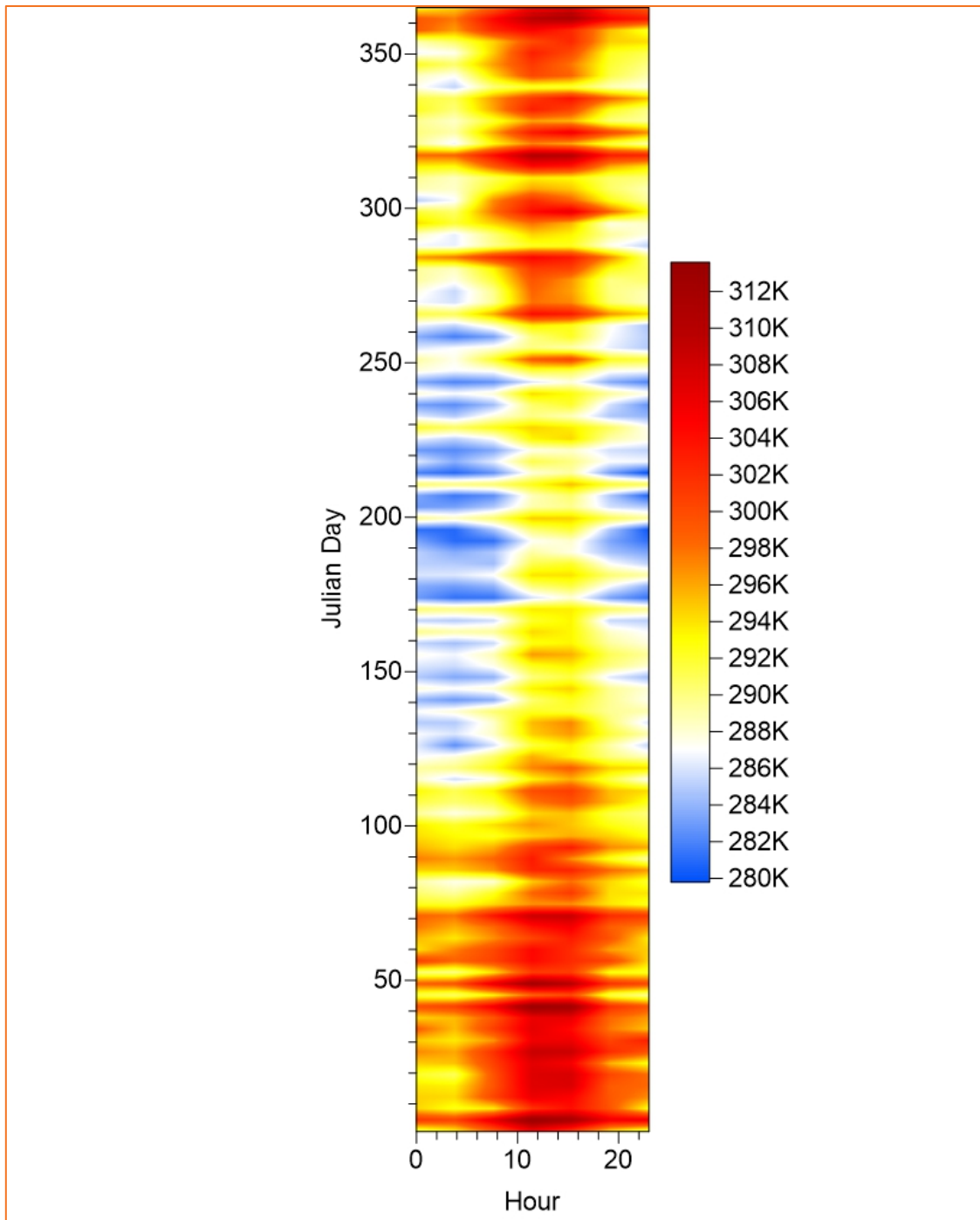
Appendix Figure 8: Julian Day-time plot of wind direction (left) and wind speed (right).



Appendix Figure 9: Surface wind vectors for 04:00 on 20 January 2015 overlain on land-use and terrain data.

Temperature

The diurnal and annual cycle of modelled surface temperatures extracted for a point corresponding to the Iluka operations during 2015 is presented as a day-time plot. Appendix Figure 4 shows that, as expected, highest temperatures generally occur during the afternoon hours from November until mid-April. Lowest modelled temperature of 279 K (6°C) occurred between 00:00 and 07:00 on 14 July (Julian day 195) with highest modelled temperature of 313 K (40°C) occurring on 11 January (Julian day 11).



Appendix Figure 10: Julian Day-time temperature plot – 2015 (extracted from CALMET)

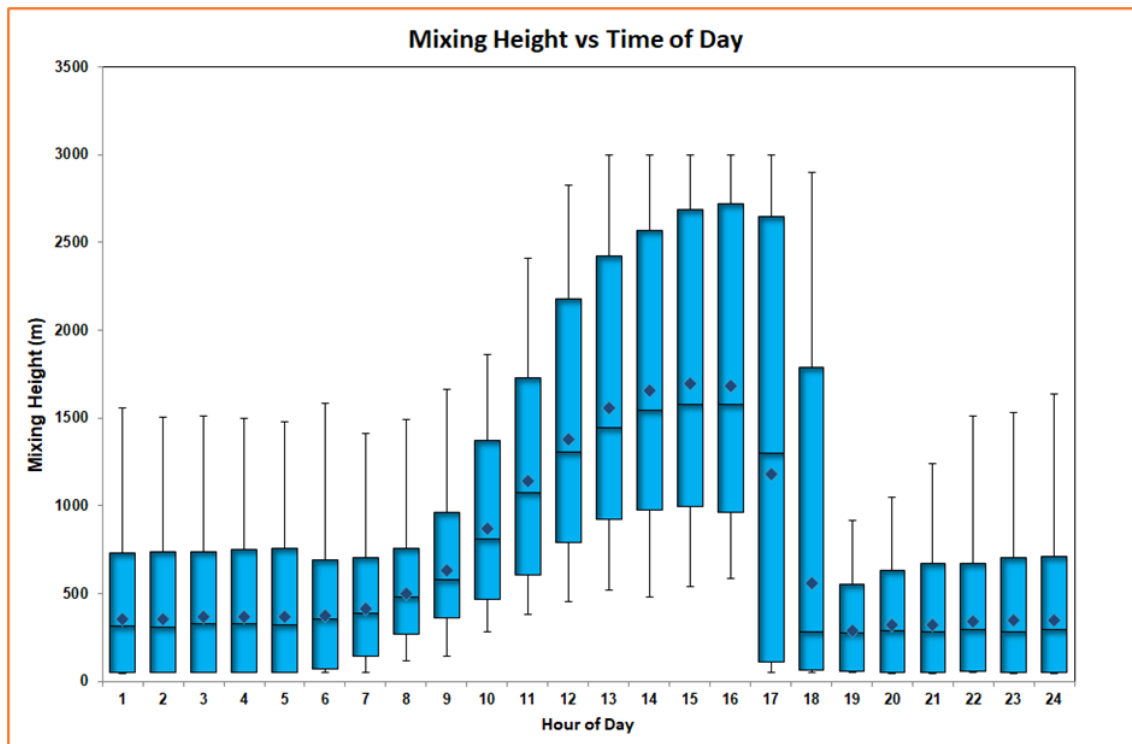
Mixing Height

Mixing height is the depth of the atmospheric surface layer beneath an elevated temperature inversion. It is an important parameter within air pollution meteorology. Vertical diffusion or mixing of a plume is limited by the mixing height, as the air above this layer tends to be stable, with restricted vertical motion.

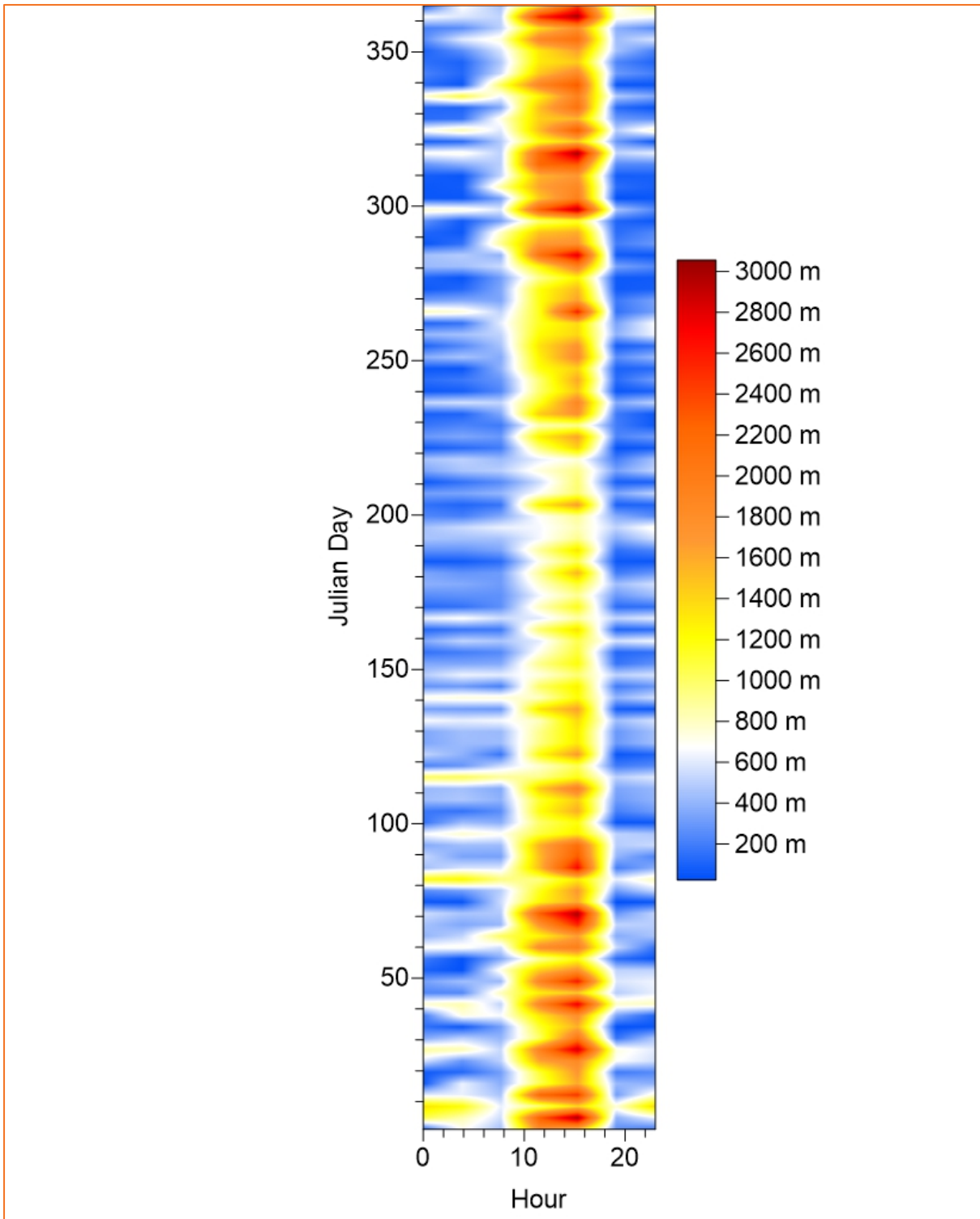
A series of internal algorithms within CALMET is used to calculate mixing heights for the subject site where it is assumed that mixing height is formed through mechanical means (wind speed) at night and through a mixture of mechanical and convective means (wind speed and solar radiation) during the day (Scire et al. 2011). During the night and early morning when the convective mixed layer is absent or small, the full depth of the planetary boundary layer (PBL) may be controlled by mechanical turbulence. During the day, the height of the PBL during convective conditions is then taken as the maximum of the estimated (or measured if available) convective boundary layer height and the estimated (or measured if available) mechanical mixing height. It is calculated from the early morning potential temperature sounding (prior to sunrise), and the time varying surface heat flux to calculate the time evolution of the convective boundary layer.

The hourly variation of mixing height over the year is summarised in Appendix Figure 11, with a clear diurnal cycle evident. At night, mixing height is normally below 500 m and after sunrise it typically increases to between 1,000 m and 2,700 m in response to convective mixing generated by solar heating of the Earth's surface. A rapid reduction in mixing height commences around sunset when convective mixing ceases and a mechanical mixing regime is re-established (Appendix Figure 7).

As expected, maximum mixing heights are lower (higher) during the winter (summer) months due to reduced (increased) solar insolation while mixing heights occasionally remain high during the night due to mechanical mixing resulting from strong winds (Appendix Figure 12).



Appendix Figure 11: Statistics of hourly mixing heights – 2015 (extracted from CALMET).



Appendix Figure 12: Julian Day-time plot of mixing heights – 2015 (extracted from CALMET).

Atmospheric Stability

An important aspect of pollutant dispersion is the level of turbulence in the lowest 1 km or so of the atmosphere, known as the planetary boundary layer (PBL). Turbulence controls how effectively a plume is diffused into the surrounding air and hence diluted. It acts by increasing the cross-sectional area of the plume due to random motions. With stronger turbulence, the rate of plume diffusion increases. Weak turbulence limits diffusion and contributes to high plume concentrations downwind of a source.

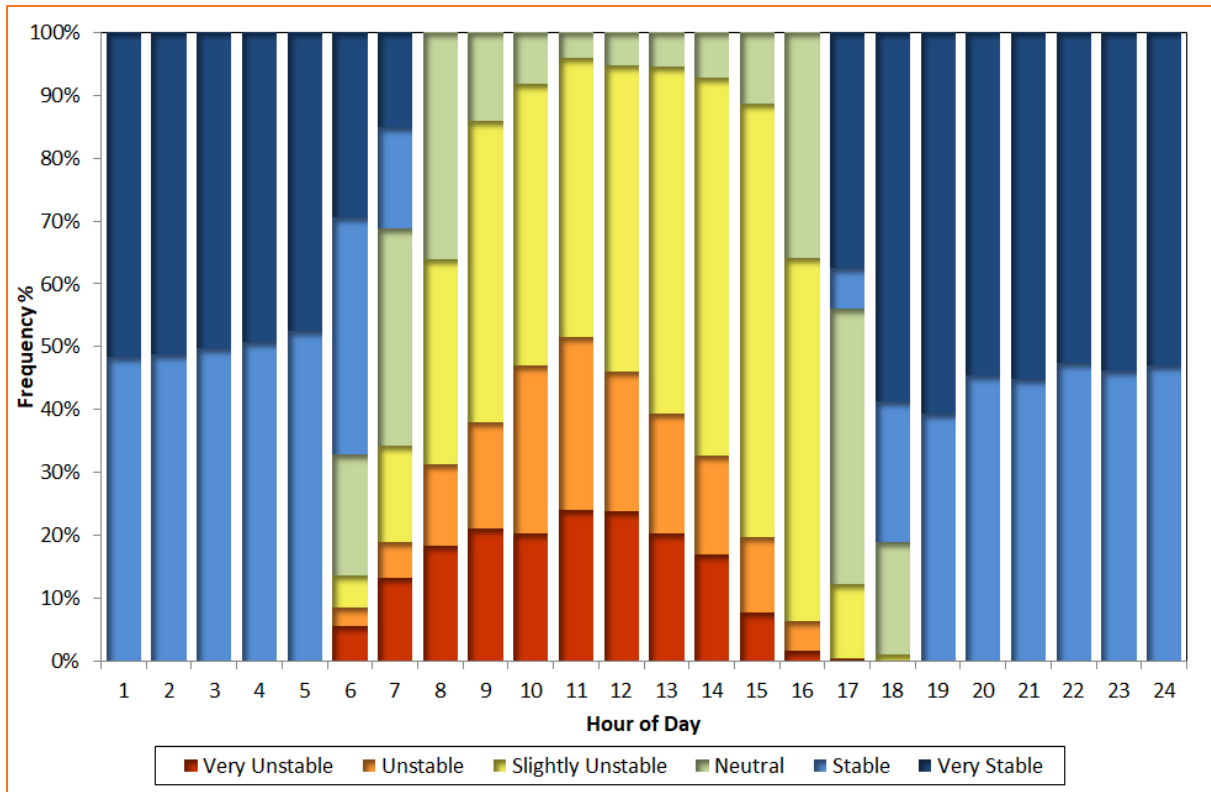
Turbulence is generated by both thermal and mechanical effects to varying degrees. Thermally driven turbulence occurs when the surface is being heated, in turn transferring heat to the air above by convection. Mechanical turbulence is caused by the frictional effects of wind moving over the earth's surface and depends on the roughness of the surface as well as the flow characteristics.

Turbulence in the boundary layer is influenced by the vertical temperature gradient, which is one of several indicators of stability. Plume models use indicators of atmospheric stability in conjunction with other meteorological data to estimate the dispersion conditions in the atmosphere.

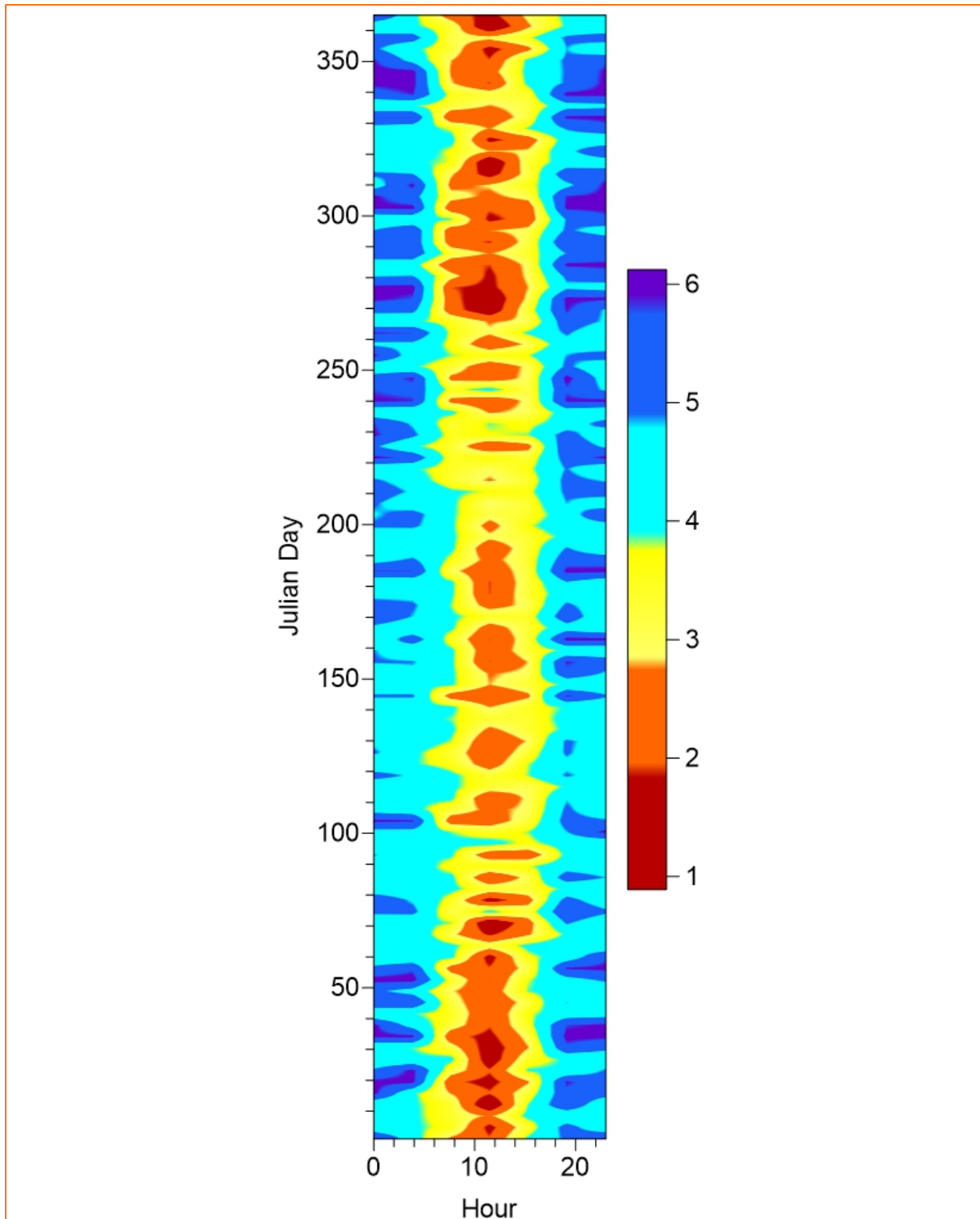
Stability can be described across a spectrum ranging from highly unstable through neutral to highly stable. A highly unstable boundary layer is characterised by strong surface heating and relatively light winds, leading to intense convective turbulence and enhanced plume diffusion. At the other extreme, very stable conditions are often associated with strong temperature inversions and light winds, which commonly occur under clear skies at night and in the early morning. Under these conditions, plumes can remain relatively undiluted for considerable distances downwind. Neutral conditions are linked to windy and/or cloudy weather, and short periods around sunset and sunrise, when surface rates of heating or cooling are very low.

The stability of the atmosphere plays a large role in determining the dispersion of a plume and it is important to have it correctly represented in dispersion models. Current air quality dispersion models (such as AERMOD and CALPUFF) use the Monin-Obukhov Similarity Theory (MOST) to characterise turbulence and other processes in the PBL. One of the measures of the PBL is the Monin-Obukhov length (L), which approximates the height at which turbulence is generated equally by thermal and mechanical effects (Seinfeld and Pandis 2006). It is a measure of the relative importance of mechanical and thermal forcing on atmospheric turbulence.

Because values of L diverge to $+$ and $-$ infinity as stability approaches neutral from the stable and unstable sides, respectively, it is often more convenient to use the inverse of L (i.e., $1/L$) when describing stability. Appendix Figure 13 shows the frequency of stability over the year by hour of the day, with reference to the widely known Pasquill-Gifford classes of stability. The relationship between L and stability classes is based on values derived by Golder (1972) set out in NSW DEC (2005). Note that the reference to stability categories here is only for convenience in describing stability. The figure shows that stable and very stable conditions occur for most of the time at night. Atmospheric instability increases during the day and reaches a peak around midday when solar insolation is at its maximum. Appendix Figure 14 shows that the frequency and intensity of slightly unstable and very unstable conditions increases during the spring and summer. Very unstable conditions occur on occasions between Julian days 268 and 78 (September to March).



Appendix Figure 13: Statistics of hourly stability class – 2015 (extracted from CALMET).



Appendix Figure 14: Julian Day-time plot of stability – 2015 (extracted from CALMET).

Appendix B – Emission Rates

Appendix Table 3: PM₁₀ emission rate for extraction – statistical summary

Source Id	Maximum (g/s)	99th Percentile (gs)	95th Percentile (gs)	90th Percentile (gs)	70th Percentile (g/s)	Average (g/s)
Load	0.17	0.17	0.17	0.17	0.17	0.09
Doz1	1.13	1.13	1.13	1.13	0.00	0.33
Unload1	0.06	0.06	0.06	0.06	0.06	0.03
FEL1	0.09	0.09	0.09	0.09	0.09	0.05
HR1	0.04	0.04	0.04	0.04	0.04	0.02
HR2	0.04	0.04	0.04	0.04	0.04	0.02
HR3	0.04	0.04	0.04	0.04	0.04	0.02
HR4	0.04	0.04	0.04	0.04	0.04	0.02
HR5	0.04	0.04	0.04	0.04	0.04	0.02
HR6	0.04	0.04	0.04	0.04	0.04	0.02

Appendix C – Emission Parameters

Appendix Table 4: Model parameters (volume sources)

Source Id	Easting	Northing	Effective Height	Sigma Y	Sigma Z
Load	336158	6692373	3	125.0	1.40
Doz1	336181	6692397	2	25.0	0.93
Unload1	335846	6692332	2	12.5	0.93
FEL1	335861	6692315	2	12.5	0.93
HR1	336154	6692477	3.3	9.8	3.08
HR2	336057	6692509	3.3	9.8	3.08
HR3	335961	6692509	3.3	9.8	3.08
HR4	335963	6692411	3.3	9.8	3.08
HR5	335930	6692348	3.3	9.8	3.08
HR6	335851	6692347	3.3	9.8	3.08

Appendix Table 5: Model parameters (area sources)

Source Id	Easting1	Easting2	Easting3	Easting4	Northing1	Northing2	Northing3	Northing4
WE1	336081	336221	336220	336081	6692421	6692422	6692305	6692306
WE2	335828	335877	335877	335827	6692336	6692336	6692285	6692286
WE3	335852	335899	335899	335854	6692481	6692480	6692438	6692439
WE4	335833	335882	335883	335835	6692609	6692610	6692568	6692569

